(Front cover)

Doctoral Thesis

Fuel and material utilization of a waste shiitake (*Lentinula edodes*) mushroom bed derived from hardwood chips

Regional Environment Creation,
The United Graduate School of Agricultural Sciences,

JIANG　ZHUOQIU

(Iwate University)

2023 年 9 月

TABLE OF CONTENTS

ABSTRACT 1

要旨 5

CHAPTER ONE　INTRODUCTION 8

1. Mushroom industry in Japan 8

2. Examples of waste mushroom bed utilization in China 9

3. Objectives in this study 10

CHAPTER TWO　CHARACTERISTICS OF CALORIFIC VALUE IN TERMS OF ELEMENTAL COMPOSITION AND ASH CONTENT 12

1. Introduction 12

2. Material and methods 14

2.1 Details of the cultivation bed 14

2.2 Moisture content (MC) tests 16

2.3 Preparation of powder samples 16

2.4 Elemental analysis and ash content tests 17

2.5 Calorific value tests 18

3. Results and discussion 19

3.1 Moisture contents of waste mushroom beds 19

3.2 Ash contents and elemental composition 22

3.3 Calorific values 26

3.4 Substance flow during Shiitake mushroom bed cultivation 32

4. Conclusions 38

CHAPTER THREE THERMAL CONDUCTIVITY OF COMPRESSION-DRIED WASTE MUSHROOM BEDS 40

1. Introduction 40

2. Material and methods 43

2.1 Preparing waste mushroom beds with various densities 43

2.2 Wood and wood-based materials for comparison 47

2.3 Measuring thermal conductivity 48

2.4 A heat-flow model for predicting substance thermal conductivity 50

2.5 Predicting the substance thermal conductivity 53

3. Results and discussion 54

3.1 Thermal conductivity of the heat bridge (substance) 54

3.2 Relationship between the density and thermal conductivity 57

3.3 Thermal conductivity of the heat bridge along the heat-flow direction 62

4. Conclusions 66

CHAPTER FOUR MECHANICAL PROPERTIES OF COMPRESSION-DRIED WASTE MUSHROOM BEDS 67

1. Introduction 67

2. Material and methods 70

2.1 Preparation of test specimens for mechanical properties 70

2.2 Internal bond strength (IB) tests 72

2.3 Compressive tests 73

2.4 Consolidation tests of powder samples 76

3. Results and discussion 78

3.1 Internal bond strength (IB) 78

3.2 Elastic modulus of substance (E_s) 82

3.3 Elastic modulus in the waste mushroom bed height direction 86

3.4 Compressive yield strength and strain in the waste mushroom beds height direction 90

4. Conclusions 92

CHAPTER FIVE MANUFACTURING AND PERFORMANCE OF BINDER-LESS BOARDS 93

1. Introduction 93

2. Material and methods 95

2.1 Raw materials 95

2.2 Boards manufacture 96

2.3 Mechanical properties and water resistance (TS・WA) tests..... 99

2.4 Surface darkening measurement (L^* test) 101

3. Results and discussion..... 102

3.1 Temperature, density, crack, and L^* of the I-Boards..... 102

3.2 Internal bond strength (IB) of the I-Boards 107

3.3 Bending strength (MOR) and young's modulus (MOE) of the I-Boards..... 110

3.4 Water resistance (TS・WA) of the I-Boards 114

3.5 Effect of skin chips on the board properties..... 117

4. Conclusions..... 119

CHAPTER SIX FUTURE PROSPECTS..... 120

REFERENCES 122

Chapter one 122

Chapter two 122

Chapter three..... 123

Chapter four 125

Chapter five 125

ACKNOWLEDGMENTS 127

LIST OF ABBREVIATIONS 128

Chapter two 128

Chapter three 129

Chapter four 130

Chapter five 130

LIST OF TABLES 132

Chapter two 132

Chapter three 132

Chapter four 132

Chapter five 133

LIST OF FIGURES 134

Chapter one 134

Chapter two 134

Chapter three 134

Chapter four 135

Chapter five 136

ABSTRACT

This study aims to recycle shiitake waste mushroom beds (WMBs), which are generated in the cultivation of shiitake mushroom using hardwood chip beds, for use as fuel and material.

First, to understand the fuel characteristics of WMB, the moisture content (MC) at the time of disposal and after 1 month of disposal, as well as its calorific value, ash content, and elemental composition, were investigated. The moisture content on a wet basis (MC_w) was 78% at the time of disposal and was as high as 63% even 1 month after disposal. It is considered that the slow drying process is caused by the low moisture permeability of the skin of mushroom bed, and therefore it is preferable to crush the WMB before drying. Comparing the gross calorific value on a dry basis of the WMB with that of the cultivation raw wood, the value inside of the WMB was similar, while that of its skin was significantly lower (by 11%). The reason for this lies in the significantly higher ash content and nitrogen content compared to those of raw wood. When analyzed from the combustion heat of the contained elements, it was found that both the cultivation raw wood and the WMB had almost no hydrogen contributing to combustion due to their high oxygen content, and they were dependent on the heat generation of carbon. As a result of finding the relationship between the net calorific value that can be used as a boiler fuel and MC_w, for example, the value at an MC_w of 50% was calculated to be 7.6 MJ/kg, which was almost the same as that of Sugi (*Cryptomeria Japonica*) sapwood and bark. The ash content of the WMB was about 7%, which is close to that of bark and about 10 times that of the wood used for the cultivation bed. When the WMB is used as boiler fuel, appropriate ash treatment is required as in the case of using bark.

As for material utilization of WMBs, two viewpoints can be considered: one is to utilize the characteristics of the internal structure, and the other is to crush the WMBs and use them as raw as

materials. One of the characteristics of WMBs is their internal structure after drying. The mushroom bed, which was originally a deposit of raw material chips, changes to a structure in which the mycelium and decay residue are integrated as the mycelium spreads. This structure is similar to that of lightweight particleboard (PB) and insulation fiberboard (IFB), suggesting the possibility that WMBs can be converted into a new wood-based insulation material. Therefore, as one of the material utilizations, this study aimed to clarify the thermal insulation performance, the mechanism of thermal insulation, and the strength performance of the WMBs after drying, and to explore the possibility of using them as thermal insulation material.

When WMBs were collected, those that did not lose their shape accounted for about 90% of the total, and of these, about 10% had a relatively homogeneous internal structure (few coarse voids) after drying. In other words, if only WMBs with a homogeneous internal structure are targeted, the available resources are less than 1/10 of the amount of WMBs generated. Therefore, in order to remove and homogenize the coarse voids inside the WMBs, the WMBs were compression-dried at four levels of thickness, and the relationship between air-dry density and thermal conductivity was investigated in the density range of about 150-600 kg/m^3. A linear relationship was found between the density and the thermal conductivity of the compression-dried WMBs. At densities of 200-300 kg/m^3, the thermal conductivity of the WMBs was comparable to that of the wood and slightly greater than that of the IFB. On the other hand, at densities of 500-600 kg/m^3, the thermal conductivity was lower than that of wood and similar to that of wood-based panel materials. In addition, the substance thermal conductivity was calculated using a heat-flow model, and the values were 0.288 W/mK for WMB, 0.368 W/mK for mycelium, and 0.218 W/mK for raw wood. The same heat-flow model was applied to WMBs to obtain the substance thermal conductivity along the heat-flow direction, suggesting that the WMB substance also has anisotropic thermal conductivity.

Next, concerning the strength of the WMBs, the relationship between internal bond strength (IB) and compressive properties with air-dry density was investigated, and the elastic modulus of substance, which is the basis of strength properties, was obtained from consolidation tests of the WMBs, mycelium, and the raw wood. The results showed that even when the density was increased to about 600 kg/m^3, the IB of the compressed WMB was almost the same as that of commercial IFB with a density of about 250 kg/m^3. The increase in IB was small relative to the increase in density. The reason for this is possibly due to the severe decrease in the cohesion of the internally decayed wood and the difficulty of generating new hydrogen bonds due to the hydrophobic nature of the mycelium even when the density is increased by compression-drying. The elastic modulus of substance of the WMB was 0.80 GPa, significantly lower than the 0.87 GPa of the raw wood. On the other hand, the elastic modulus of substance of the mycelium itself was 1.6 times (1.42 GPa) that of the raw wood. The substance of the WMB is a mixture of decay residue of wood substance and mycelium. This suggests that the elastic modulus of substance of the decayed wood was significantly low. When the WMBs were compression-dried, the increase in elastic modulus was greater than the relative increase in density. From this, it can be interpreted that coarse voids gradually decreased due to the increase in density, the number of contact points of load-resisting elements (substance) increased, resulting in planar contact, and the contribution of mycelium itself, which has a high compressive elastic modulus, also increased. The yield stress and yield strain of the compression-dried WMBs were found to be equal to or greater than those of commercial IFB.

In order to use the WMBs as raw materials, the manufacturing method and performance of a binder-less board (self-adhesive board) were investigated. The skin of the WMBs is water-repellent, which may have a negative impact on self-adhesion, but from the perspective of resource utilization, it is desirable to use all of the WMBs (skin + inside) as raw materials for the binder-less boards.

Therefore, in this study, three types of raw materials (inside, skin, and whole WMBs) were used to produce binder-less boards with a target density of 1.0 g/cm^3 and a target thickness of 5 mm by keeping the press temperature constant at 210±10 ℃. The chip size, and hot-pressing schedule [pressure for relaxation period (residual pressure), with/without the second compression] were varied to determine the appropriate manufacture conditions. As a result, a board thickness and density were closest to the target values under the condition of with the second compression using small chips less than 2 mm derived from inside the WMBs. However, at the highest residual pressure of 1.5 MPa, the boards tended to suffer internal cracking. The manufacturing conditions that provided the boards with the best mechanical properties was a combination of using the chips of less than 2 mm derived from the inside of WMBs, residual pressure of 1.0 or 1.5 MPa at the relaxation period, and with the second compression. Under these conditions, darkened test specimens were obtained, with lightness L^* in the range of 35–50, suggesting the ability to perform self-adhesion. On the other hand, board thickness and density with chips derived from skin and whole WMBs were similar to those with chips derived from the inside, but the mechanical properties were inferior, and significant internal cracking occurred in chips less than 2 mm. As feared, the skin material was found to be a factor in internal cracking and strength loss.

This study reveals the possibility of using shiitake WMBs made from hardwood chips as fuel and material. It is also expected that the findings obtained from this study will be applied to cultivation wastes other than shiitake mushrooms to promote the recycling of resources.

要 旨

本研究は、広葉樹チップを用いたシイタケ菌床栽培で排出される廃菌床（以下、廃菌床）を、燃料や材料としてリサイクル利用することを目指している。

まず、廃菌床の燃料特性を把握するため、廃棄時および廃棄 1 ヶ月後の含水率、発熱量、灰分、元素組成などを調べた。その結果、廃棄時の湿量基準含水率（MC_w）は 78%、1 ヶ月放置後でも 63%であった。廃菌床の乾燥が遅い原因として表面の透湿性の低さが考えられるため、廃菌床は乾燥前に粉砕することが望ましい。廃菌床の乾燥時の発熱量を原料チップと比べると、廃菌床の内部ではほぼ同等であったが、表面部の方は約 11%低かった。この理由を元素組成から分析すると、廃菌床表面部では木材と比べて窒素と灰分の含有量が著しく高いことが挙げられた。さらに、酸素含有量の多さから水素はほとんど燃焼に寄与せず、廃菌床の発熱量が炭素の発熱に依存することが発熱量の理論計算から示された。また、ボイラー燃料として利用可能な発熱量を含水率との関係から調べると、MC_wが 50%で発熱量は 7.6 MJ/kg となり、スギの辺材や樹皮の値とほぼ同等であることが分かった。また、廃菌床の灰分は約 7%と高く、これは樹皮の値と同等で原料チップに対して約 10 倍であった。

廃菌床の材料利用の方向性として、内部構造の特性を活かす視点、粉砕して原料化する視点の二つが考えられる。廃菌床の特性の一つは、乾燥後の内部構造にある。最初は原料チップの堆積状態にあった菌床が、菌糸の蔓延に伴って腐朽残渣と菌糸が一体化した構造に変化している。これは軽量パーティクルボードや軟質繊維板（IFB）と類似した構造であり、廃菌床が新たな木質系断熱材に転換できる可能性を示唆する。そこで、本研究では材料利用の一つとして、乾燥後の廃菌床の断熱性能、断熱性の発現メカニズム、強度性能などを明らかにし、断熱材としての利用可能性を探ることを目的とした。

廃菌床を回収する際、形状が崩れないものは全体の約 9 割であり、そのうち乾燥後に比較的

均質な内部構造（粗空隙が少ない）を持つものは約 1 割であった。つまり、均質な内部構造を持つ廃菌床だけを対象とすると、利用できる資源は廃菌床発生量の 1/10 以下に過ぎない。そこで、廃菌床内部の粗空隙を排除して均質化するため廃菌床の厚さを 4 レベルで圧縮乾燥し、気乾密度 150–600 kg/m^3 の範囲で断熱性能および強度特性を調べた。圧縮乾燥された廃菌床の密度と熱伝導率の間に直線関係が認められた。密度 200–300 kg/m^3 程度では、廃菌床の熱伝導率は木材素材のそれと同等であり、IFB のそれより若干大きかった。一方、密度 500–600 kg/m^3 程度では、木材のそれよりも低く、木質パネルの断熱性に近接した。さらに、熱伝導モデルを用いて実質熱伝導率を算出した結果、その値は廃菌床で 0.288 W/mK、菌糸で 0.368 W/mK、原料チップで 0.218 W/mK であった。また、同じ熱伝導モデルを廃菌床に適用して、熱流方向の実質熱伝導率を求めた結果、廃菌床実質にも熱伝導率の異方性があることが示唆された。

次に廃菌床の強度に関して、内部結合力と圧縮特性を気乾密度との関係を調べるとともに、強度特性の基礎となる実質の弾性率を、廃菌床、原料チップおよび菌糸自体の圧密試験から決定した。その結果、圧縮乾燥により廃菌床の密度を 600 kg/m^3 程度に増加させても、内部結合力は市販の密度 250 kg/m^3 程度の IFB とほぼ同等であった。内部結合力の増加は、密度の増加に対して僅かであり、その理由として、内部の腐朽木材の凝集力低下が激しいこと、圧縮乾燥で密度を高めても菌糸の疎水性により新たな水素結合が発生しにくいことが考えられた。また、廃菌床の実質弾性率は 0.80 GPa で、原料チップの 0.87 GPa と比較して僅かに低かった。一方、菌糸自体の実質弾性率は原料チップの 1.6 倍（1.42 GPa）であった。廃菌床は菌糸と木材の腐朽残渣の混合体であるため、この結果は木材実質の腐朽残渣の弾性率が著しく低いことを示唆する。また、廃菌床を圧縮乾燥すると、圧縮弾性率の増加率は密度の増加率よりも大きくなった。これより、密度増加により粗空隙が徐々に減少し、荷重の抵抗要素（実質）の接触点が増えて面状接触となり、高い圧縮弾性率をもつ菌糸自体の寄与も増えたと解釈できる。圧縮乾燥された廃菌床の降伏応力と降伏ひずみは、市販の IFB のそれと同等以上であることが確認された。

廃菌床を原料化して材料利用するために、バインダレスボード（自己接着ボード）の製造方法と性能を調べた。廃菌床表面部には撥水性があるため自己接着への悪影響が危惧されるが、資源の有効利用の観点からは廃菌床の全て（表面部 + 内部）をボード原料に使うことが望ましい。そこで本研究では、3 種類の原料（廃菌床の内部、表面部、廃菌床の全て）を用い、プレス温度を 210 ± 10 ℃で一定とし、目標密度 1.0 g/cm^3、目標厚さ 5 mm のバインダレスボードを作製した。その際、原料小片の粒度、熱圧スケジュール（息抜き時の残圧 0.5–1.5 MPa、第二圧締の有無）を変化させ、適切な製造条件を調べた。その結果、ボードの厚さと密度が最も目標値に近くなる条件は、廃菌床内部由来の 2 mm 以下の小片を用いて第二圧締を行う条件であった。しかしながら、息抜き時の残圧が最も高い 1.5 MPa の場合、ボードの内部割れが生じ易かった。機械的性質が最も優れる製造条件は、廃菌床内部由来の 2 mm 以下の小片を用い、息抜き時残圧が 1.0 MPa または 1.5 MPa、第二圧締がある組み合わせであった。この条件では暗色化された試験体が得られ、明度 L^*は 35–50 の範囲に存在し、自己接着能力の発揮が確認された。一方、廃菌床全体および表面部由来の小片を用いてもボード厚さと密度は内部由来小片の場合と同等であったが、機械的性質は劣り、2 mm 以下の小片では顕著な内部割れが発生した。危惧されたとおり、表面部由来の原料は内部割れおよび強度低下の要因となることが確認された。

本研究により、広葉樹チップを原料とするシイタケ廃菌床の燃料および材料利用の可能性が見えてきた。また、本研究で得られた知見がシイタケ以外の菌床栽培の廃棄物にも応用され、資源循環が進むことを期待する。

CHAPTER ONE　INTRODUCTION

1. Mushroom industry in Japan

Mushroom production in each country is on the rise due to the recent boom in health foods. According to FAO statistics (Food and Agricultural Organization of the United Nations, 2017 results) [1-1], there are 30 countries that produce more than 1 million tons per year, with a total of 10.18 million tons. There are 43 countries with less than 1 million tons, but because their production in total is tens of thousands of tons, the total production of the world is approximately 10.2 million tons. The growth in mushroom production is supported by the conversion from raw wood cultivation to mushroom bed cultivation.

According to Japanese government statistics [1-2], the total production of mushrooms in Japan is 4.56 million tons (2018 results). Among several kinds of mushrooms, shiitake mushrooms are the largest on a production value basis, and the number of large-scale shiitake mushroom bed cultivation farms is increasing. In addition, the mushroom production industry, as one of the industries that utilize local resources in agricultural and mountainous villages, serves a major role in stabilizing the local economy and securing employment opportunities. However, the large amount of by-products generated in the process of its production, such as waste mushroom beds (WMBs) discharged from mushroom bed cultivation, if improperly disposed of, can cause not only a waste of resources but also environmental pollution and other problems.

2. Examples of waste mushroom bed utilization in China

With the increase in demand for fungus foods, the mushroom industry has grown rapidly, and the disposal of WMBs has become a serious problem. The following is an example of the use of WMBs in China. Huangsongdian town, located in the suburbs of Jilin Province's Jiaohe City (approximately 30 km west of the city center) [1-3], is currently known as the " Hometown of wood ear in China" and has three pellet manufacturing plants (**Figure 1-1:** production volume about 3000 tons per year) that use wood ear WMBs as raw material. The plant utilizes WMBs to contribute to local waste disposal, and at the same time, the pellets produced are supplied to rural residents, thereby contributing to a shift from coal to wood fuel as an energy source with a smaller environmental impact. In addition, a thermal power plant in the region directly burns the pulverized WMBs to supply electricity to the local community, creating an energy self-sufficient production system in the region.

Figure 1-1 Pellet fuel production process from wood ear WMBs

3. Objectives in this study

Figure 1-2 shows the production process at the shiitake farm in the Kuji area of the Iwate prefecture, Japan. The purpose of this study is to collect basic data for fuel and material utilization of the shiitake WMBs shown in **Fig. 1-3**. We are considering two viewpoints on material use: insulation material and binder-less board production. Specifically, the study was organized into the following four chapters.

In the chapter two, the fuel characteristics of a WMB derived from hardwood chips were investigated. This involved studying it's the moisture content (MC) at the time of disposal and after 1 month of disposal, as well as its calorific value, ash content, and elemental composition.

In the chapter three, the thermal conductivity of compression-dried WMBs were measured to examine their potential use as a thermal insulation material, and the position of their thermal insulation performance was investigated.

In the chapter four, the internal bond strength (IB) and compressive properties of WMBs were investigated in relation to air-dry density, and the position of the strength performance was investigated for WMBs that will be used as insulation materials.

In the chapter five, the manufacture of binder-less boards using chips derived from WMBs was also investigated.

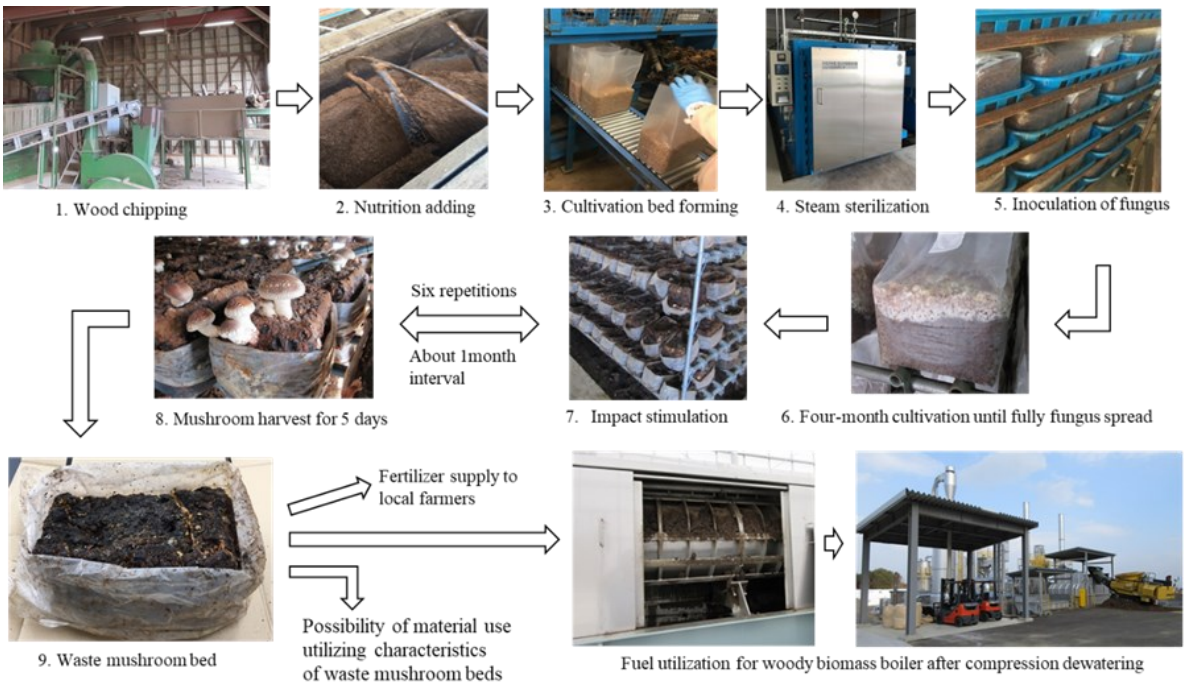

Figure 1-2 Production process of Shiitake mushroom using hardwood chip cultivation beds

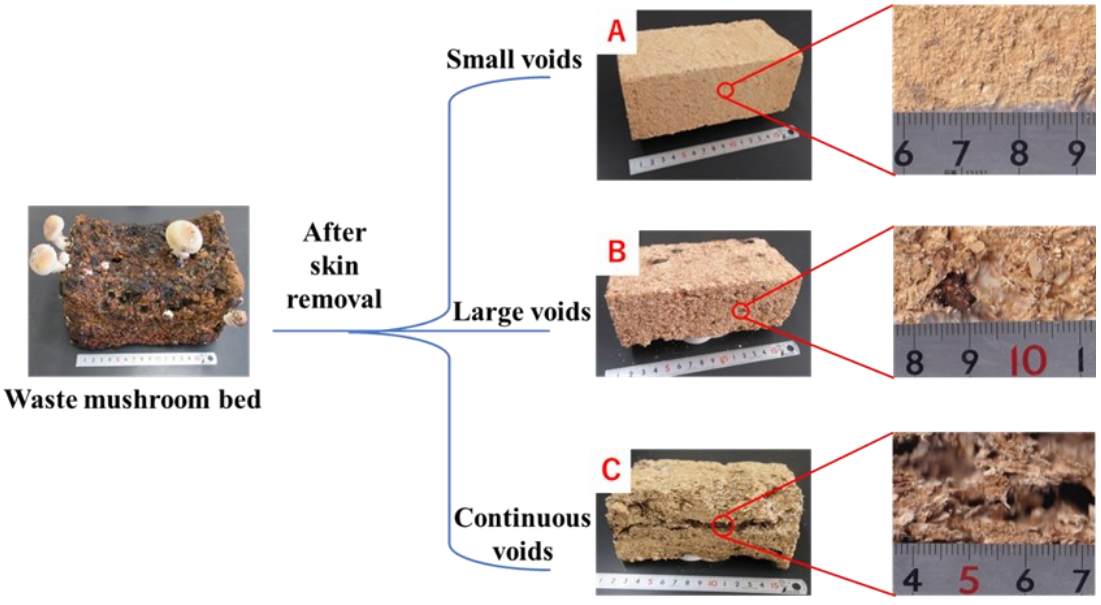

Figure 1-3 Three types of voids inside the dried shiitake WMB

CHAPTER TWO

CHARACTERISTICS OF CALORIFIC VALUE IN TERMS OF ELEMENTAL COMPOSITION AND ASH CONTENT

1. Introduction

Figure 1-2 shows the production process at the shiitake farm in the Kuji area of the Iwate prefecture, Japan. At this shiitake farm, hardwood logs collected from a nearby area are chipped to form a cultivation bed, which is disposed of after about 11 months through six times of harvesting. Traditionally, the treatment of WMBs was to provide fertilizer to local farmers, but as the number of WMBs has increased (currently more than 1 million per year), their effective use has become a serious problem.

In this chapter, we collect basic data for the fuel of the WMB. The MC of WMBs at the time of disposal and after one month of disposal, as well as the ash content, elemental composition, and calorific value, are shown as basic properties for fuel utilization. In particular, the calorific value of the WMB is discussed in comparison with that of undecayed wood (raw wood) and the mycelium itself. Then, differences in the calorific values among these materials are also discussed from the viewpoint of their elemental composition. Furthermore, the substance flow from mushroom bed preparation to disposal is discussed through the results of elemental analysis and an ash content test.

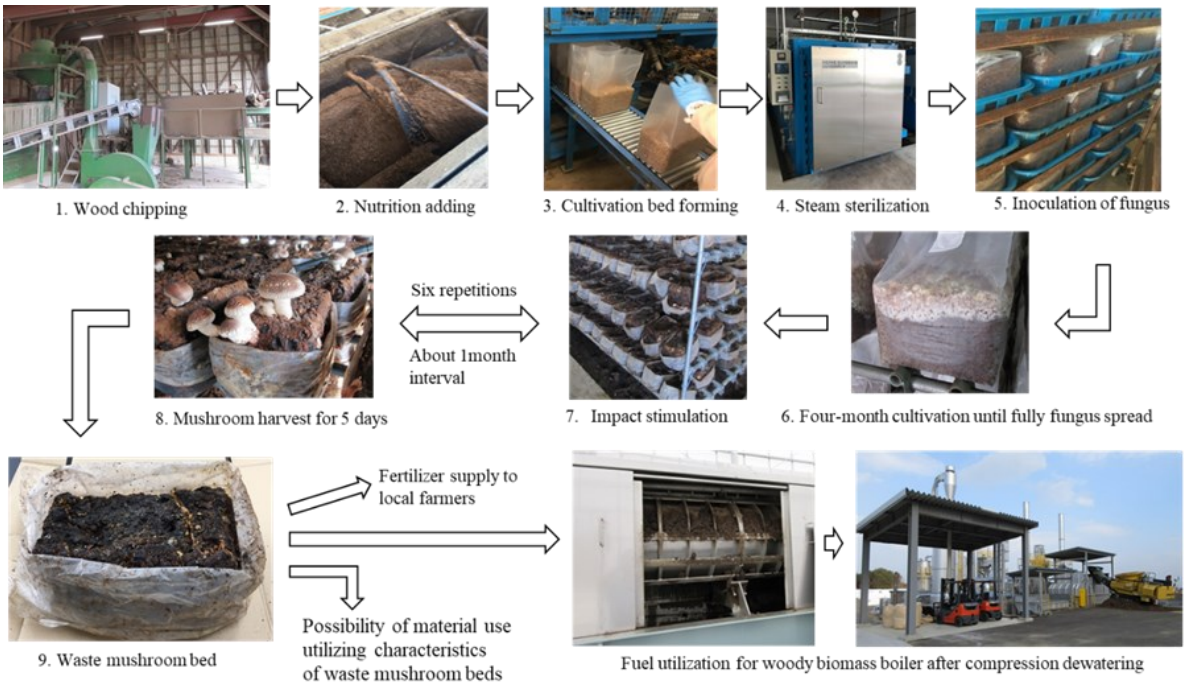

Figure 1-2　Production process of Shiitake mushroom using hardwood chip cultivation beds

2. Material and methods

2.1 Details of the cultivation bed

It is necessary to know the details of the cultivation beds, because the fuel or material properties of the WMBs are dependent on them. Therefore, the tree species and density of the raw wood, the size of the pieces after chipping, and the weight of the cultivation bed were investigated at the shiitake cultivation farm shown in **Fig. 1-2**. More than 90% of the hardwood logs were mizunara (*Quercus crispula*). A total of 20 mizunara disks with a diameter of 8–20 cm and a thickness of 2 cm were collected from a log stockyard, dried to an air-dried state (13% of the MC on a dry basis, MC_d), and their density was measured. In addition, 50 pieces of raw wood chip samples were randomly extracted from a chip stockyard, dried to an air-dry state, and the dimensions were measured. Furthermore, 30 cultivation bed samples were randomly extracted in each of Steps 3 and 5 shown in **Fig. 1-2** and they were then weighed.

The results of the above measurements are listed in **Table 2-1**. The mean dimensions of raw wood chips were 10.1 mm in width (R), 1.9 mm in thickness (T), and 7.7 mm in length (L), which are much smaller than those dimensions of the raw wood chips used in the paper industry. In Step 2 of **Fig. 1-2**, nutrients and water are added to the raw wood chips, and the MC on a wet basis, MC_w, is adjusted to about 60%. Nutrients (details will be described later) make up about 10% of the total weight of the cultivation bed. The mean weight of the cultivation bed including a plastic forming bag was 2888 g before steam sterilization. The mean weight after steam sterilization decreased by 36 g to 2852 g although about 10–13 g of inoculative fungus was added. The dimensions of the cultivation bed were about 12 cm in width, 20 cm in length, and 10 cm in height.

As shown in **Fig. 1-2**, it takes about 4 months before fungus spread fully into the cultivation bed after fungus inoculation, and then shiitake harvesting is repeated six times with an interval of 1

month. The total yield of shiitake mushroom from one cultivation bed was 913 g (2017 results), and the cultivation beds become WMBs about 11 months after preparation.

Table 2-1 Details of the cultivation bed (mean±std. ; n [1])

Raw material density (Air-dried, kg/m^3)	Chip dimensions (Air-dried, mm)	Weight per bed including forming bag [2] (g)	
		Before sterilization	After fungus inoculation
	n = 50		
n = 20	R [3]: 10.1±1.0	n = 30	n = 30
780±66	T [4]: 1.9±0.2	2888±47	2852±39
	L [5]: 7.7±0.8		

1) n : The number of samples 2) The weight of plastic forming bag (13 g)

3) R : Radial direction (width) 4) T : Tangential direction (thickness)

5) L : longitudinal direction (length)

2.2 Moisture content (MC) tests

Within 3 days of the last harvest, 100 WMB samples were randomly extracted from a cultivation house, taken out of the plastic forming bag, and weighed. A histogram of the weight was created with a class of 50 g, and then about 1/3 of the samples were extracted from each class and their MC_w were obtained by the oven-drying method ($n = 36$).

Another MC test was performed on the WMBs that had been left for 1 month to examine their drying properties. After the last harvest, they were transferred from a cultivation house to a well-ventilated greenhouse with a concrete soil for a waste yard. Although the temperature in the greenhouse was unknown, the mean temperature in the region during this period was 19 °C according to the local meteorological data. The same testing procedure as the sampling within 3 d after disposal was applied to these WMBs and their MC_w were determined ($n = 39$).

2.3 Preparation of powder samples

Powder samples were used in the tests of elemental analysis, ash content, and calorific value, which are described below. There are four types of samples: the skin of the WMB, the inside of the WMB, the mycelium, and the raw wood used for the cultivation bed. About 100 g of chip samples were prepared for both the skin and the inside from several WMBs within 3 d after disposal. The skin chips were collected by scraping the surface of the WMB with a knife. The chip samples of mycelium were prepared from the stem part of the shiitake fruiting body, because it was difficult to take out only the mycelium from the inside of the WMB. First, these four chip samples in an air-dry state were powdered using a Willey mill. Then, they were classified by a three-stage sieve, and the following three kinds of fractions were prepared: F1: 0.5–2 mm; F2: 0.15–0.5 mm; F3: less than 0.15 mm.

2.4 Elemental analysis and ash content tests

Carbon (C), hydrogen (H), and nitrogen (N) were quantified using a fully automatic elemental analyzer (Yanoko CHN Corder MT-6). F2 powder of each sample was used, and the samples were left for 5 d in an air-conditioned laboratory where the device was placed to prevent moisture absorption/desorption during analysis. Approximately, 2 mg of each sample was used for each analysis and weighed to within an accuracy of 1 μg. Three replicate analyses were conducted, and the ash content was also measured automatically through the analysis. To calculate the oven-dry weight of the samples, the MC_d, during the analysis was determined by an oven-drying method using about 2 g of the remaining sample.

After the analysis, however, three types of samples other than the mycelium showed a small amount of detected nitrogen, hence other highly accurate tests were necessary. Therefore, nitrogen was quantified for these samples using another analyzer (SUMIGRAPH NC-22A). About 100 mg of oven dry F2 sample was used for each analysis and weighed with an accuracy of 10 μg. Three replicate analyses were performed.

Among ash measurements obtained through the elemental analysis, the raw wood chips did not meet the precision required for analysis due to the lack of a detected amount of ash. Therefore, an ash content test by the usual determination method [2-1] was added. About 1 g of oven-dry F1 sample was weighed in a melting pot with an accuracy of 0.1 mg. This was heated at 600 °C for 8 h to obtain ash, and then the ash weight was measured with the same accuracy. The ratio of the dry ash weight to the oven-dry sample weight was defined as the ash content (%). Five replicate tests were performed for the three types of samples other than the mycelium.

2.5 Calorific value tests

In accordance with JIS M8814 [2-2], a gross calorific value (H_h) was determined for the four types of samples using an automatic bomb calorimeter (Shimadzu CA-4P). Approximately 1 g of F1 sample was weighed per test with an accuracy of 0.1 mg, and three replicate tests were performed. Furthermore, the MC at the time of the test, MC_w, was measured by an oven-drying method using 2–3 g of the sample. The MC_w was used to calculate gross calorific values on a dry basis.

3. Results and discussion

3.1 Moisture contents of waste mushroom beds

Figure 2-1 shows two weight histograms of a WMB. One is within 3 days after disposal and the other is 1 month later. Statistical data for the wet weight of 100 samples and on an oven-dry weight of the extracted samples are listed in **Table 2-2**. First, focusing on within 3 days after disposal, the wet weight was 1235 g on mean and had a coefficient of variation (*COV*) of 14%. The variation on the wet weight is affected not only by the amount of moisture that is included but also by the weight of the substance, because the oven-dry weight was not constant and had a *COV* of about 9%. Their MC_w, was about 78% on mean and had a *COV* of about 6%.

Second, focusing on 1 month after disposal, the wet weight was 772 g on mean and had a *COV* of 16%. As discussed above, this variation is affected not only by the amount of moisture included but also by the weight of substance, because the oven-dry weight was not constant and had a *COV* of about 16%. Their MC_w was about 63% on mean with a *COV* of about 11%. The mean MC_w decreased from 78 to 63% after being left for about 1 month. The MC on a dry basis is easier to intuitively understand the drying properties from, so when converted, its MC_d decreases from 379% to 181%. This indicates that the amount of moisture was about 3.8 times the substance weight within 3 d after disposal, and 1.8 times after being left for 1 month. This also suggests that a 1-month natural drying process is not long enough to obtain a good woody biomass fuel. The slow drying is presumed to be due to the low moisture permeability of the skin of the WMB. As will be described later, the skin is browned due to the deposition of melanin pigment. It is speculated that this browning results in the low moisture permeability. Therefore, when the WMB is used as a boiler fuel, it is preferable to expose the inside through a crushing process followed by drying.

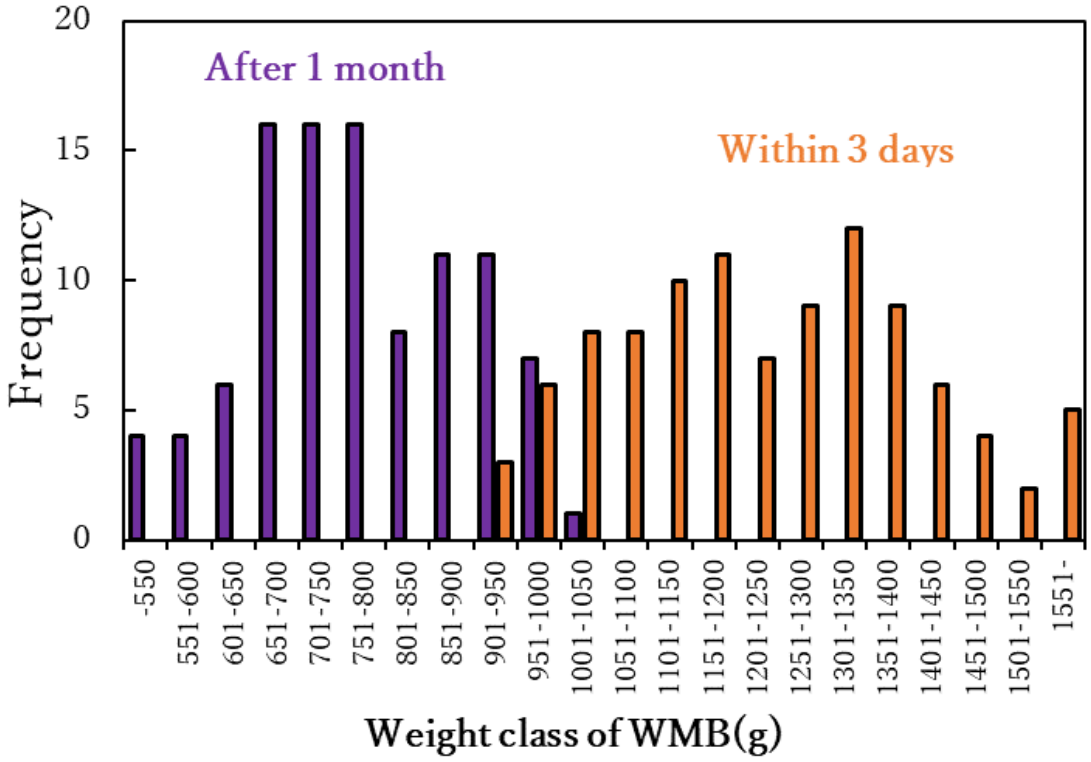

Figure 2-1　Weight histogram of WMB (n =100 for each)

Table 2-2　Weight and moisture content of WMB (mean ± std.)

	Within 3 days	After 1 month
Wet weight (g)	1235±173	772±122
(COV[1], n[2])	(0.140, 100)	(0.158, 100)
Oven-dry weight (g)	249.1±21.5	275.0±43.0
(COV, n)	(0.086, 36)	(0.157, 39)
MC_w[3] (%)	78.2±4.5	63.4±6.5
(COV, n)	(0.057, 36)	(0.105, 39)

1) COV: Coefficient of variation　2) n: The number of samples

3) MC_w: Moisture content on a wet basis

Focusing on the oven-dry weights shown in **Table 2-2** again, they had a *COV* of about 9% and 16% for the samples within 3 days and on 1 month after disposal, respectively. Although the reason for the difference of *COV* between the two sample groups is not clear, these variation means that the degree of wood decay varies to some extent from sample to sample. This suggests that there will be a concern of density variation when using as a block material shown in **Fig. 2-2**, while it is not a big problem when using as boiler fuel.

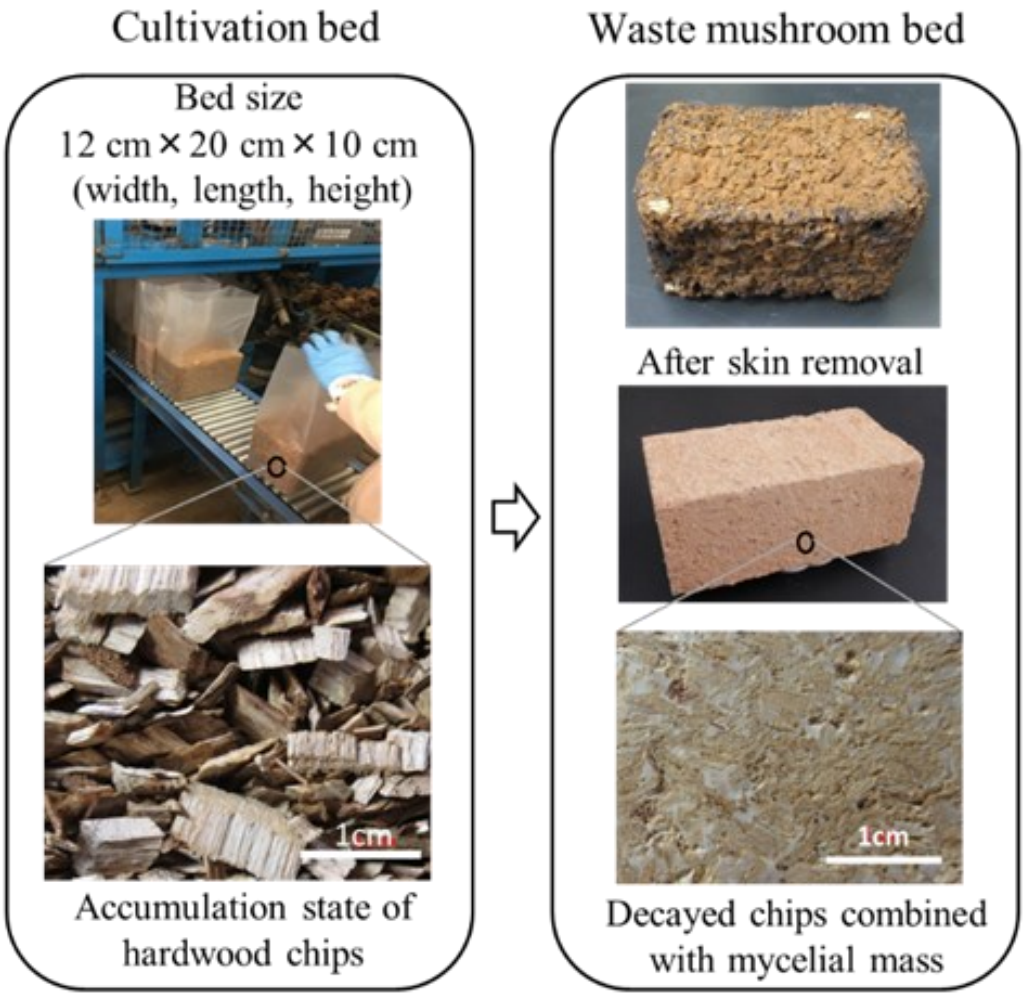

Figure 2-2　　Changes in the structure of a mushroom bed

3.2 Ash contents and elemental composition

Figure 2-3 shows the results of the ash content tests. The raw wood showed a value of about 0.7%, which is close to the values reported [2-3] for live oak (0.6%) and black oak (0.5%). Conversely, the ash content of WMB was about 7%, which is 10 times the value of raw wood. There was no significant difference in ash contents between the inside and the skin, and the mean ash content became 6.78% when the law of mixing was applied assuming a weight ratio of inside to skin of 10:1. The WMB is a mixture of decayed wood residues and mycelium. The ash content of the mycelium itself was 3.4%, while that of the WMB was about double. The reason for this is considered to result from the nutrients added to the raw wood during the cultivation bed preparation. The ash content of nutritional supplements is as high as 4–8% (details will be described later). During shiitake cultivation, the elements that make up the ash move to some extent in the fruit bodies that are repeatedly harvested, and they are lost in small amounts by elution into supplemental water. Except for these two systems, the ash constituent elements remain in the mushroom bed, and it is considered that the ash content is concentrated due to the decrease in the overall weight due to biodegradation. The high ash contents of the WMB measured in this study are comparable to those of hardwood bark. For example, Kofujita [2-4] reported that the ash contents of mizunara (*Quercus crispula*) bark and buna (*Fagus crenata*) bark were 5.7% and 7.3%, respectively. The disadvantage of using bark as a boiler fuel is the high ash content compared to wood chips [2-5]. When using the WMB as fuel, the treatment of ash will be necessary, as with bark.

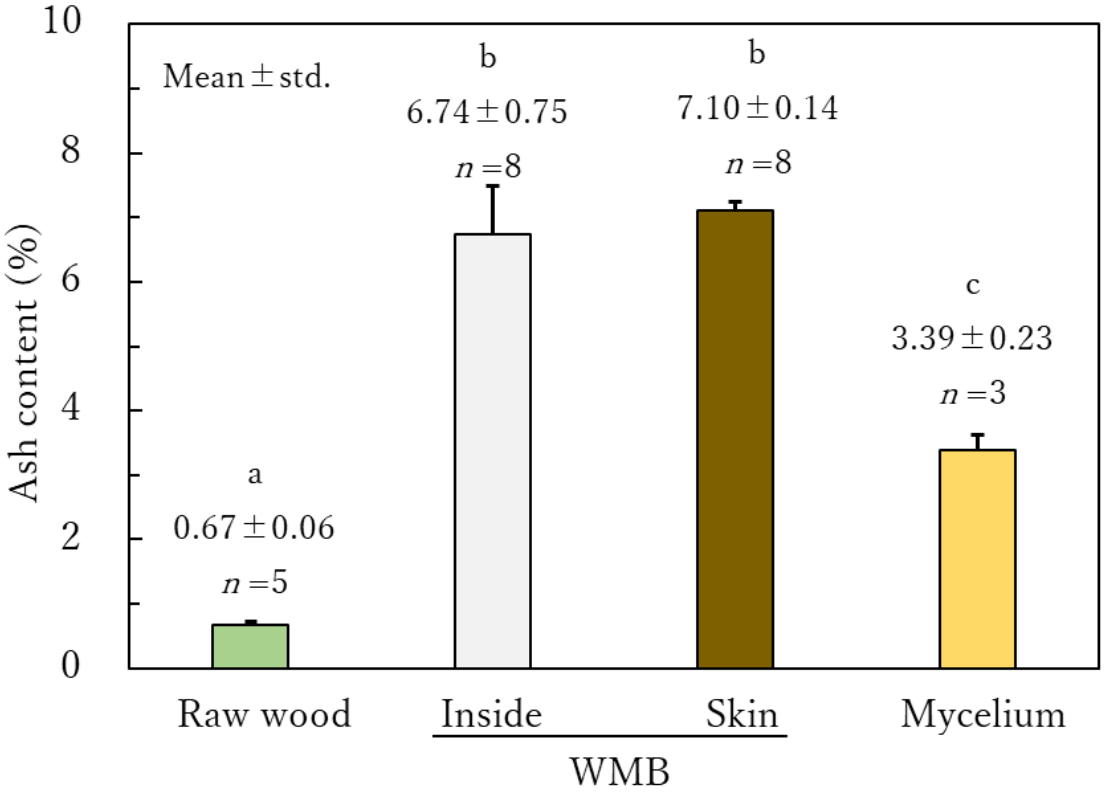

Figure 2-3　Results of the ash content tests

Means with different letters are significantly different at $P = 0.05$

Table 2-3 lists the results of the elemental analysis. The air-dry base contents of C, H, and N of each sample are shown together with their MC_d values. These values were converted to oven-dry base values using the formulas shown below the table. Here, a simple moisture correction was done for C and N (only for mycelium), and in addition to this, bound water was deducted for H. Furthermore, the content of oxygen (O) was obtained by subtracting the sum of these three elements and ash from the entire system. The values for the whole WMB in Table 2-3 were calculated from the law of mixing, assuming a weight ratio of inside to skin of 10:1. The C, H, and O contents of the WMB (whole) were slightly lower than those of the raw wood. This is thought to be due to the higher ash content than that of raw wood as discussed above. Conversely, the nitrogen content was about four times greater in the WMB. This is because the nitrogen content of the skin is about 10 times that of raw wood, in addition to the high nitrogen content inside of the WMB. It is considered that the high nitrogen content of the skin is due to the inclusion of a dark brown melanin pigment. The formation of the melanin pigment is believed to occur, because mycelium protects its territory from other bacteria and prevents water loss [2-6].

These elemental composition data will be used later in the discussion of calorific value and in the calculation of the substance flow during shiitake mushroom bed cultivation.

Table 2-3 Results[1] of the elemental analysis

		Air-dry-base content (%)				Oven-dry-base content[2] (%)			
		MC_d[3]	C	H	N	C	H	N	O
Raw wood		9.2	44.68 (0.33)	5.96 (0.02)	-	48.79 (0.36)	5.49 (0.02)	0.16 (0.02)	44.89 (0.38)
WMB	Inside	9.4	40.98 (0.46)	5.62 (0.06)	-	44.84 (0.50)	5.10 (0.06)	0.53 (0.02)	42.79 (0.55)
	Skin	13.6	40.70 (0.28)	5.30 (0.01)	-	46.24 (0.31)	4.51 (0.01)	1.57 (0.01)	40.59 (0.32)
	Whole	-	-	-	-	44.94	5.05	0.62	42.60
Mycelium		9.7	41.41 (0.06)	6.39 (0.03)	2.07 (0.09)	45.41 (0.07)	5.93 (0.03)	2.27 (0.09)	42.99 (0.20)

1) Data are shown as a mean of 3 replicate tests; values in parenthesis show standard deviations.

2) Oven-dry-base $C(\%) = C(\%) \times (100+MC_d)/100$

$$H(\%) = H'(\%) \times (100+MC_d)/100 - MC_d \times 2/18$$

$$N(\%) = N'(\%) \times (100+MC_d)/100$$

$$O(\%) = 100 - (C(\%) + H(\%) + N(\%) + \text{Ash content (\%)})$$

where, $C'(\%)$, $H'(\%)$, and $N'(\%)$ are the air-dry-base carbon, hydrogen and nitrogen percentages, respectively.

3) MC_d: dry-base moisture content

3.3 Calorific values

The results of calorific value tests are as follows: H_h (mean ± std.) and MC_w for the raw wood was 18.08 ± 0.28 MJ/kg and 7.9%, respectively; 17.55 ± 0.36 MJ/kg and 7.3% for the inside of the WMB, respectively; 15.54 ± 0.65 MJ/kg and 11.1% for the skin of the WMB, respectively; and 16.40 ± 0.02 MJ/kg and 9.2% for the mycelium, respectively. To compare the gross calorific values on a dry basis (H_{ho}) among the samples, these H_h values were converted to H_{ho} using the following **Eq. (2-1)**:

$$H_{ho} = \frac{H_h \times 100}{100 - MC_w} \tag{2-1}$$

Figure 2-4 compares the H_{ho} values among the samples. The H_{ho} value of oak wood [2-7] was reported to be 18.4 MJ/kg to 22.1 MJ/kg, therefore the H_{ho} value of the raw wood (19.63 MJ/kg) obtained in this chapter is reasonable. Although the H_{ho} value of the inside of the WMB was not significantly reduced compared to the raw wood, that of the skin was about 11% lower than that of the raw wood. Assuming a weight ratio of the inside to skin of 10:1, the H_{ho} value for the whole WMB is calculated to be 18.81 MJ/kg from the law of mixing, which was 4–5% lower compared to the raw wood. Focusing on the H_{ho} value of the mycelium (18.06 MJ/kg), this value was 8% lower compared to the raw wood and had no significant difference compared to both the inside and the skin of the WMB. This result suggests that the presence of mycelia is not the main factor that reduces the H_{ho} of the WMB.

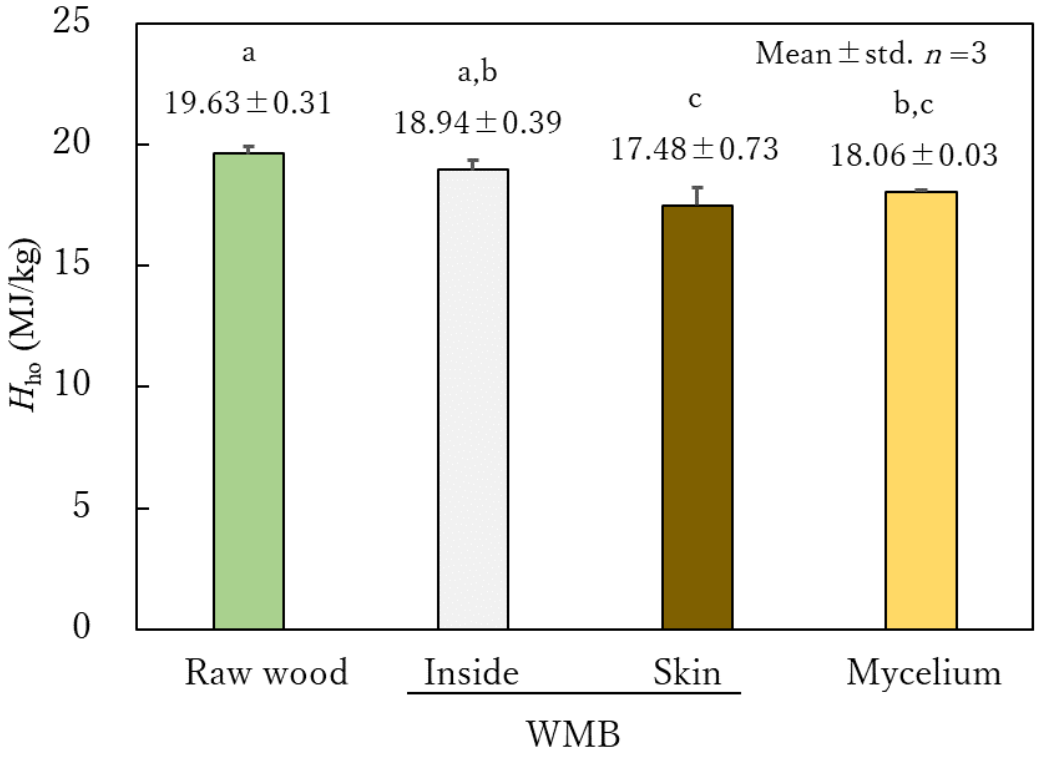

Figure 2-4　Gross calorific values on a dry basis (H_{ho})

Means with different letters are significantly different at $P = 0.05$

Generally, the calorific value of a woody biomass fuel is affected by the amount of ash. Also, nitrogen in fuel does not contribute to heat generation. Therefore, the correction values (H_{ho}') of the H_{ho} values excluding ash and nitrogen were calculated using the following **Eq. (2-2)**:

$$H_{ho'} = \frac{H_{ho} \times 100}{100 - \text{Ash content}\,(\%) - N(\%)} \qquad (2\text{-}2)$$

Substituting the ash content (%) shown in **Fig. 2-3** and N(%) shown in **Table 2-3** into the **Eq. (2-2)**, the values of $H_{ho'}$ for the raw wood, inside of the WMB, skin of the WMB, and mycelium were determined to be 19.79 MJ/kg (100%), 20.42 MJ/kg (103%), 19.14 MJ/kg (97%), and 19.15 MJ/kg (97%), respectively. Here, the value in parentheses is the ratio to the value of the raw wood. Compared to the differences among the samples shown in **Fig. 2-4**, the differences in the correction values were smaller. From this analysis, it was found that the differences in H_{ho} among the samples were due to the amounts of ash and nitrogen.

The calorific value of a fuel is the sum of the combustion heat values of the combustible components, and the H_{ho} value of wood and bark can be estimated by **Eq. (2-3)** in general [2-8].

$$H_{ho} = 33.94\,C + 142.5\,(H - \frac{O}{8}) \qquad (2\text{-}3)$$

Here, C, H, and O are the weights (kg) of carbon, hydrogen, and oxygen contained in 1 kg of oven dry fuel, respectively. The variable ($H - O/8$) of the second term is called the "effective hydrogen" of the system. The oxygen contained in the fuel is not used as oxygen for combustion, and usually a portion of the hydrogen is combined with this oxygen to form bound water. Therefore, the amount of hydrogen contained in the bound water (H_2:O=2: 16=1:8), that is, $O/8$, is subtracted

from the amount of contained hydrogen. The values of $H-O/8$ using the results shown in **Table 2-3** for the raw wood, the inside of the WMB, the skin, and the mycelium were –0.0015 kg, –0.0025 kg, –0.0056 kg, and 0.0056 kg, respectively. From these results, it was found that there was no effective hydrogen other than the mycelium and that the heat generated by the effective hydrogen in the mycelium was only 0.8 MJ/kg. In other words, the mycelium can be expected to generate a small amount of heat from hydrogen, while the other three are all from carbon. The calculated values of H_{ho} according to **Eq. (2-3)** are 16.56 MJ/kg (84%), 15.22 MJ/kg (80%), 15.69 MJ/kg (90%), and 16.21 MJ/kg (90%) for the raw wood, the inside of the WMB, the skin of the WMB, and the mycelium, respectively. Here, the values in parentheses are the ratios to the measured values shown in **Fig. 2-4**. The values calculated by **Eq. (2-3)** were underestimated by up to 16% of the actual measured value. A similar underestimation was observed when applying **Eq. (2-3)** to coniferous bark and wood [2-5]. Although **Eq. (2-3)** underestimates the measurements, it can clarify the properties of woody biomass fuels in which the presence of oxygen reduces the available hydrogen for combustion.

The gross calorific values obtained on a dry basis, H_{ho}, which have been discussed so far, are a basic indicator of calorific value. The gross calorific value at a MC of MC_w (%) is shown using **Eq. (2-4)**, which is a modification of **Eq. (2-1)**. These calorific values include the latent heat of condensation (H_s) of water vapor because the water vapor generated by combustion cannot escape outside of the bomb calorimeter. Usually, in boiler combustion, water vapor in exhaust gas is diffused into the atmosphere without being condensed. Therefore, the amount of heat that can be used is called the net calorific value (H_n), and this is the value obtained by subtracting H_s from H_h (**Eq. (2-6)**). The value of H_s can be calculated from **Eq. (2-5)** [2-5, 2-8]. Here, h is the weight ratio of hydrogen in the fuel. For example, from **Table 2-3**, the value of h in the WMB (whole) is 5.05%

at a MC_w of 0% and 2.53% at a MC_w of 50%.

$$H_h = \frac{H_{ho}\,(100 - MC_w)}{100} \qquad (2\text{-}4)$$

$$H_s = \frac{2.512\,(9 \times h + MC_w)}{100} \qquad (2\text{-}5)$$

$$H_n = H_h - H_s \qquad (2\text{-}6)$$

Figure 2-5 shows the relationship between H_n and MC_w. It was found that the H_n of the WMBs was 4–5% lower than that of the raw wood in any MC range. The WMBs will generate an H_n of 7.6 MJ/kg when they are dried up to about an MC_w of 50%. This value is almost the same as the H_n of general woody biomass fuel. For example, H_n values at a MC_w of 50% have been reported to be 7.5 MJ/kg and 8.0 MJ/kg for sapwood and bark of sugi (*Cryptomeria Japonica*), respectively [2-5].

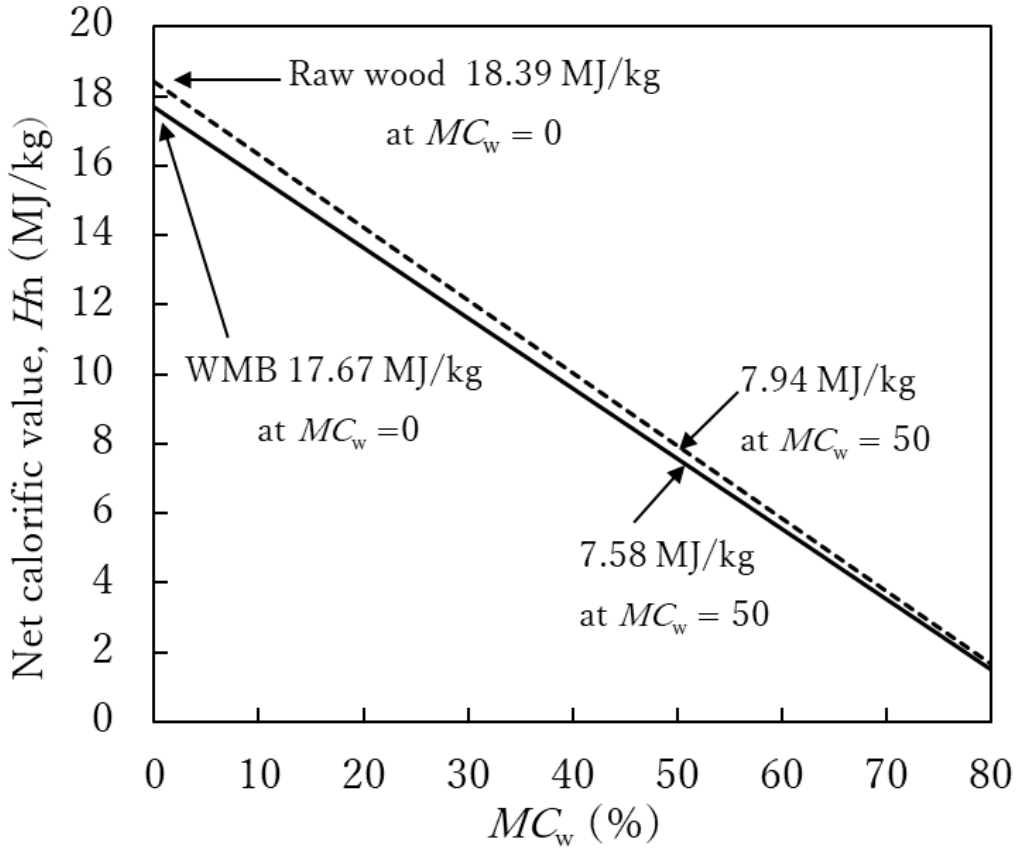

Figure 2-5 Relationships between MC_w and the net calorific value for both the WMB (whole) and the raw wood

3.4 Substance flow during Shiitake mushroom bed cultivation

In this section, we discuss the substance flow during the shiitake cultivation by comparing the weight composition of the cultivation bed at the time of preparation and at the time of disposal.

First, the weight composition of one cultivation bed was determined using the following procedure (the results are shown in **Table 2-4**). In Step 2 of **Fig. 1-2**, raw wood with a volume of 6 m^3 and 310 kg of nutrients (90 kg of rice bran and 220 kg of wheat bran) are placed into the mixer, and water is added to adjust the MC_w to 60%. From this batch, 1080 cultivation beds are made. Therefore, the weight of one batch in the mixer become 3105 kg, because the mean weight of one cultivation bed is 2875 g when the forming bag is deducted (see **Table 2-1**). Because the MC_w is 60%, the moisture weight is 1863 kg, and thus, the total oven-dry weight of the chips and nutrients is 1242 kg. To divide this oven-dry weight into raw wood and nutrients, the oven-dry weight of the nutrients is calculated via the following calculation. If the MC_w values of rice bran and wheat bran are 10.3% [2-9] and 13.4% [2-10], respectively, the oven-dry weights are calculated to be 80.7 kg and 190.5 kg, respectively. Therefore, the oven-dry weight of the raw wood is 970.8 kg. When these values are divided by the number of cultivation beds (1080), the weight composition per cultivation bed is obtained as follows: moisture: 1725 g; raw wood oven-dry weight: 898.9 g; rice bran oven-dry weight: 74.8 g; and wheat bran oven-dry weight: 176.4 g. Also, because the mean weight of the inoculum is 11.5 g, if the MC_w of the inoculum is equivalent to that of the shiitake fruiting body (90.3%) [2-9], the oven-dry weight of the inoculum becomes 1.12 g. Summing these values together, the oven-dry weight of the cultivation bed becomes 1151.2 g.

Table 2-4 Weight composition of the cultivation bed

Components	Weight per mixer batch (kg)	Weight per bed (g)
Water	1863	1725
—The values below are oven-dry weight—		
Raw wood	970.8	898.9
Rice bran	80.7	74.8
Wheat bran	190.5	176.4
Inoculum	–	1.12 (Total: 1151.2)

Next, the weights of the four elements (C, H, N, and O) and ash constituting one cultivation bed in an oven-dry state (1151.2 g) were determined by the following procedure. First, the composition ratios of C, H, N, O, and ash for raw wood, rice bran, wheat bran, and inoculum used in the calculation are shown in the upper half of **Table 2-5**. Here, the values for the raw wood and inoculum are the same as those shown in **Table 2-3** and **Fig. 2-3**, and the values of the rice bran and wheat bran were obtained from literature [2-11, 2-12]. Second, the weights of the four elements and the ash in each component are calculated by multiplying their oven-dry weight by the composition ratio, and then the total weights of each element and ash are calculated (see the lower half of **Table 2-5**). This calculation revealed that the ratio of elements to the oven-dry weight of the cultivation bed was 48.4% for carbon, 5.7% for hydrogen, 0.6% for nitrogen, 43.6% for oxygen, and 1.7% for ash.

The weights of the four elements (C, H, N, O) and ash in one WMB are determined. They were calculated by multiplying the mean oven-dry weight (249.1 g; within 3 days after disposal, see **Table 2-2**) by their composition ratio (whole bed) shown in **Table 2-3** and an ash content of 6.78%. **Table 2-6** compares the calculation results with the values of the cultivation bed, also shows the values calculated from the total yield of the fruiting bodies. Because the yield of shiitake mushrooms per bed is 913 g, if its MC_w is 90.3% [2-9], the oven-dry weight will be 88.6 g. The weights of the four elements (C, H, N, and O) and ash in this dry weight were calculated from the ratios of the inoculum shown in **Table 2-5**.

Table 2-5 Elemental weight composition of an oven-dry cultivation bed

Components	C	H	N	O	Ash	Total
			—Ratios used for the calculation (%)—			
Raw wood	48.79	5.49	0.16	44.89	0.67	100.0
Rice bran	48.10	6.98	2.63	34.39	7.90	100.0
Wheat bran	46.30	5.98	2.26	41.16	4.30	100.0
Inoculum	45.41	5.93	2.27	42.99	3.39	100.0
			—Weight (g)—			
Raw wood	438.6	49.3	1.4	403.5	6.1	898.9
Rice bran	36.0	5.2	2.0	25.7	5.9	74.8
Wheat bran	81.7	10.5	4.0	72.6	7.6	176.4
Inoculum	0.50	0.07	0.03	0.48	0.04	1.12
Total[1)]	556.8	65.1	7.4	502.3	19.6	1151.2
	(48.4%)	(5.7%)	(0.6%)	(43.6%)	(1.7%)	(100%)

1) Values in parentheses are a percentage of the total weight

Table 2-6　Comparison of the elemental weight composition between the cultivation bed and WMB in an oven-dry base

	C	H	N	O	Ash	Total
Cultivation bed [a] (g)	556.8	65.1	7.4	502.3	19.6	1151.2
WMB [b] (g)	112.0	12.6	1.5	106.1	16.9	249.1
Weight loss $(1-b/a)\times 100$ (%)	79.9	80.6	79.7	78.9	13.8	78.4
Shiitake mushroom[1)] (g)	40.2	5.3	2.0	38.1	3.0	88.6

1)　Sum of six repeated harvests from one cultivation bed

From **Table 2-6**, the following can be observed regarding the substance flow in shiitake mushroom bed cultivation. First, there was a weight loss of about 78% from a cultivation bed weight of 1151 g to a WMB weight of 249 g. This loss is mainly due to mycelium respiration and proliferation, fruiting body formation, and repeated fruiting body harvesting. In addition, it is considered that some of the amino acids were leached out and moved to wastewater due to the watering operation during cultivation. Second, the weight losses of the four elements C, H, N, and O were in the range of 79–81% and were close to each other. One of the reasons for this is considered to be that shiitake mushrooms are white-rot fungi, and they attack all of the chemical constituents of the cell wall [2-13]. In other words, because lignin has a higher carbon content than cellulose and hemicellulose [2-5], it is considered that the carbon residual rate increases when lignin cannot be decomposed. To discuss the changes in these four elements in detail, it will be necessary to examine the changes in the major chemical components of wood before and after decay. Third, the weight loss of ash was about 14%, which was significantly lower than that of the four elements. As already mentioned in the section pertaining to the ash results, the ash was concentrated throughout a cultivation from 1.7% ash in the cultivation bed (**Table 2-5**) to 6.8% ash in the WMB. The fourth is the movement of nitrogen. Of the 7.4 g of nitrogen contained in the cultivation bed, 1.5 g remained in the WMB, and 2.0 g was transferred to the fruiting bodies. Therefore, it is considered that a difference of 3.9 g was leached as various amino acids into supplemental water during cultivation. Finally, we focus on the C/N ratio of the WMB. Itoh [2-10] reported that the yield was maximized when the C/N ratio of the shiitake cultivation bed was 70–80. When the C/N ratio was calculated using the values shown in **Table 2-6**, it was about 75 for both the cultivation bed and WMB. This result suggests the possibility that the WMB can be mixed with the cultivation bed and reused.

4. Conclusions

The findings obtained from this work are summarized as follows:

(1) The shiitake mushroom bed at the time of disposal contained about 3.8 times the oven-dry weight of moisture, and even after 1 month of natural drying, it contained about 1.8 times the oven-dry weight of moisture. The slow drying is presumed to be due to the low moisture permeability of the skin of the WMB. Therefore, it is necessary to crush the WMB and then dry it before using it as a boiler fuel.

(2) The ash content of the WMB was about 7%, which was close to that of bark and about 10 times that of the wood used for the cultivation bed. When the WMB is used as a boiler fuel, appropriate ash treatment is required as in the case of using bark.

(3) The gross calorific value on a dry basis (H_{ho}) inside of the WMB was 18.9 MJ/kg, which was not significantly lower than that of cultivation bed raw wood. However, the H_{ho} of the skin of the WMB was significantly lower by 11% than that of the cultivation bed raw wood because of its higher ash and nitrogen contents. As a result, the H_{ho} of the whole WMB was 18.8 MJ/kg, which was 4–5% lower than that of the cultivation bed raw wood. The H_{ho} of mycelium itself was 18.1 MJ/kg, which was significantly lower by 8% than that of the cultivation bed raw wood due to its significantly higher nitrogen and ash contents. When analyzed considering the combustion heat of the contained elements, it was found that both the cultivation bed raw wood and the WMB had almost no hydrogen contributing to combustion due to the high oxygen content, and they were dependent on the heat generation of carbon.

(4) The relationship between the net calorific value and moisture content on a wet basis (MC_w) was obtained for the WMB. The net calorific value was 4–5% lower than that of the cultivation bed raw wood at any moisture content level, and it was 7.6 MJ/kg at an MC_w of 50%, which was

almost the same as that of sugi (*Cryptomeria Japonica*) sapwood and bark.

(5) Comparing the oven-dry weight of the WMB with that obtained at the time of preparing the cultivation bed, the weight loss was about 78%. The weight losses of the four elements C, H, N, and O were in the range of 79–81% and were close to each other. Conversely, the weight loss of ash was about 14%, which was significantly lower than that of the four elements, such that the ash was concentrated through cultivation from 1.7% in the cultivation bed to 6.8% in the WMB.

CHAPTER THREE

THERMAL CONDUCTIVITY OF COMPRESSION-DRIED WASTE MUSHROOM BEDS

1. Introduction

Natural growing mycelium is attracting attention as a new binder for wood-based molding materials. For example, Grown. bio [3-1] in the Netherlands cultivates mycelium using wood chip pieces and agricultural wastes as a medium in a molding formwork to produce interior goods and packaging, building, and construction materials. The campus benches of the University of British Columbia [3-2] are also made from mycelium and alder sawdust. Furthermore, the fire protection performance [3-3] and sound absorption properties [3-4] of wood-based molding materials are being explored.

However, the structure of the WMB is similar to the wood-based molding materials above. If it can be used as a material, it will help reduce the mushroom industry's waste. In this chapter, we explore the possibility of using the WMBs as insulation material. For example, if the dried WMB is installed under the floor, heat insulation from the ground surface can be expected. When the WMB is dried, the decayed chips are bonded with the mycelia, resulting in a lightweight particleboard (PB) or insulation fiberboard (IFB) structure (**Fig. 1-3**). However, the homogeneous WMBs with small voids between decayed chips were only one-fifth of the total (**Fig. 1-3(A)**). The remaining have scattered or continuous coarse voids unfavorable for thermal insulation due to heat convection (**Fig. 1-3(B) & (C)**). Therefore, this chapter attempts compression-drying to eliminate the coarse voids and use WMBs as much as possible. The WMBs were compressed to various degrees in the height direction, and specimens with various densities were removed to evaluate the thermal

conductivity. Furthermore, the thermal conductivities of wood and wood-based materials with various densities were measured, and the positioning of the thermal insulation performance of compression-dried WMBs was investigated.

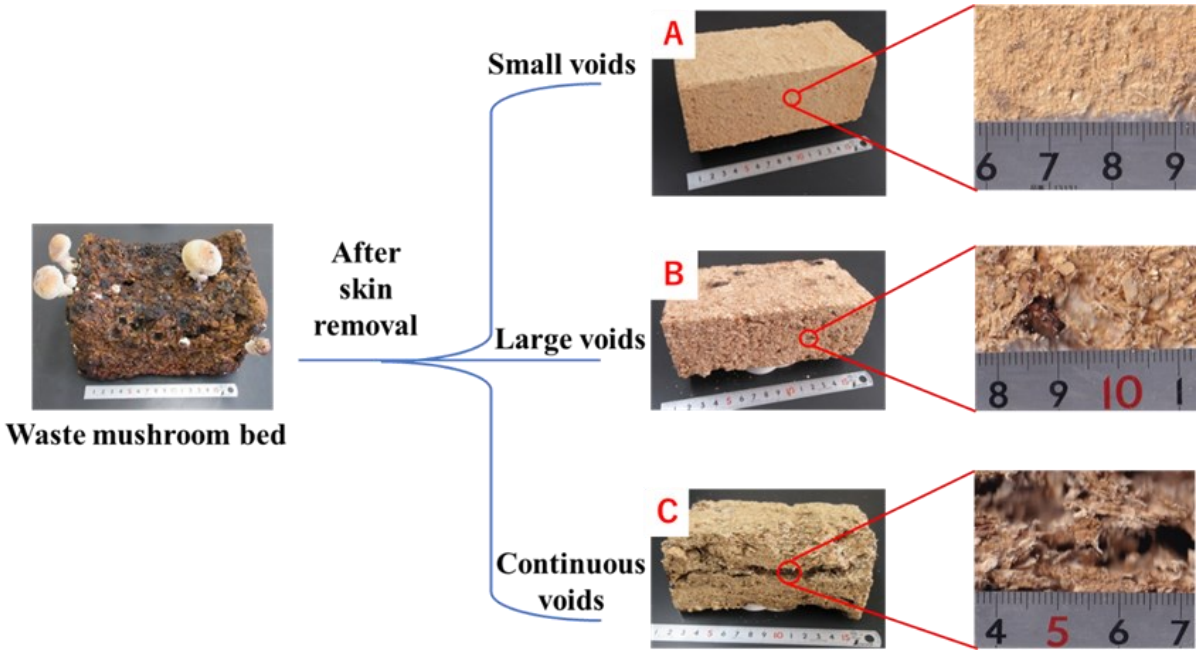

Figure 1 – 3 Three types of voids inside the dried WMB

The thermal insulation performance of a WMB is affected by coarse voids and the thermal conductivity of the WMB substance (a mixture of decayed chip and mycelium), serving as a heat bridge. Therefore, the powder mats' thermal conductivity of the WMB was measured, and a heat-flow model was applied to estimate the thermal conductivity of the heat bridge. Similar estimates were made for raw wood and mycelium. To further investigate whether there is anisotropy in the substance thermal conductivity of the WMB, the substance thermal conductivity along the heat-flow direction was determined using the same heat-flow model.

2. Material and methods

2.1 Preparing waste mushroom beds with various densities

After being harvested five times, one hundred WMBs were collected from the farm shown in **Fig. 1-2**. The WMB's dimensions were approximately 130 mm wide, 210 mm long, and 120 mm high. They were distributed into five groups of 20 per group for equal mean weights. H_{120} was the uncompacted WMB (120 mm high) group, dried at 105 ℃ to an oven-dry state and cured to an air-dry state. The air-dry density distribution of H_{120} from 190–220 kg/m^3 (**Fig. 3-1(a)**). H_{60}, H_{50}, H_{30}, and H_{25} are the WMB groups to be compacted to 60, 50, 30, and 25 mm in height, respectively. **Fig. 3-2** show a 200 kN press installed with formwork bottom dimensions of 130 × 210 mm to compact the WMBs and the cross section of the formwork. The WMBs were heated in a microwave oven to a central temperature of approximately 90 ℃ before being placed in the formwork. After reaching the target height, the formwork's upper and lower plates were fixed with two metal rods for each plate (**Fig. 3-2(d)**), and the compacted WMBs were dried at 105 ℃ to an oven-dry state. Then, they were left in an ordinary experimental room at least for 2 months until they become air-dry state (MC_d: 10–12%). **Figs. 3-1(b)–(e)** show the air-dry density distribution of H_{60}, H_{50}, H_{30}, and H_{25}, respectively. The above compaction operations were used to prepare WMBs with densities from 190–670 kg/m^3.

The inclination angle of the decayed chips with respect to the horizontal plane was measured using the WMB before drying. The height direction of the decayed chip was almost perpendicular to the fiber. One side skin (210 mm long, 120 mm high) was cut off, and the cut surface was photographed at seven compacted heights of 120 (compaction rate: 0%), 110 (8%), 100 (17%), 90 (25%), 80 (33%), 70 (42%), and 60 mm (50%) using a universal testing machine (**Fig. 3-3**). Each photo was analyzed using imaging software (Adobe Photoshop) to obtain 200 inclination angles.

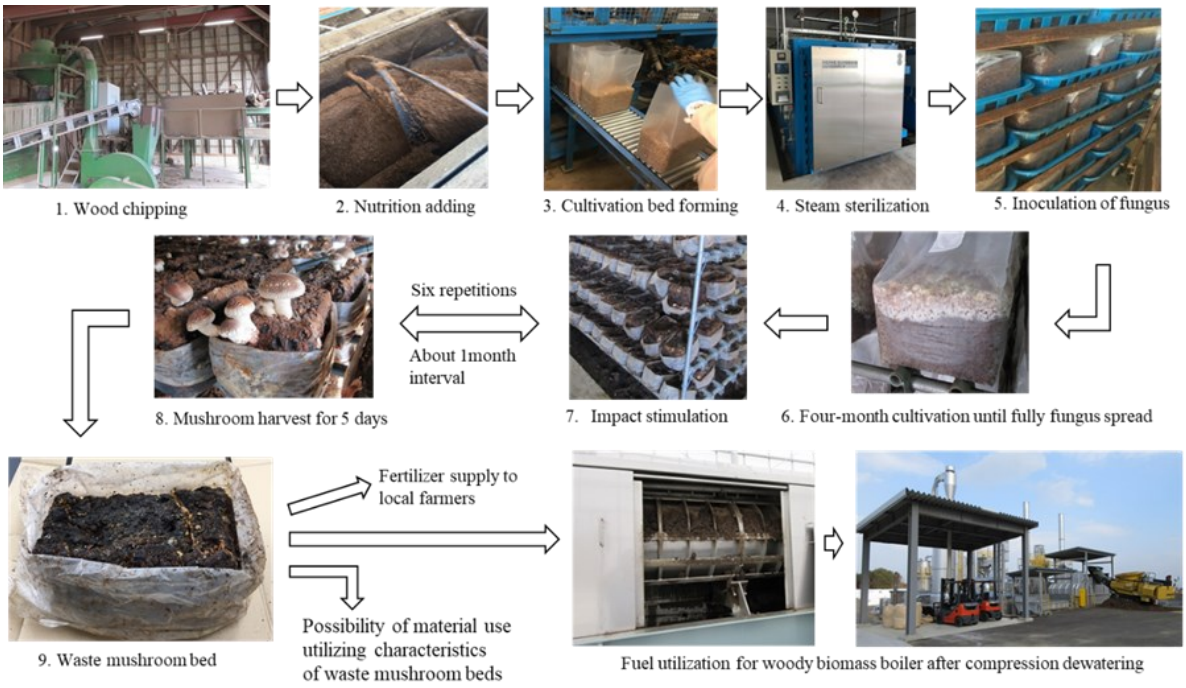

Figure 1 – 2 Production process of Shiitake mushroom using hardwood chip cultivation beds

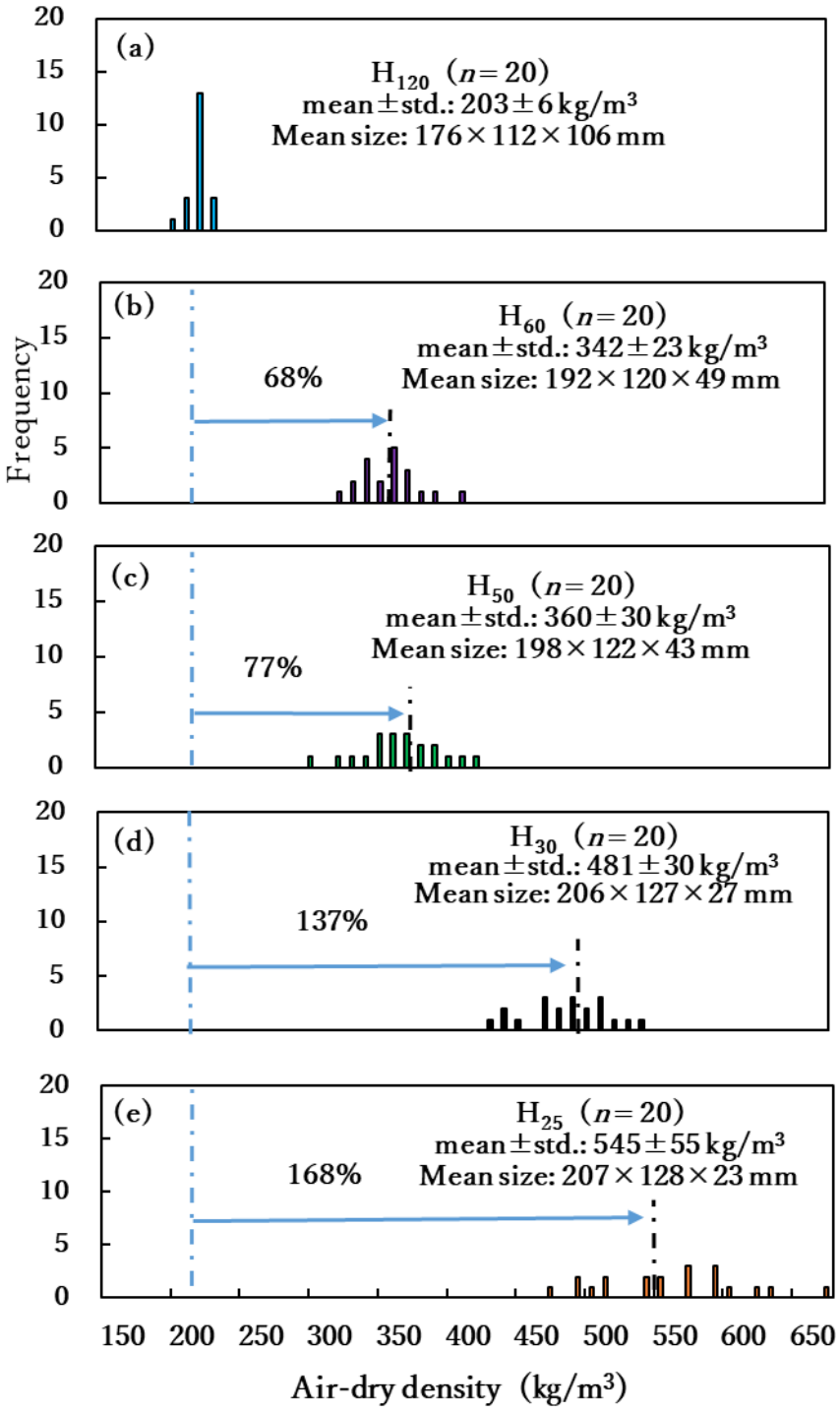

Figure 3-1 Air-dry density distribution of the WMB

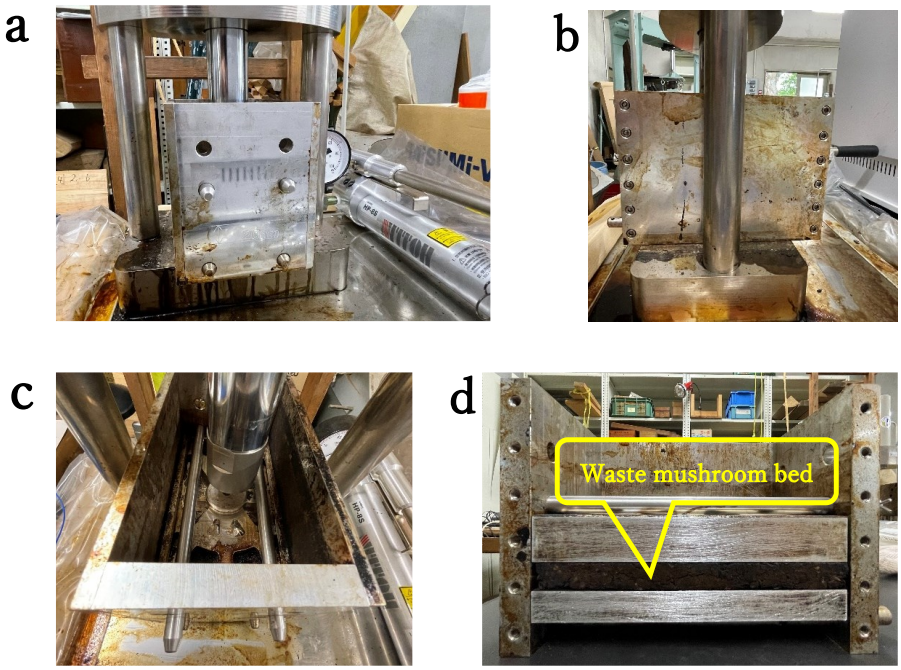

Figure 3-2　Compaction equipment for the WMB

(a: front view, b: side view, c: top view, d: cross section of compression formwork)

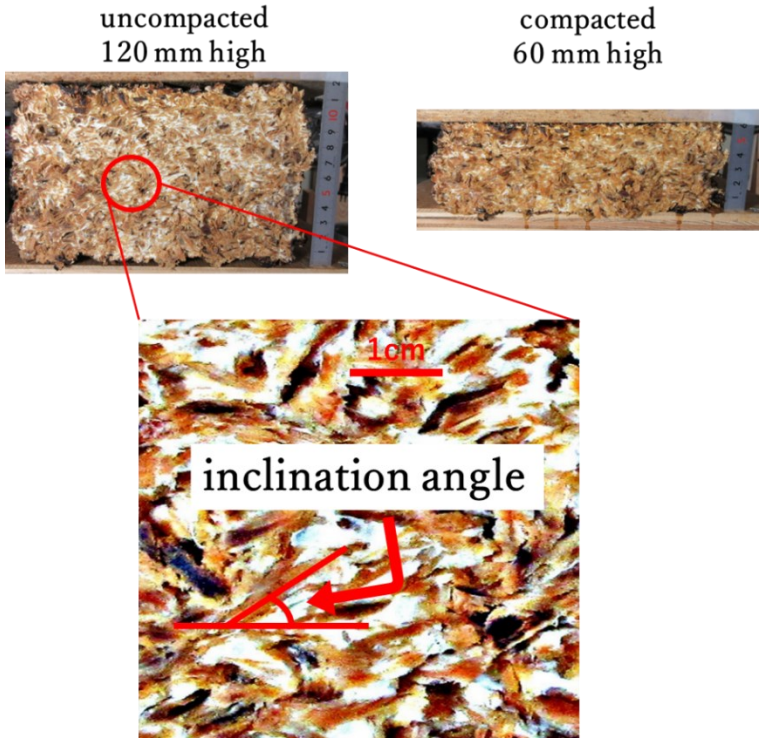

Figure 3-3　Cut surface of the WMB for chip inclination angle measurement

2.2 Wood and wood-based materials for comparison

The following control materials were used: balsa (*Ochroma pyramidale*), kiri (*Paulownia tomentosa*), sugi (*Cryptomeria japonica*), douglas fir (*Pseudotsuga menziesii*), yellow cedar (*Chamaecyparis nootkatensis*), insulation fiberboard (IFB), plywood, medium-density fiberboard (MDF), oriented strand board (OSB), and particleboard (PB). Test specimens of 100 mm wide, 100 mm long, and 12 mm high (perpendicular to the fiber, MC_d: 10–12%) were obtained from the master board for thermal conductivity measurements. **Table 3-1** shows the mean densities and the number of test specimens.

Table 3-1 Wood and wood-based panels for thermal conductivity measurement

Wood			Wood-based panels		
Tree species	Mean density[1] (kg/m^3)	n[2]	Type	Mean density (kg/m^3)	n
balsa	129	2	IFB[3]	269[4], 251[5], 244[6], 354[7]	6[4), 5), 6)], 2[7]
kiri	251	2	plywood	438[8], 618[9]	2[8), 9)]
sugi	347	5	MDF	622	2
douglas fir.	447	9	OSB	705	2
yellow cedar	536	2	PB	811	2

1) Moisture content: 10–12% 2) n: the number of test specimens 3) Insulation fiberboard
4) T-Class IFB: 12 mm high 5) T-Class IFB: 15 mm high 6) T-Class IFB: 20 mm high
7) Sheathing IFB 8) Lauan plywood 9) Softwood plywood

2.3 Measuring thermal conductivity

Thermal conductivity was measured using the comparison method with a standard plate [3-5] (JIS A 1412-2: 1999). In this method, the test specimen and standard plate are overlapped and placed between the upper high-temperature plate and the lower low-temperature plate. When the vertical downward heat-flow reaches a steady state, the test specimen's thermal conductivity (λ) can be calculated using **Eq. (3-1)**.

$$\lambda = \lambda_0 \times \frac{\triangle\theta_0}{d_0} \times \frac{d}{\triangle\theta} \qquad (3\text{-}1)$$

where λ_0, $\triangle\theta_0$, and d_0 are the thermal conductivity, the temperature difference between upper and lower surfaces, and the height of the standard plate, respectively. d and $\triangle\theta$ are the test specimen's height and the temperature difference between its upper and lower surfaces, respectively. The standard plate used was glass wool with a known thermal conductivity and was certified by the US National Institute of Standards and Technology (NIST, SRM1450d). Its height and air-dry density were 25.2 mm and 118 kg/m^3, respectively. The temperatures of the upper and lower plates were 40 ℃ and 20 ℃, respectively. The mean temperature of the specimens ranged from 24–26 ℃. Measurements were taken twice on one test specimen by reversing the upper and lower surfaces.

Test specimens with dimensions of 100 mm wide, 100 mm long, and 12 mm high were obtained from the WMB groups of H_{120}, H_{60}, H_{50}, H_{30}, and H_{25} to allow for various densities (MC_d: 10–12%). **Table 3-2** shows the number of test specimens and the mean densities. The test specimen's height direction is the same as the WMBs.

Table 3-2 Densities of the WMB for thermal conductivity measurement

	H_{120}	H_{60}	H_{50}	H_{30}	H_{25}
Density[1] (kg/m^3) (mean ± std.[2])	208 ± 42	287 ± 32	328 ± 54	408 ± 53	483 ± 65
The number of specimens	12	11	11	13	10

1) Moisture content: 10–12% 2) std.: standard deviation

2.4 A heat-flow model for predicting substance thermal conductivity

The series–parallel heat-flow model comprising two elements, substances (cell wall, heat bridge), and voids (intracellular pore) was applied to estimate the thermal conductivity of charcoal [3-6], fiber-based insulation materials [3-7], and PB [3-8] (**Fig. 3-4**). Assume that a single cell is square with a circular inner pore, and because it is symmetric, it can be divided into four equal parts. If the void's ratio is $V(0 < V < 1)$, the substance's ratio is $1 - \sqrt{V}$. In this model, the parallel part of the void is connected in series with the substance, where λ_s indicates the thermal conductivity of the substance. If the thermal conductivity of the parallel part is λ_p, **Eq. (3-2)** is valid because the sum of the thermal resistance of the parallel part $(1 - \sqrt{V})/\lambda_s$ and that of the adjacent part $\sqrt{V}/\lambda_p$ becomes the entire thermal resistance $1/\lambda$. **Equation (3-3)** shows the mixed law based on the ratio of the void and substance and their respective thermal conductivities. **Equation (3-4)** shows the entire model's λ thermal conductivity, obtained by substituting **Eq. (3-3)** into **Eq. (3-2)**.

The void ratio V is obtained from the oven-dry density ρ_{o} and the substance density ρ_{h} using **Eq. (3-5)**—the value in the oven-dry state. The V used in **Eq. (3-4)** is in the air-dry state, so a correction to the air-dry state is necessary (not made in this study).

$$\frac{1}{\lambda} = \frac{1-\sqrt{V}}{\lambda_s} + \frac{\sqrt{V}}{\lambda_p} \qquad (3\text{-}2)$$

$$\lambda_p = \sqrt{V}\,\lambda_a + (1-\sqrt{V})\lambda_s \qquad (3\text{-}3)$$

$$\lambda = \frac{1}{\frac{(1-\sqrt{V})}{\lambda_s} + \frac{\sqrt{V}}{\lambda_p}} = \frac{1}{\frac{(1-\sqrt{V})}{\lambda_s} + \frac{\sqrt{V}}{\sqrt{V}\,\lambda_a + (1-\sqrt{V})\lambda_s}}$$

$$= \frac{\lambda_s\{\sqrt{V}\,\lambda_a + (1-\sqrt{V})\lambda_s\}}{\lambda_s(1+V-\sqrt{V}) + \lambda_a(\sqrt{V}-V)} \qquad (3\text{-}4)$$

$$V = \left(1 - \frac{\rho_o}{\rho_h}\right) \qquad (3\text{-}5)$$

Figure 3-4 A heat-flow model applied to the WMB

2.5 Predicting the substance thermal conductivity

Powder samples were prepared to measure the substance density ρ_h and substance thermal conductivity λ_s using the following procedures. Approximately 500 g chip samples were prepared for the inside from several WMBs, the mycelium, and the raw wood used for the cultivation bed. Because removing only the mycelium from the WMB was challenging, mycelium chip samples were prepared from the stem part of the shiitake fruiting body. First, these three air-dried chip samples were powdered using a Willey mill. Then, they were classified using a three-stage sieve, and the following two fractions were prepared: F4: 0.250–0.355 mm for the λ_s test, and F5: less than 0.150 mm for the ρ_h test. The pycnometer method [3-9] was used to determine the ρ_h. Ten measurements were conducted on each sample using a 50 ml pycnometer. The test results were as follows: WMB: 1.622 g/cm^3, mycelium: 1.550 g/cm^3, and raw wood: 1.569 g/cm^3 (see **Table 3-3**).

The λ_s was estimated by measuring the thermal conductivity λ of the powder mats using the comparison method with the standard plate described above. The powder mats were prepared with various densities using the F4 powder: 270–400 kg/m^3 for the WMBs (n = 28), 290–445 kg/m^3 for the mycelium (n = 25), and 320–460 kg/m^3 for the raw wood (n = 25). The mats were prepared over various densities to examine whether the voids between the powders could be treated as static air. The mats were hand-formed in formwork with internal dimensions of 100 mm wide, 100 mm long, and 12 mm high. The mean mat MC_d was 8.1%, 7.9%, and 9.0% for the WMB, the mycelium, and the raw wood, respectively.

Once the powder mat's λ was obtained, the λ_s was estimated from the heat-flow model shown above. Because the wood λ_s is anisotropic and the powders in the mat are randomly oriented, the λ obtained using this method can be the mean value of the directions parallel and perpendicular to the fiber. The powder mat of the WMB and mycelium can be considered similarly.

3. Results and discussion

3.1 Thermal conductivity of the heat bridge (substance)

Typically, the thermal conductivity of fiber insulation materials, such as glass wool, takes minimum values regarding their densities [3-10]. At lower densities, the thermal conductivity increases due to heat convection transfer in the voids, and at higher densities, it increases due to increased heat bridges. A similar trend would apply to the results of the powder mat thermal conductivity tests (**Fig. 3-5**). The thermal conductivity (λ_m) of the WMBs and raw wood decreased as the density increased. The results indicate that the mat's air voids can be treated as static air at approximately 400 kg/m^3 for the WMB and 450 kg/m^3 for the raw wood. However, the λ_m of mycelium showed an increasing trend with the density, indicating that the air voids in the mat can be treated as static air at a density of approximately 300 kg/m^3. Therefore, the mean density ρ_{m} and λ_m used in the model calculations were 399 kg/m^3 and 0.0675 W/mK, 330 kg/m^3 and 0.0712 W/mK, 451 kg/m^3 and 0.0632 W/mK for the WMBs, the mycelium, and the raw wood, respectively. These mean densities were obtained using five data plots, and the λ_m values were obtained from the regression line in **Fig. 3-5**. The λ_s was determined using the following procedure. First, the powder mat's λ was calculated using **Eq. (3-4)**, given an arbitrary value for λ_s. Then, the λ was compared to the λ_m, and the comparison was repeated for the λ calculated with 0.001 W/mK increments of the λ_s. Finally, the optimal λ_s was determined when the λ was closest to the λ_m.

Table 3-3 lists the values used in the model calculations and the optimal λ_s. The λ_s of the WMB was 0.288 W/mK, 1.3 times higher than that of raw wood (0.218 W/mK). The substance of the WMB is a mixture of decay residue of wood substance and mycelium. The λ_s of the WMB is higher than that of raw wood because the mycelium (0.368 W/mK) is 1.7 times higher than that of raw wood. However, further research is needed to determine the λ_s of the decayed chip substance.

Figure 3-5 Relationship between the density and thermal conductivity for the powder mat

Table 3-3　Values used in model calculations and the optimal substance thermal conductivity λ_s

Mat type	Substance density ρ_h			Powder mat			Thermal conductivity (W/mK)		
	Powder sample	n	Mean [1] ± std. [2] (g/cm³)	Powder sample	ρ_m [3] (kg/m³)	V [4] (%)	λ_a [5]	λ_m [6]	λ_s
WMB	F5	10	1.622 [a] ± 0.046	F4	399	75.4	0.026	0.0675	0.288
Mycelium			1.550 [b] ± 0.031		330	78.7		0.0712	0.368
Raw wood			1.569 [a/b] ± 0.076		451	71.3		0.0632	0.218

1) Means with different letters are significantly different at $P = 0.05$ among the three samples

2) std.: standard deviation

3) Air-dry density at which the voids in the mat can be treated as static air ($n = 5$, MC_d: 7.9–9.0%)

4) Values calculated using **Eq. (3-5)**

5) Value corresponding to a specimen temperature of approximately 25 ℃

6) Values on the regression line in **Fig. 3-5**

3.2 Relationship between the density and thermal conductivity

Figure 3-6 shows the relationship between the density and thermal conductivity of the WMB test specimens, where the mean temperatures were 24–26 ℃, and a linear relationship was recognized between the density and thermal conductivity. A closer examination was conducted in **Table 3-4** to investigate the differences in thermal conductivity among the test specimen groups with the same density band. Focusing on the mean density of 259 kg/m^3, the mean thermal conductivity of H_{60} (0.051 W/mK) and H_{50} (0.053 W/mK) was significantly lower by 12% and 9%, respectively, than that of H_{120} (0.058 W/mK). Since the test specimens have the same density, the total amount of voids should be equivalent. Therefore, the decrease in thermal conductivity can be attributed to suppressing the heat convection transfer due to the compression breakup of the coarse voids. However, at the mean densities of 327 kg/m^3 and 426 kg/m^3, no significant difference occurred between H_{50} and H_{30} and between H_{30} and H_{25}, respectively. Therefore, the suppression of heat convection transfer is completed when the WMB is compressed to these densities.

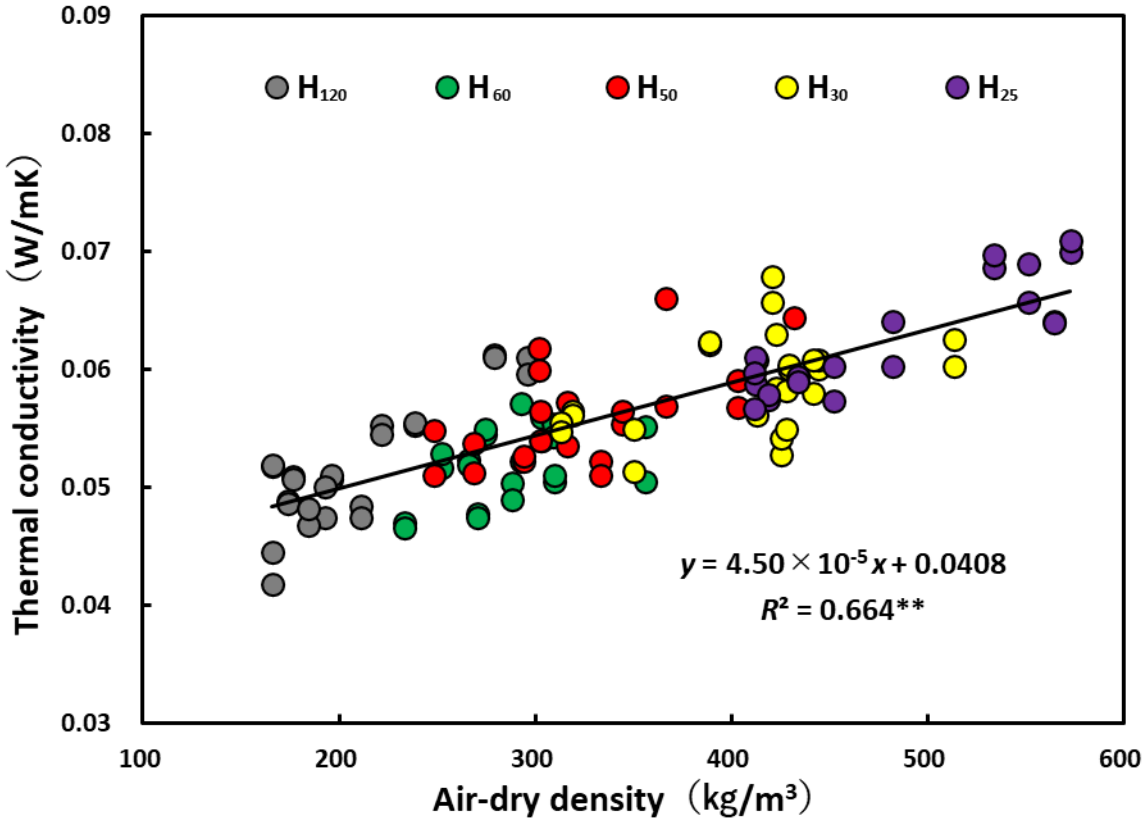

Figure 3-6　Relationship between the density and thermal conductivity of the WMB

Table 3-4 Comparison of the thermal conductivity of WMB with the same density band

WMB	*n*	Density[1] (kg/m^3)		Thermal conductivity (W/mK)
		mean	band	mean[2] ± std.[3]
H_{120}	8	259	222–296	0.058 [a] ±0.003
H_{60}	10		233–275	0.051 [b] ±0.003
H_{50}	4		248–269	0.053 [b] ±0.002
H_{50}	12	327	302–367	0.057±0.004
H_{30}	6		313–350	0.055±0.002
H_{30}	14	426	413–441	0.060±0.004
H_{25}	4		419–433	0.058±0.001

1) Moisture content: 10–12%

2) Means with different letters are significantly different at $P = 0.05$

3) std.: standard deviation

Figure 3-7 shows the relationship between density and thermal conductivity for the comparison materials. Regression equations were obtained from the wood plus plywood group (A) and the wood-based panel group other than plywood (B). The regression line of the WMB (C) was between those of groups (A) and (B). Focusing on the density range of 200–300 kg/m^3, the thermal conductivity of the WMB was greater than that of the IFB. This is because the WMB contains coarser voids than IFB, and heat convection transfer might have affected the thermal conductivity of the WMB. As shown in **Table 3-3**, the thermal conductivity of the heat bridge (substance) was higher for the WMB (0.288 W/mK) than for the wood (0.218 W/mK), which could also be a reason. However, in the density range of 500–600 kg/m^3, the thermal conductivity of the WMB was similar to that of group (B), indicating that most voids inside the WMB were more finely divided. Furthermore, the surface of the WMBs may have a lower heat radiation rate than that of wood due to the large number of small voids inside and the surface is inhomogeneous [3-11]. A lower heat radiation rate would reduce radiative heat transfer, resulting in lower thermal conductivity.

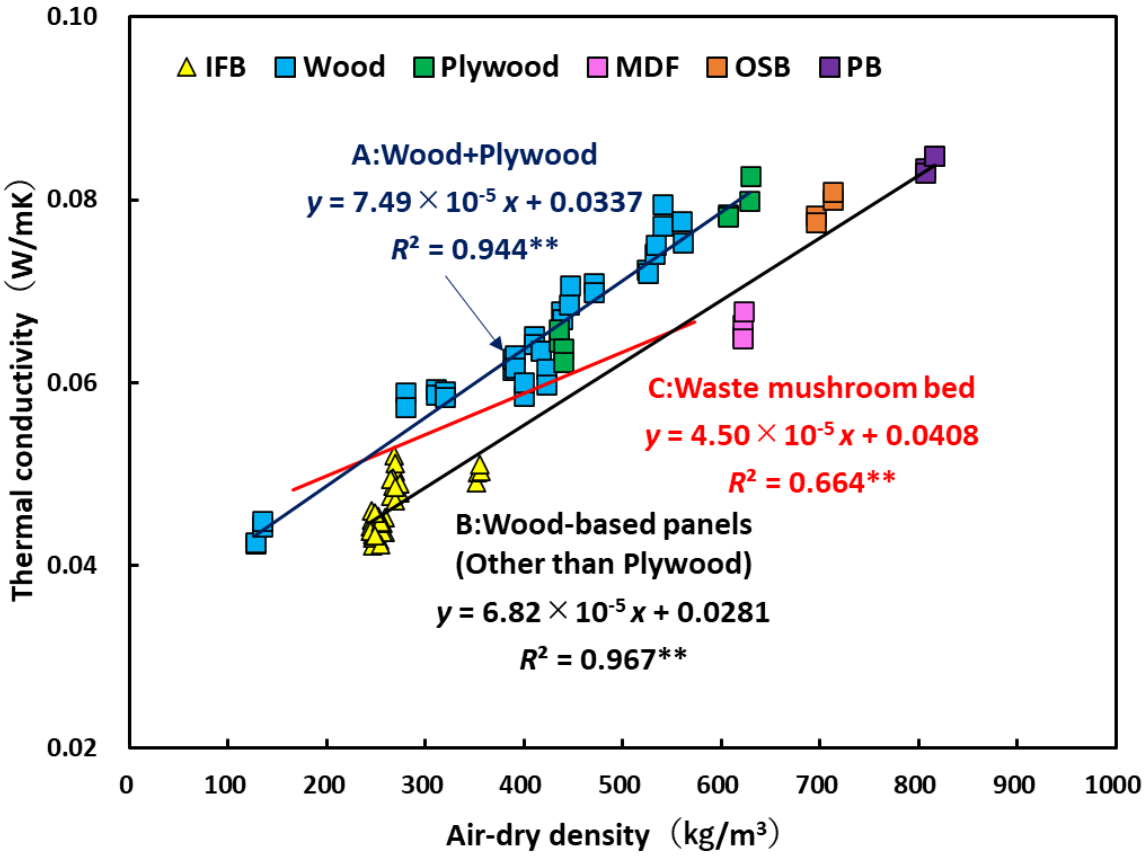

Figure 3-7　Relationship between the density and thermal conductivity for the WMB and comparison materials

3.3 Thermal conductivity of the heat bridge along the heat-flow direction

Figure 3-8 shows the relationship between the compaction degree along the height direction of the WMB and the inclination angle of the decayed chips. The inclination angle decreased as the compaction degree increased. If the WMB substance's thermal conductivity is anisotropy similar to that of the wood substance, i.e., that in the fiber parallel direction is greater than in the fiber perpendicular direction, the smaller the inclination angle, the lower the substance thermal conductivity along the heat-flow direction. The anisotropy in the thermal conductivity of the WMB substance was examined using the heat-flow model (**Eq. (3-4)**) in the following manner.

The substance thermal conductivity along the heat-flow direction of the WMB was determined in the same way as for λ_s described above. However, since the thermal conductivity of the coarse void λ_a depends on the density of the WMB, the λ_a was varied (**Fig. 3-9**). For the WMB with a density of 400 kg/m^3 or higher, λ_a was assumed to be 0.026 W/mK for static air. However, because the λ_a of the WMB with a density of less than 400 kg/m^3 is unknown, this value was changed to increase with the decreasing density. The degree of increase was determined from literature values as follows. Sekino [3-11] et al. reported λ_a of 0.045 W/mK and 0.033 W/mK for wood shaving insulation panels and carbonized wood shaving mats, respectively, with a density of approximately 90 kg/m^3. Therefore, considering that λ_a of the WMB of the same density would be similar to these, three levels were set at a density of 90 kg/m^3 (**Fig. 3-9**): 20% increase in static air (0.031 W/mK), 50% increase (0.039 W/mK), and 80% increase (0.047 W/mK).

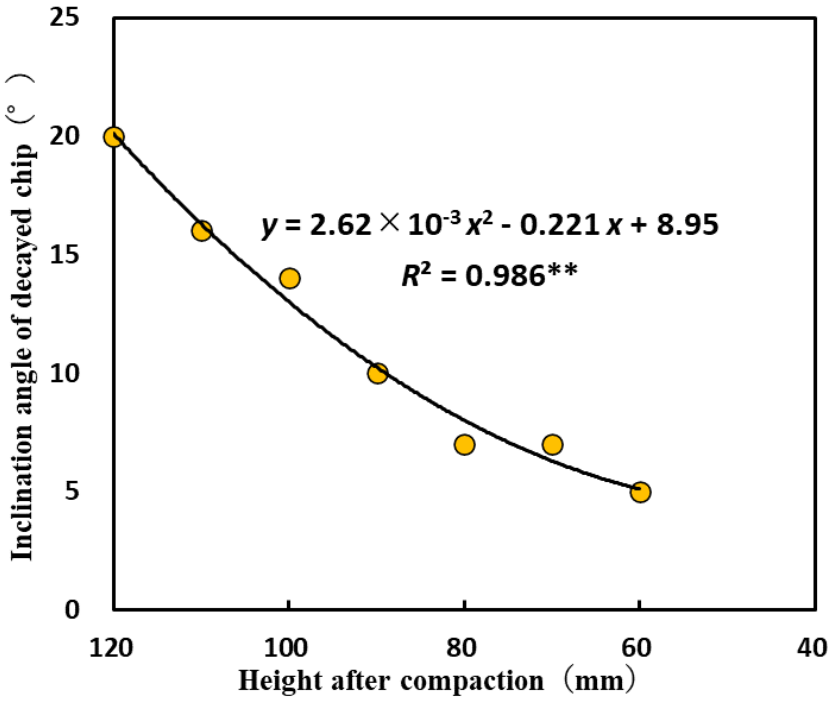

Figure 3-8　Relationship between the height of the WMB after compaction and inclination angle of the decayed chip

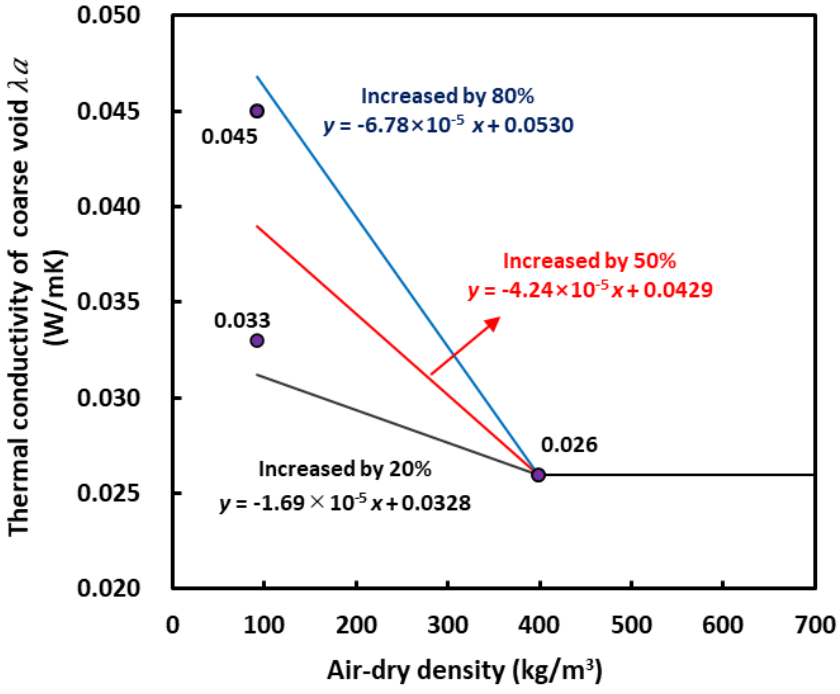

Figure 3-9　Thermal conductivity of the coarse void varying with a WMB density

Figure 3-10 shows the WMB's estimated thermal conductivity along the heat-flow direction. For the density of 400 kg/m^3 or higher, the substance thermal conductivity along the heat-flow direction decreased slightly with the increasing density. The values in the regression equation were 0.227 W/mK, 0.199 W/mK, and 0.196 W/mK for densities of 400 kg/m^3, 500 kg/m^3, and 600 kg/m^3, respectively. This trend is why the slope of the regression equation shown in **Fig. 3-7** is smaller than that of wood. Now, focusing on plots with a density of less than 400 kg/m^3, when λ_a was increased by 80% of static air, many plots appeared with values smaller than 400 kg/m^3 or higher. This result contradicts the hypothesis because the substance thermal conductivity along the heat-flow direction should increase as the decayed chip inclination angle increases with decreasing density. In the case of a 50% increase, values higher than those at a density of 400 kg/m^3 or higher began to appear. Furthermore, for a 20% increase, values higher than those at a density of 400 kg/m^3 or higher appeared. These results indicate that the WMB substance has anisotropic thermal conductivity similar to wood. However, further investigation is required to determine the specific degree of anisotropy of the substance's thermal conductivity.

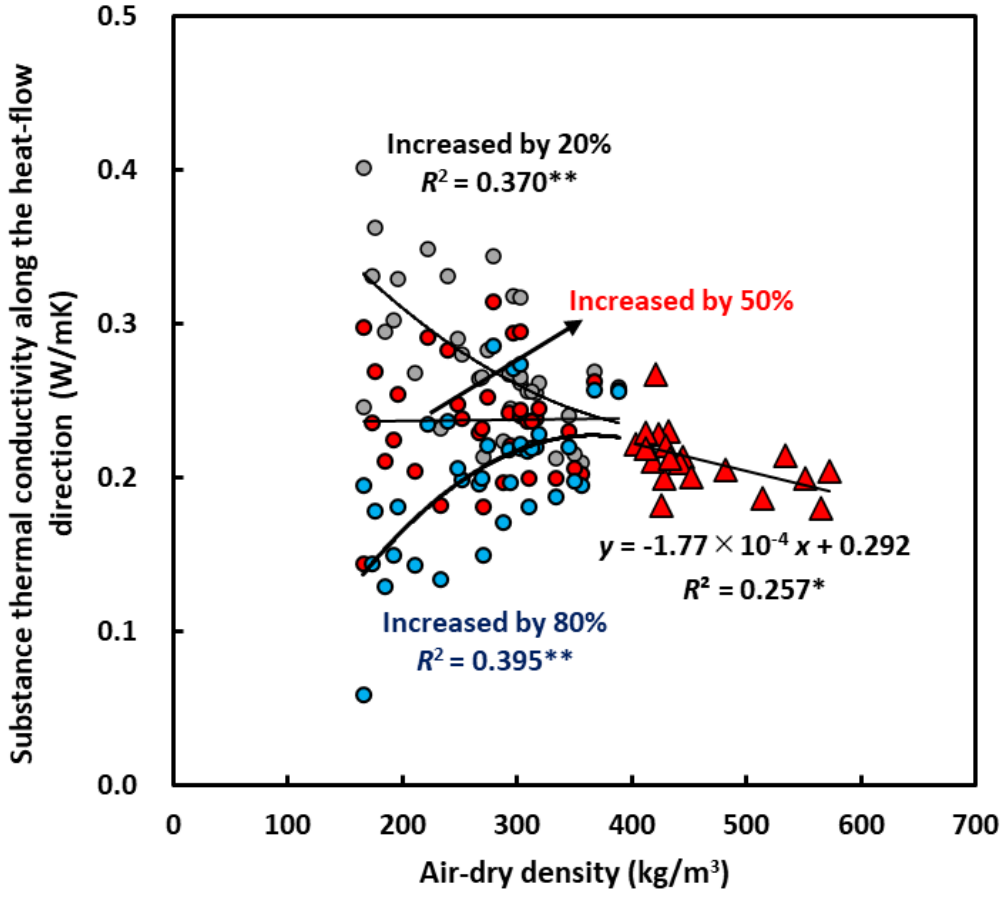

Figure 3-10 WMB's estimated substance thermal conductivity along the heat-flow direction

4. Conclusions

The findings obtained from this work are summarized as follows.

（1） The substance thermal conductivity λ_s of the WMB was 0.288 W/mK, 1.3 times higher than that of raw wood (0.218 W/mK), which could be attributed to the higher λ_s of the mycelium (0.368 W/mK) contained in the WMB substance. However, the λ_s of the decayed chip substance has not been measured in this study and should be investigated in the future.

（2） A linear relationship was recognized between the density and thermal conductivity of the WMB. A closer examination of this relationship revealed a decrease in the thermal conductivity due to compression-drying in the density range of 220–300 kg/m^3, indicating a suppression effect of heat convection transfer due to the breakup of the coarse voids. The thermal conductivity of the WMB was greater than that of the IFB with the same density because the WMB contained coarser voids than the IFB, resulting in higher heat convection transfer and the thermal conductivity of the heat bridge was high. However, the thermal conductivity of the WMB at a density of 500–600 kg/m^3 was similar to the value on the regression line of the wood-based panels other than plywood.

（3） Substance thermal conductivity along the heat-flow direction was determined using model calculations for WMBs of various densities. The results indicate that the WMB substance has anisotropic thermal conductivity similar to that of wood.

CHAPTER FOUR

MECHANICAL PROPERTIES OF COMPRESSION-DRIED WASTE MUSHROOM BEDS

1. Introduction

In the chapter three, the possibility of using WMBs as an insulation material was examined. As shown in **Fig. 4-1**, WMBs were compression-dried at four levels (compressed WMBs) and the relationship between air-dry density and thermal conductivity was investigated in the density range of about 150–600 kg/m^3. The results showed that there was a linear relationship between density and thermal conductivity. At densities of 200–300 kg/m^3, the thermal conductivity was more than that of T-class IFB at the same density: however, at densities of 500–600 kg/m^3, the thermal conductivity was lower than that of wood and similar to that of wood-based panel materials. From this, 300–600 kg/m^3 were considered to be an appropriate range for the density to be reached by compression-drying.

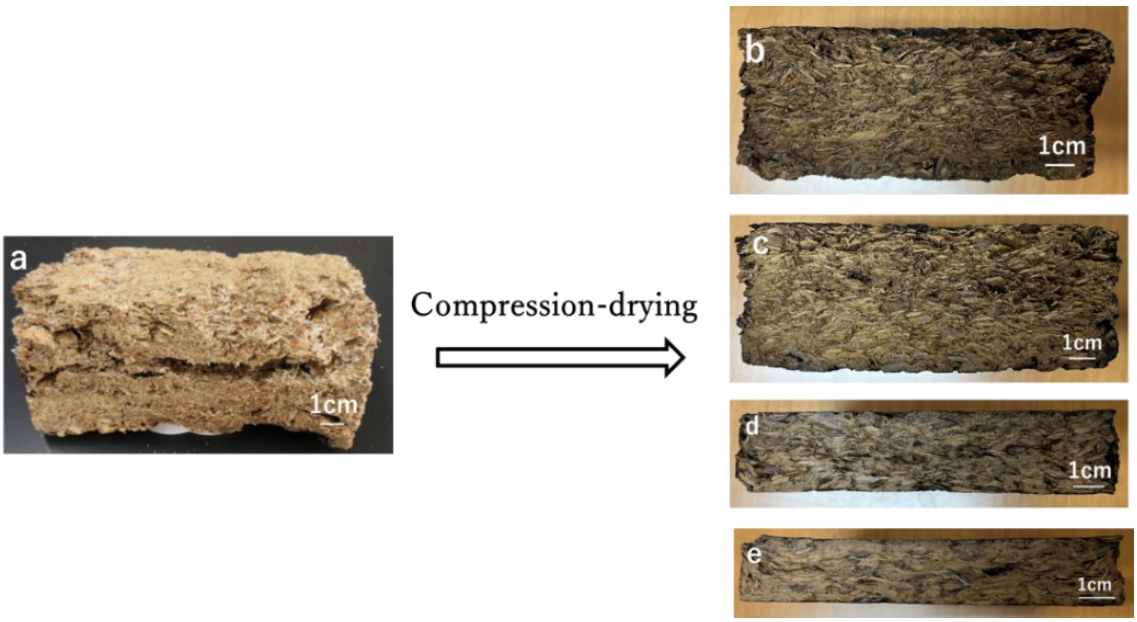

Figure 4-1 Elimination of internal voids by compression drying (four levels of the heigh)

a: 120 mm high (before compression, uncompressed WMBs),

b: 60 mm high, c: 50 mm high, d: 30 mm high, e: 25 mm high

In this chapter, as the basic strength properties of WMBs for insulation, the internal bond strength (IB) and compressive properties are investigated in relation to the density. The compressive behavior of the WMBs in the height direction is considered to be similar to the transverse compressive behavior of wood. Therefore, the same evaluation indices as the transverse compression test, namely, transverse elastic modulus, yield strain, and yield stress, were examined. The purpose of this study was to compare these properties with those of commercially available IFB and to determine the position of strength performance.

Moreover, with the aim of obtaining a fundamental understanding of the mechanical properties of decayed wood, the elastic modulus of the substance with WMB powder was determined. This elastic modulus was calculated from the stress – strain diagram obtained by the consolidation test. Similar measurements were made for raw wood and mycelium, to estimate the position of the elastic modulus of the substance of the WMBs.

2. Material and methods

2.1 Preparation of test specimens for mechanical properties

WMBs consist of two groups: uncompressed and compressed WMBs. **Figure 4-2** shows the density distribution of these two groups used in the study described in the chapter three. From these WMBs, test specimens with dimensions of 50 mm long, 50 mm wide, and 10–12 mm high were obtained. The density of the test specimens ranged from about 100–600 kg/m^3 (MC_d: 10–12%), but test specimens in the density range of 145–605 kg/m^3 were used, because the test specimens in the density range of 140 kg/m^3 or less broke during the cutting process. The height of the test specimen was in the direction of chip accumulation, namely, the height of the WMB, and the strength measurements were made in this direction.

Commercially made IFBs of three different thicknesses (12, 15, and 20 mm) were used as control materials. These are materials specified by JIS A5905 [4-1]and manufactured for tatami mat core materials (called T-IB in JIS). A number of test specimens were produced from the product samples of each material with dimensions of 50 mm long, 50 mm wide, and of the product thickness.

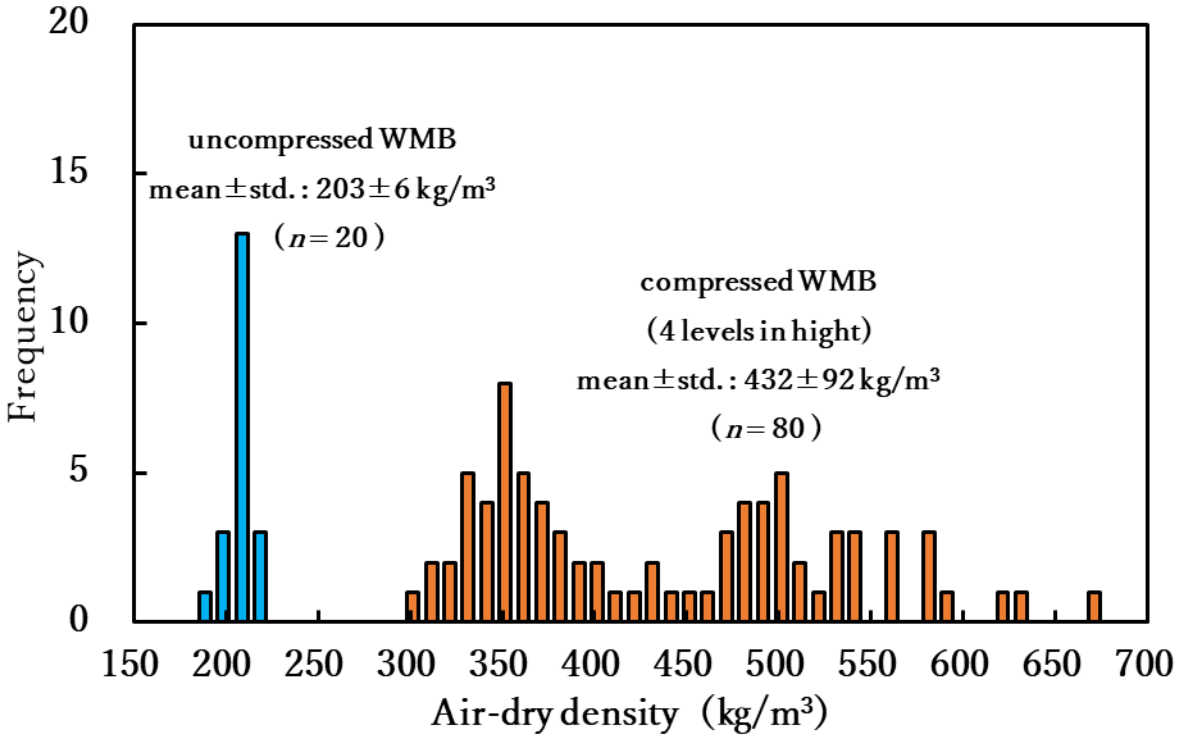

Figure 4-2 Air-dry density of the WMBs

2.2 Internal bond strength (IB) tests

Table 4-1 shows the number of test specimens, and the range of the densities and the mean values for the IB test. Tests were conducted according to JIS A5905 [4-1] and the loading speed was 2 mm/min. The *IB* was obtained by dividing the maximum load P_{max} by the load surface A (50 × 50 mm), as shown in **Eq. (4-1)**.

$$IB = \frac{P_{max}}{A} \qquad (4\text{-}1)$$

Table 4-1 Internal bond strength test specimens and their densities

Type		n[1)]	Air-dry density[2)] (kg/m^3)	
			range	mean
Waste mushroom bed (WMB)	uncompressed	35	145–288	213
	compressed	28	259–605	416
Insulation fiberboard (IFB)	12 mm	13	258–276	265
	15 mm	17	238–254	246
	20 mm	8	236–244	239

1) The number of test specimens 2) Values at moisture content of 10–12%

2.3 Compressive tests

Table 4-2 shows the number of test specimens, and the range of the densities and the mean values for the compressive test. The test specimens were loaded to 25% compressive strain in the height direction using a universal testing machine at a loading speed of 0.5 mm/min. Compression load and strain were recorded at 2 s intervals. These data were converted to stress-strain data, and a strain (X) – stress (Y) diagram was produced, as shown schematically in **Fig. 4-3**.

The yield point (yield strain ε_y, yield stress σ_y) is the coordinate of the maximum stress that will not cause compressive failure and the strain at that time. However, when using the material, the stress should be less than half of the yield stress. The yield point was determined by the procedure shown below. First, the regression line of the elastic region was obtained, and the elastic modulus E (**Eq. (4-2)**) was determined from the slope of the regression line. The point at which a measured stress value falls 1% below the stress on the regression line for the first time is the yield point, and its y – coordinate is σ_y. When the upper and lower surfaces of the test specimens are not completely parallel, curved portions may appear in front of the elastic region. The x – coordinate ε_y was obtained by exclusion of this curvature portion. Compressive properties were evaluated using three indices: E, σ_y, and ε_y.

$$E = \frac{\sigma_y}{\varepsilon_y} \tag{4-2}$$

Table 4-2 Compressive test specimens and their densities

Type		n[1)]	Air-dry density[2)] (kg/m^3)	
			range	mean
Waste mushroom bed (WMB)	uncompressed	23	163–276	215
	compressed	22	255–574	427
Insulation fiberboard (IFB)	12 mm	13	258–268	261
	15 mm	13	238–249	245
	20 mm	12	234–241	237

1) The number of the test specimens 2) Values at moisture content of 10–12%

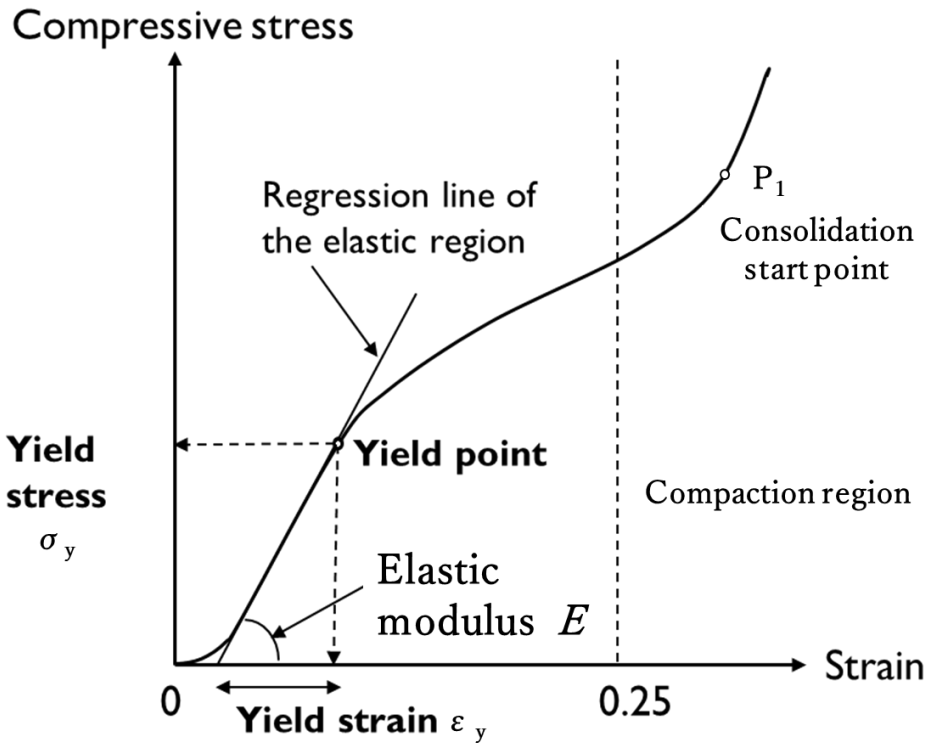

Figure 4-3 Schematic draw of the stress-strain curve of the compressive test

2.4 Consolidation tests of powder samples

To determine the elastic modulus of the substance, the WMBs, raw wood, and the mycelium powder samples were compressed. If the powder sample is compressed into a region above its substance density, the elastic modulus of the substance can be estimated from its stress-strain relationship. A universal testing machine with a maximum load of 50 kN was used. The powder sample was placed in a metal cylinder with an inner diameter of 16.04 mm and pressed with a metal piston (the photo in **Fig.4-4**). The cross-sectional area of the cylinder is 2.02 cm^2, so if a 1.52 g powder sample is compressed to a thickness of 5.00 mm, its density becomes 1.50 g/cm^3. Therefore, the 1.50 g powder sample was inserted and compressed at a loading speed of 1.2 mm/min until a thickness of 4.50 mm was reached. The density at 4.50 mm thickness is 1.67 g/cm^3, which is greater than the substance density [WMB: 1.622 kg/m^3, raw wood: 1.569 kg/m^3, mycelium: 1.550 kg/m^3 (see **Table 3-3**, in chapter three)] of the samples. The date were recorded at 0.5 s intervals.

As shown in **Fig.4-4**, the compressive stress σ of the powder sample in the cylinder gradually increases until the voids in the sample completely disappear, after which σ increases linearly with decreasing thickness d. The linear region is thought to reflect only the elastic modulus of substance E_s. Therefore, E_s can be determined by **Eq. (4-3)** using two points in the linear region, P_1 (d_1, σ_1) and P_2 (d_2, σ_2), as described in **Fig. 4-4**.

$$E_S = \frac{(\sigma_2 - \sigma_1) \times d_1}{d_2 - d_1} \qquad (4\text{-}3)$$

Powder samples were prepared for the raw wood, interior of several WMBs, and the mycelium (shiitake fruiting body). First, these three air-dried chip samples were powdered using a Willey mill. Then, the powder samples were classified with a sieve. Two sizes of samples (F6: 0.25–0.36 mm, F7: less than 0.15 mm, MC_d: 9.7–9.9%) were tested to determine whether there is any effect of particle size on the elastic modulus obtained in the consolidation test (five replicates). The E_s obtained in this study does not reflect the anisotropy, resulting in composite E_s for the strong and weak directions.

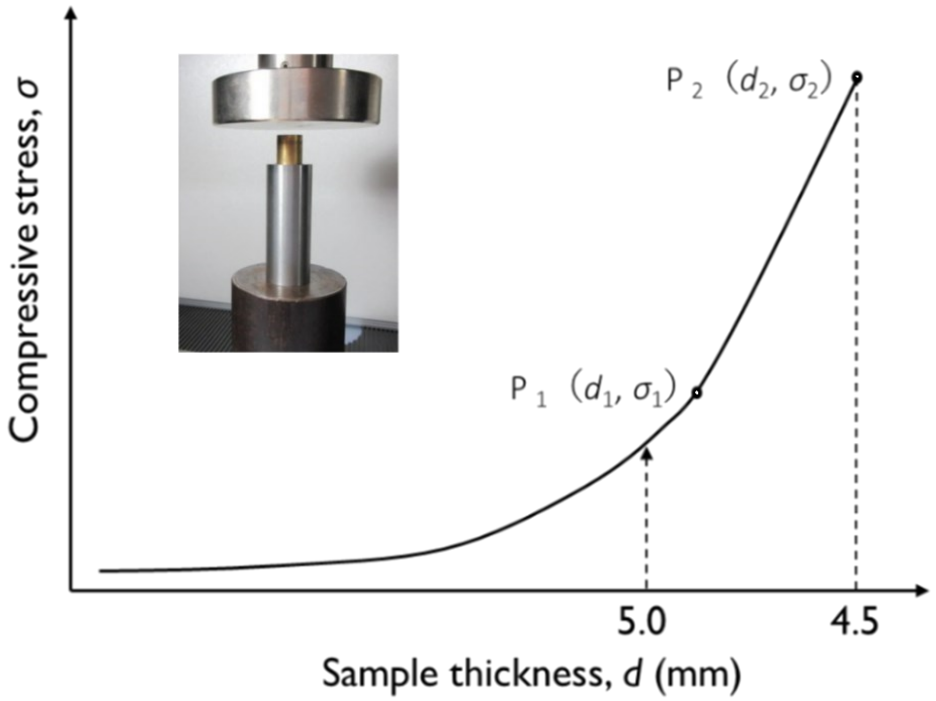

Figure 4-4 Schematic draw of the stress-thickness curve of the powder consolidation test

3. Results and discussion

3.1 Internal bond strength (IB)

Figure 4-5 shows the results of the IB tests on the density of the test specimens. Although there was a significant positive correlation between the density and *IB* for the WMB test specimens, the increase in *IB* was small relative to the increase in density. **Table 4-3** shows the densities classified into three density bands (less than 200 kg/m^3, 200–300 kg/m^3, and more than 300 kg/m^3) and compares the mean of these *IB*s. For a density of 200–300 kg/m^3, there was no significant difference in the mean *IB* values between the uncompressed and compressed WMBs. This is because the original low-density WMBs, namely, those with a high degree of decay and a high percentage of mycelium present, will increase in density after compression-drying. However, owing to the hydrophobic surface of the mycelium [4-2], it can hardly be expected that there would be any adhesive force between the mycelium or between the mycelium and decayed chips by hydrogen bonding. On the other hand, the mean value of *IB* for the compressed WMBs with densities of more than 300 kg/m^3 was significantly higher (by about 38%) than that of the uncompressed WMBs with densities of more than 200 kg/m^3. The reason for this is that the compressed WMBs with densities of more than 300 kg/m^3 are originally high in density; that is, they have a higher percentage of chips with a lower degree of decay, and the entanglement of decayed chips by compression-drying and the formation of new hydrogen bonds may have increased the bonding strength. Additional experiments at higher compressions are needed to confirm this.

Next, the measured *IB* results (mean ± std.) for the control material, IFB, were determined to be 68.4 ± 11.5 kPa, 40.6 ± 6.5 kPa, and 52.6 ± 8.7 kPa for thicknesses of 12, 15, and 20 mm, respectively. The mean value of each is plotted in **Fig. 4-5**, which tended to be higher than the plot for WMBs. The mean *IB* of the three IFBs was 52.6 kPa (std.: 15.1 kPa, n = 38), which was

significantly about two times greater than the *IB* of the WMBs (mean 28.4 MPa, std.: 16.6 MPa, *n* = 18) in the same density range (236–276 kg/m^3). To obtain the same level of *IB* as IFBs with a density of about 250 kg/m^3, the density of compressed WMBs should be increased to about 500–600 kg/m^3. The reason for the low *IB* of the compressed WMBs may be a significant decrease in the cohesive strength of the decayed wood.

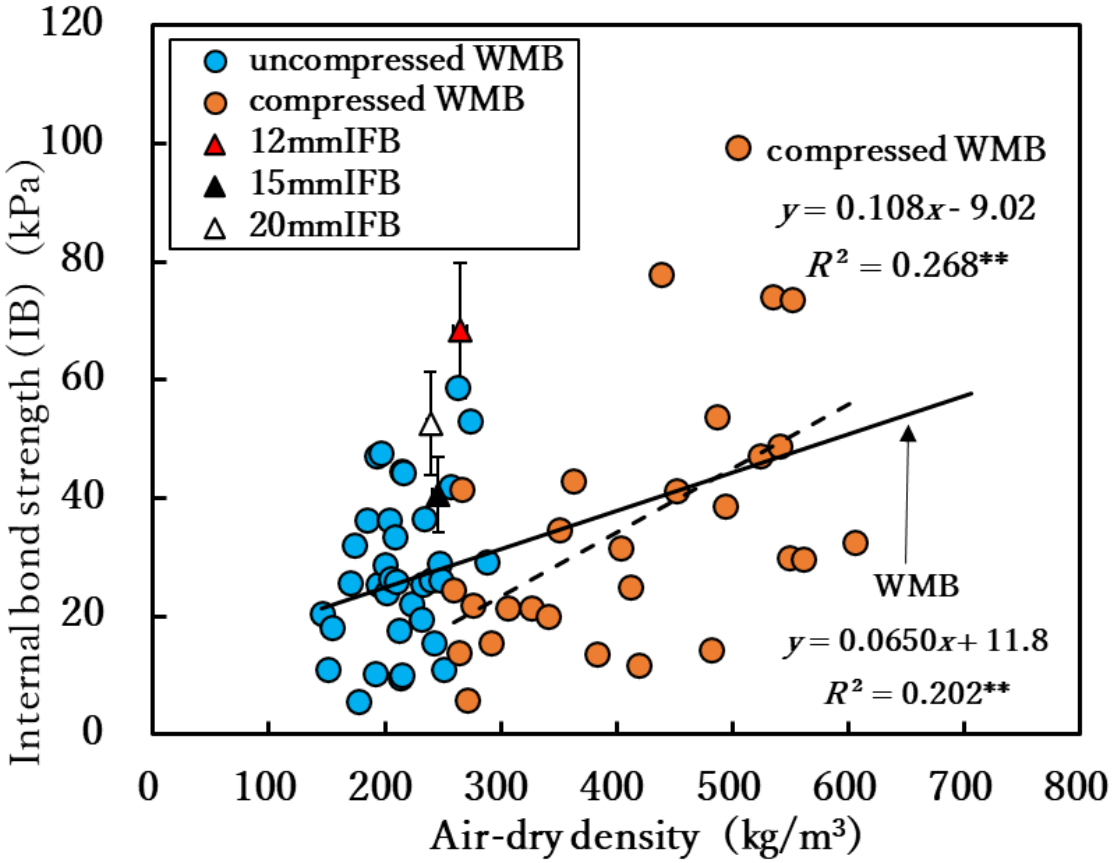

Figure 4-5 Relationships between the density and the *IB* of the WMB and IFB

Table 4-3 *IB* values (mean[1)] ± std.[2)]; kPa) at different density bands of WMB

Density [3)] bands	Uncompressed	Compressed
Less than 200 kg/m^3	25.5[a] ± 14.3 (n [4)] = 11)	–
200 – 300 kg/m^3	29.1[a/b] ± 12.9 (n = 24)	20.6[a] ± 12.2 (n = 6)
More than 300 kg/m^3	–	40.2[a/c] ± 23.3 (n = 22)

1) Averages with different letters are significantly different at P=0.05

2) std.: standard deviation 3) Values at moisture content of 10–12%

4) n : the number of test specimens

3.2 Elastic modulus of substance (E_s)

Figure 4-6 shows an example of the powder sample thickness (X)— stress (Y) relationship obtained from a consolidation test. At a thickness of less than approximately 6 mm, a linear relationship is observed. Since this linear relationship reflects the elastic behavior of the compacted powder, E_s can be obtained if the slope of this line can be determined. P_2 is the coordinate at maximum stress and P_1 is determined by the following method: Fifteen consecutive plots (range of displacement is 0.15 mm) from P_2 are used to calculate the coefficient of determination R^2. Here the first plot is the start point and the 15th plot is the end point. The start point was shifted by one plot and this operation was repeated, with P_1 as the end point just before R^2 decreases. E_s was calculated using **Eq. (4-3)**.

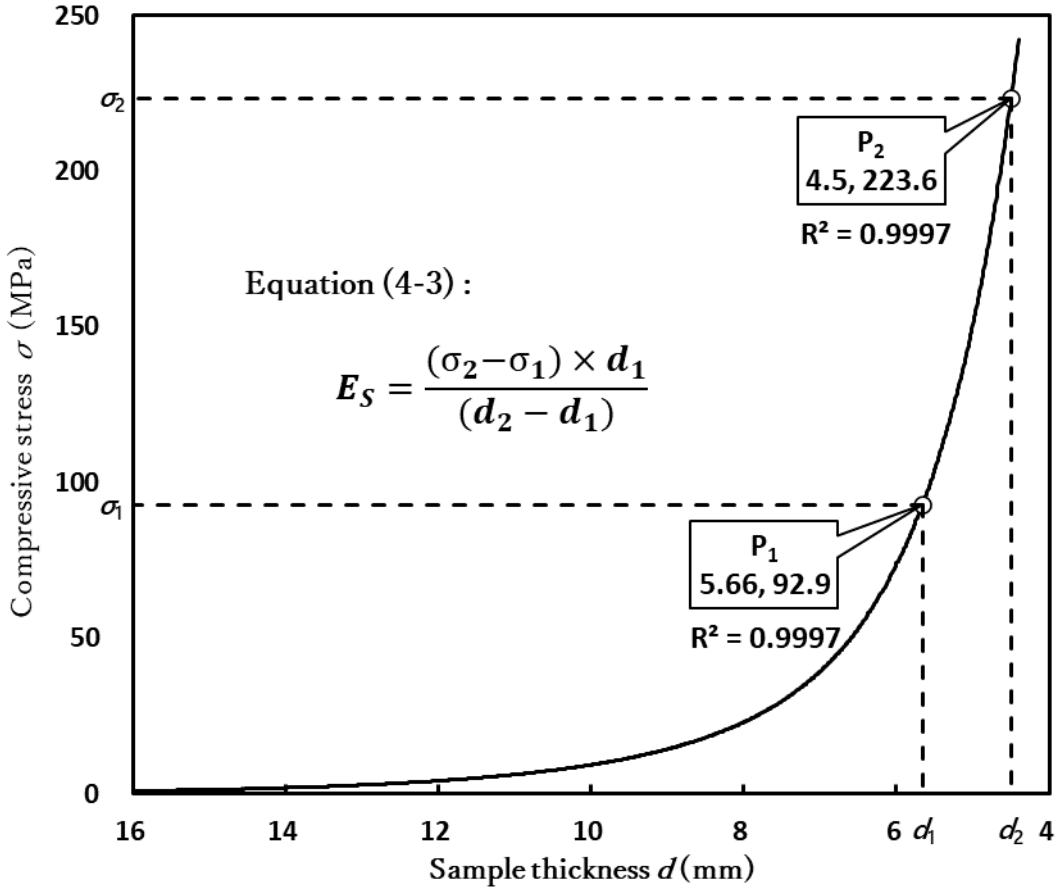

Figure 4-6 Example of the powder sample thickness - stress relationship

(WMB, F7)

Table 4-4 lists the results of E_s calculations. First, focusing on the effect of powder size on E_s, E_s values differed slightly (± 4%) between the WMBs and raw wood, depending on the powder size, but no effect was observed in the mycelium. Therefore, F6 and F7 were compared by the mean E_s of 10 samples without distinction. The E_s of the WMB was 0.80 GPa, significantly lower than that of the raw wood (0.87 GPa) by about 10%. The substance of the WMB is a mixture of decay residue of wood substance and mycelium. The E_s of the mycelium itself was 1.42 GPa, significantly about 60% higher than that of the raw wood. This suggests that the E_s of the decayed wood was significantly low.

Table 4-4　Elastic modulus of substance E_s (powder samples)

powder		n [2]	E_s (GPa)	
sample	size[1]		mean[3] ± std. [4]	mean (n =10)
Waste mushroom bed	F6	5	0.81 [a] ± 0.02	0.80[A]
	F7	5	0.78 [b] ± 0.02	
Raw wood	F6	5	0.84 [c] ± 0.01	0.87[B]
	F7	5	0.89 [d] ± 0.02	
Mycelium	F6	5	1.42 [e] ± 0.04	1.42[C]
	F7	5	1.42 [e] ± 0.03	

1) The size of powder samples: F6: 0.25-0.36mm, F7: less than 0.15mm

2) n: the number of test powder samples

3) Averages with different letters are significantly different at P = 0.05

4) std.: standard deviation

3.3 Elastic modulus in the waste mushroom bed height direction

In addition to the pattern shown in **Fig. 4-3**, the compaction behavior of the WMBs was observed in the pattern shown in **Fig. 4-7**. **Figure 4-3** shows the pattern for test specimens with a density of less than 300 kg/m^3, while the pattern in **Fig. 4-7** shows a tendency for test specimens with a density of more than 300 kg/m^3. In **Fig. 4-3**, the yield point is recognized, so E was obtained from the slope of the elastic region (**Eq. (4-2)**), but in **Fig. 4-7**, E was obtained from the slope of the line connecting the estimated consolidation start point and the origin. The consolidation start point P_1 was determined by the following method. First, the P_1 in **Fig. 4-3** was determined by the method used in the estimation of E_s. Next, a regression equation was obtained for the relationship between the density of the test specimens and the strain at P_1. The extrapolation of this regression equation was used to estimate the strain ε of P_1 in test specimens with a density of more than 300 kg/m^3, and P_1 was determined by substituting ε into the X-Y diagram in **Fig. 4-7**.

The relationship between the obtained E and the density of the WMB test specimens is shown in **Fig. 4-8(A)**. A significant positive correlation was observed between the two. However, for the test specimens with a density of more than 300 kg/m^3, the dispersion of E is large, and one of the reasons for this is the estimated error of P_1. Now, E is calculated from the regression equation ($y = 0.0385\ x - 7.17$) in **Fig. 4-8(A)**; the values are 0.53, 8.23, and 15.93 MPa for densities of 200, 400, and 600 kg/m^3, respectively. Compression-drying increased the relative amount of substance resisting loading as the coarse voids between decayed chips disappeared, and the increase in E was greater than the relative increase in density.

Now, the measured E (mean $\pm$ std.) for the control material, IFB, was 3.78 $\pm$ 0.15, 1.75 $\pm$ 0.20, and 2.85 $\pm$ 0.09 MPa for thicknesses of 12, 15, and 20 mm, respectively. These mean E values of IFBs in **Fig. 4-8(A)** tended to be slightly higher than those of WMBs. Upon comparison at the

same density band (234–268 kg/m^3), the mean E of the IFBs was 2.79 MPa (std.: 0.86 MPa, n = 38) and that of the WMBs was 1.38 MPa (std.: 0.52 MPa, n = 9). The WMBs were significantly lower by 50% than the IFBs. One reason for this is that the E_s of WMBs is lower than that of raw wood, as shown in **Table 4-4**. Other possible reasons include differences in the size of the components and the degree of inter-element adhesion.

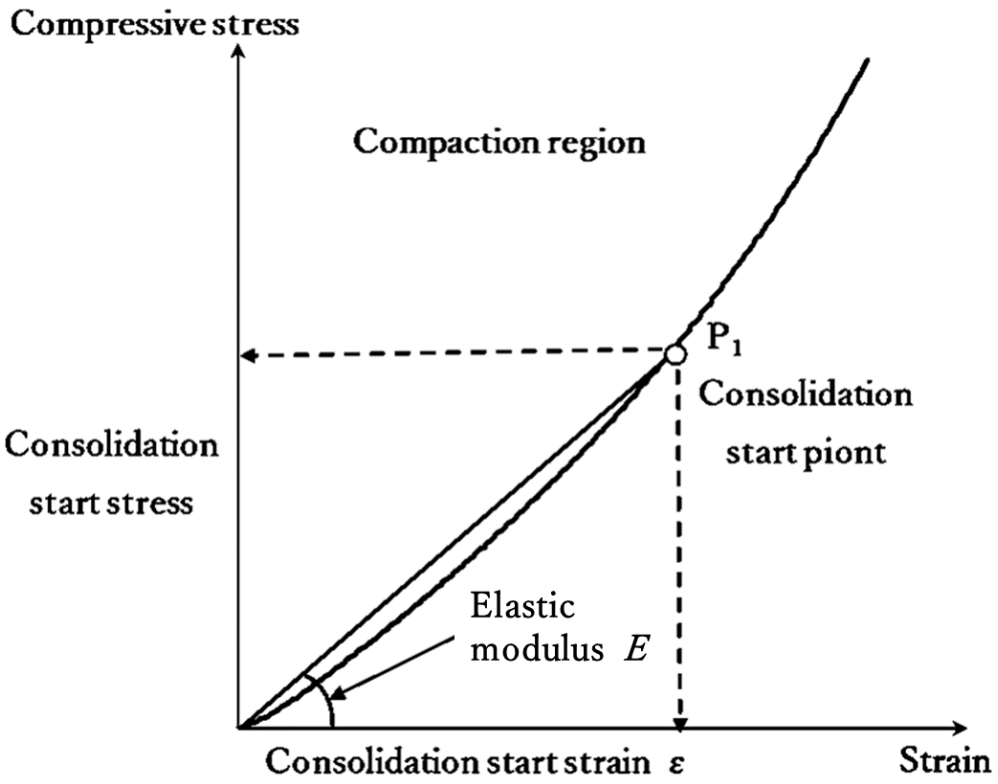

Figure 4-7　Schematic draw of the compaction behavior for the WMB

Density 300 kg/m^3 or more

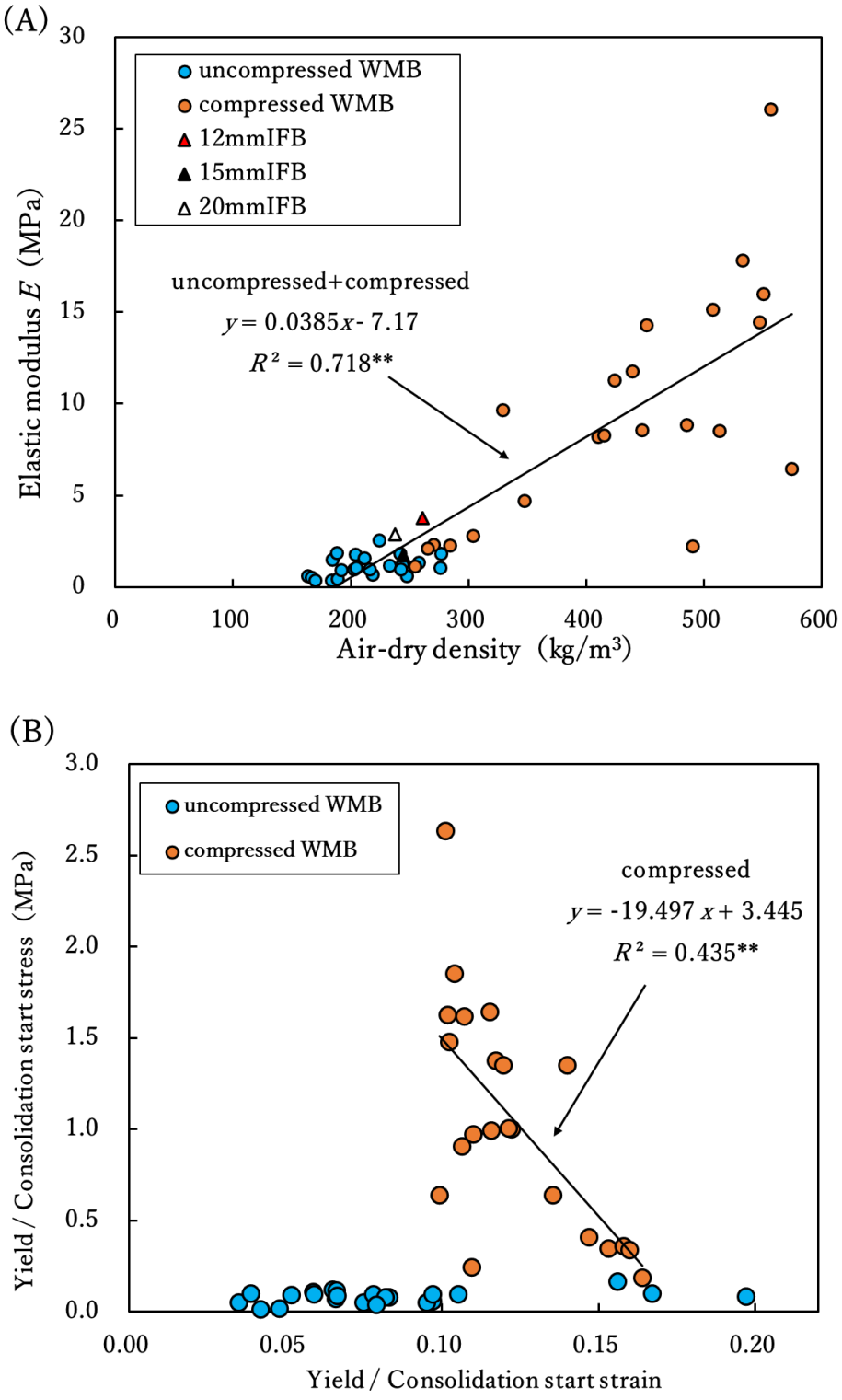

Figure 4-8　　Compression behavior of the WMB and IFB

A: relationships between the density and the *E*, B: yield point

3.4 Compressive yield strength and strain in the waste mushroom beds height direction

The yield points determined for the uncompressed (density 163–276 kg/m^3) and compressed (density 255–574 kg/m^3) WMBs are shown in **Fig. 4-8(B)**. Focusing on the uncompressed WMBs, yield stress remained at a low level and yield strain was widely distributed. This is due to the inclusion of low-density test specimens with large deformation capacity. Meanwhile, focusing on the compressed WMBs, there was a significant negative correlation between yield strain and yield stress. This is because these plots covered a wide range of densities: the higher the density, the larger the yield stress and the smaller the yield strain.

Figure 4-9 compares the yield points of WMBs and IFBs (three different thicknesses). The plots represent mean values and standard deviations. The slope of the straight line connecting the origin and the yield point represents the elastic modulus. First, the uncompressed WMB was compared to the 15 mm IFB having the lowest yield point among the three: the elastic modulus of the uncompressed WMB was significantly lower by about 55% than that of the IFB, but the yield stress was about the same, and the yield strain was significantly about 1.6 times greater. Next, the compressed WMB was compared to the 12 mm IFB having the highest yield point among the three: the elastic modulus, yield stress, and yield strain of the compressed WMB were significantly about 2.4, 6.1, and 2.7 times higher, respectively, than those of the IFB. In other words, if a WMB originally having a low density is compression-dried to increase the density, it is possible to impart compression performance exceeding that of the IFB.

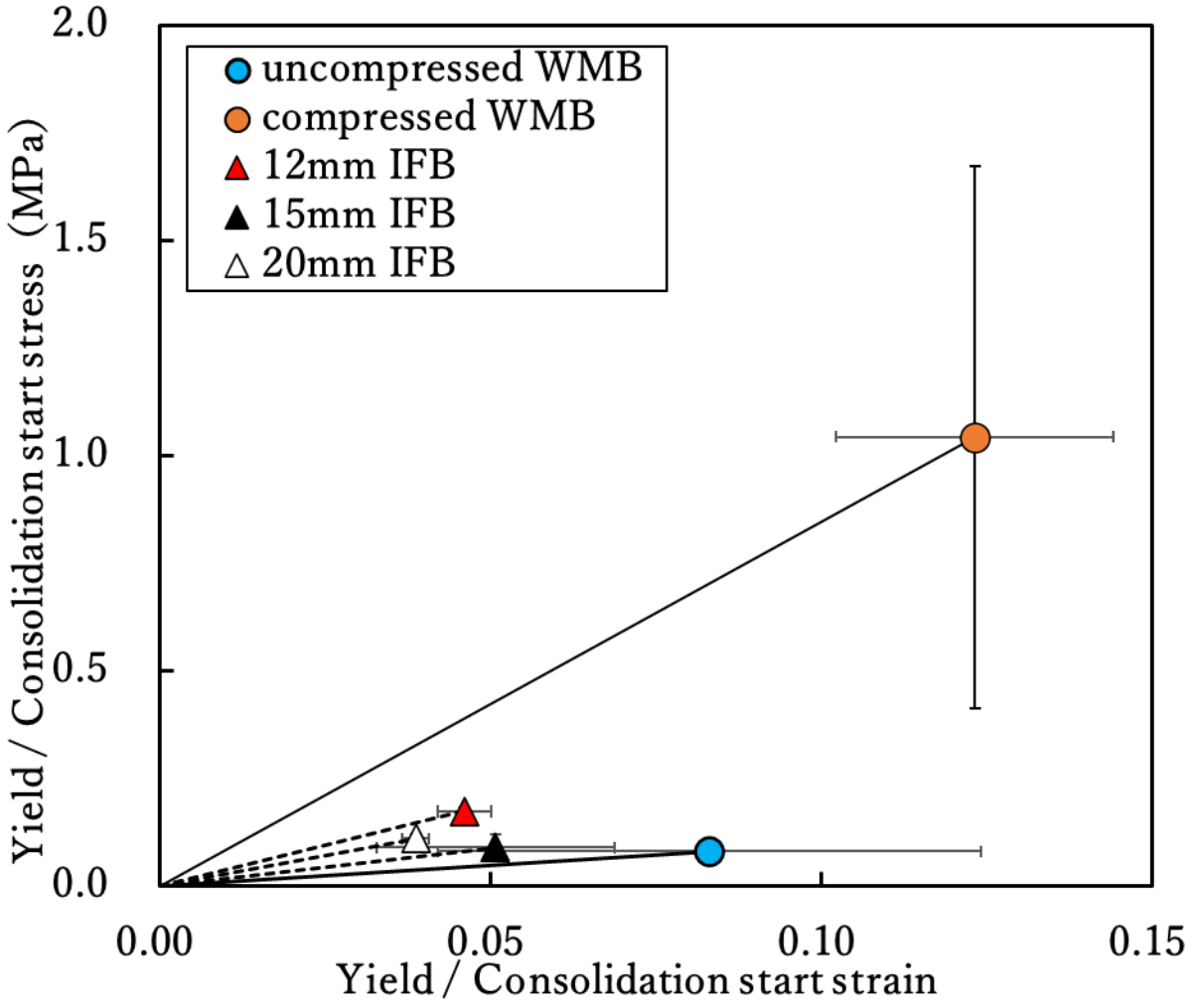

Figure 4-9 The yield point of the WMB and IFB

5. Conclusions

The findings obtained from this work are summarized as follows:

(1) The increase in IB was slight even when the WMBs were compression-dried to increase their density. The reason for this is that the mycelial surface is hydrophobic, and thus hydrogen bonds between mycelia or between mycelia and decayed chips are not expected to be strong even after compression-drying. Even when the density was increased to about 600 kg/m^3, the IB of the compressed WMB was almost the same as that of commercial IFB with a density of about 250 kg/m^3, indicating a significant decrease in the cohesive strength of the decayed wood.

(2) The elastic modulus of substance E_s of the WMB (a mixture of decay residues of wood substance and mycelium) was 0.80 GPa, significantly lower than that of the raw wood (0.87 GPa) by about 10%. The E_s of the mycelium itself was 1.42 GPa, significantly higher by about 60% than that of the raw wood. This suggests that the E_s of the decayed wood was significantly low.

(3) Compression-drying of WMBs to increase their density resulted in a slight increase in IB, but a significant increase in elastic modulus E. The uncompressed WMBs had low yield stress and a large variation in yield strain. On the other hand, the compressed WMBs had a higher yield stress and a smaller variation in yield strain. Compression-drying of WMBs provided yield stress and yield strain (compressive deformation capacity up to yield) equivalent to or greater than those of commercial IFB.

CHAPTER FIVE

MANUFACTURING AND PERFORMANCE OF BINDER-LESS BOARDS

1. Introduction

In the chapter three and four, involved analyses of the material utilization of WMBs by exploiting their shape. As described in this chapter, the manufacture of binder-less boards using chips derived from WMBs was also examined. Binder-less boards are wood-based panels produced without adhesives, utilizing the self-adhesion generated by the polymerization of wood-derived sugars and the thermoplastic flow of lignin [5-1]. Binder-less boards are an excellent technology that is safe for humans and environmentally friendly. For example, methods for manufacturing them have been investigated using various raw materials including kenaf [5-2], bagasse [5-3], and sugi bark [5-4]. The following findings [5-5] have been obtained through these studies:

a. To bring out the self-adhesion resulting from the hydrolysis of the raw material hemicellulose and the softening of lignin, it is necessary to prepare the raw material into chips of an appropriate size.

b. Insufficient water vapor inside the mat during hot-pressing reduces its self-adhesion, while excessive water vapor causes internal cracking and loss of strength. It is thus important to generate and discharge the appropriate amount of water vapor at an appropriate time.

c. The combination of temperature, pressure, and time during hot-pressing is important because extremely high hot-pressing temperatures will cause blackening and loss of strength.

Liu et al. [5-6] utilized waste wood from shiitake mushroom log cultivation to produce binder-less boards with a density of 0.8 g/cm^3. It was reported that a binder-less board made by hot-pressing

at a temperature of 220℃, pressure of 5 MPa, and press time of 10 min using raw wood that had been left to rot for 26 months had higher strength than that produced using unrotted raw wood. However, to the best of our knowledge, no reports describing research on binder-less boards made from WMBs have been published.

The skin of WMBs is water-repellent, which may prevent self-adhesion. In addition, since the elemental composition of skin differs from that of the inside, differences in chemical composition can also be inferred. From the perspective of resource utilization, it is desirable to use the whole WMBs (both inside and skin) as raw materials for binder-less boards. Therefore, the purpose of this chapter was to explore the appropriate states for manufacturing binder-less boards using WMBs. Specifically, the press temperature was kept constant at 210 ± 10 ℃, and the type of raw materials (inside, skin, and whole WMBs), chip size, and hot-pressing schedule [pressure for relaxation period (residual pressure), with/without second compression] were varied, and board properties such as the degree of darkening, mechanical properties, and the presence of internal cracks after board formation were examined. Since there is no standard for evaluating the performance of binder-less boards, the JIS standard for particleboard (PB) [5-7] was applied to the evaluation.

2. Material and methods

2.1 Raw materials

Three types of board raw materials were prepared: inside, skin (the part from the surface to a depth of 1 cm), and whole WMBs. These three raw materials were pulverized into chips with a Willey mill. The chips were then sorted with a sieve to obtain two sizes (L: 4–2 mm, S: less than 2 mm). The chips were conditioned to approximately 10% MC_d. **Table 5-1** shows the symbols used for the different types of raw material chips. According to the chapter two, the whole chips are estimated to contain about 10% skin chips.

Table 5-1 Symbols of the raw material chips

Chip size \ Type	Inside of the WMB	Skin of the WMB	Whole WMB
L: 4–2 mm	I_L	S_L	W_L
S: Less than 2 mm	I_S	S_S	W_S

2.2 Boards manufacture

The boards were manufactured in accordance with the following procedure. A heat-resistant sheet with a thickness of 0.06 mm and one thermocouple (JIS K Φ0.3, mat surface temperature: T_S) were first placed on an aluminum caul-plate. A forming box made of soft wood with a density of about 0.2 g/cm^3 and with internal dimensions of 20 × 20 cm and 35 mm high was placed on top of sheet. The target dimensions of the board were 20 × 20 cm and 5 mm high, the target density was 1.0 g/cm^3, and the raw material needed was 220 g (MC_d: 10%). One-half of the raw material was spread in the forming box to form a half mat, and then another thermocouple same as described above was placed on the center of the mat (core temperature: T_C), and the remaining material was spread to complete a particle mat. Then, the heat-resistant sheet was placed on top of the mat, after which the caul-plate was placed on top. The mat was inserted into a hot press heated to 220 ℃ together with the forming box. When the T_S reached 80 ℃, hot-pressure was started in accordance with the hot-pressing schedules shown in **Fig. 5-1**. Three replicate boards were manufactured under the conditions shown in **Table 5-2**: six conditions for I-Boards, that is, three residual pressure conditions for the relaxation period, with/without second compression; and one condition for W-Boards and S-Boards. After the mats had been inserted, the temperature of the hot press slightly decreased and was 210 ± 10 ℃.

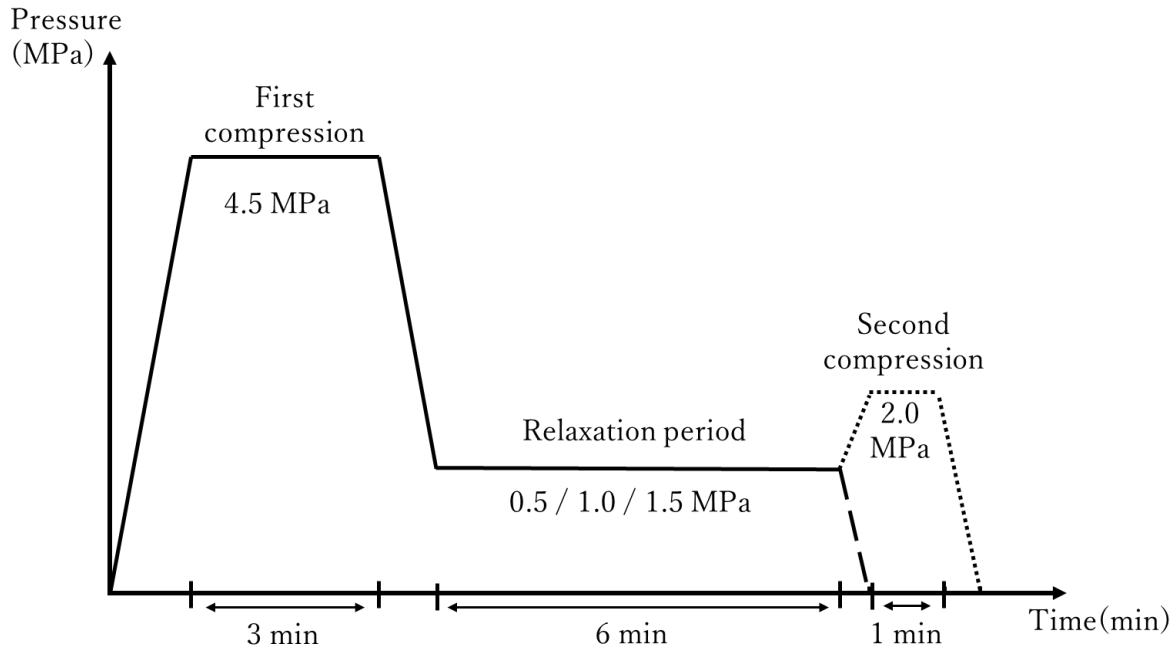

Figure 5-1　　Hot-pressing schedules of the binder-less boards

Table 5-2 Hot-pressing conditions of the binder-less boards

Board type	First compression		Relaxation period		Second compression		Symbol
	Pressure[1)] (MPa)	Time (min)	Pressure (MPa)	Time (min)	Pressure (MPa)	Time (min)	
I-Board[2)]	4.5	3	0.5	6	-	-	I_LR_5, I_SR_5
					2.0	1	I_LR_5Y, I_SR_5Y
			1.0	6	-	-	I_LR_{10}, I_SR_{10}
					2.0	1	$I_LR_{10}Y$, $I_SR_{10}Y$
			1.5	6	-	-	I_LR_{15}, I_SR_{15}
					2.0	1	$I_LR_{15}Y$, $I_SR_{15}Y$
W–Board[3)]	4.5	3	1.0	6	2.0	1	$W_LR_{10}Y$, $W_SR_{10}Y$
S–Board[4)]	4.5	3	1.0	6	2.0	1	$S_LR_{10}Y$, $S_SR_{10}Y$

1) Press closing speed: 0.45 mm/s

2) I-Board: Binder-less board made from the inside of the WMBs

3) W-Board: Binder-less board made from the whole of the WMBs

4) S-Board: Binder-less board made from the skin of the WMBs

2.3 Mechanical properties and water resistance (TS・WA) tests

The properties of the binder-less boards were measured in accordance with JIS A5908 PB [5-7]. Mechanical properties such as bending strength (MOR) and IB were measured. For the water resistance, the 24-h water immersion test was used to measure the thickness swelling rate (TS) and the water absorption rate (WA). Young's modulus in bending (MOE) was calculated from the stress-deflection diagram obtained in the bending test.

The manufactured boards were cured indoors for 2–3 weeks (winter). They were then trimmed to dimensions of 18 × 18 cm, from which 12 pcs bending test specimens with dimensions of 18× 4 cm were taken in each condition (**Fig. 5-2**). MC_d was measured using the trimmed sections and was found to be 3–4%. After the bending test, 48 pcs test specimens of 4 × 4 cm were taken in each condition, avoiding the bending breakage area in the center of the span. Test specimens with significant internal cracking as shown in **Fig. 5-3** were excluded from the tests, the thickness of each test specimen was measured at four locations, and the board density was calculated. The test specimens were then divided into two groups: an IB test group (14 pcs or more test specimens) and a water resistance test group (14 pcs or more test specimens).

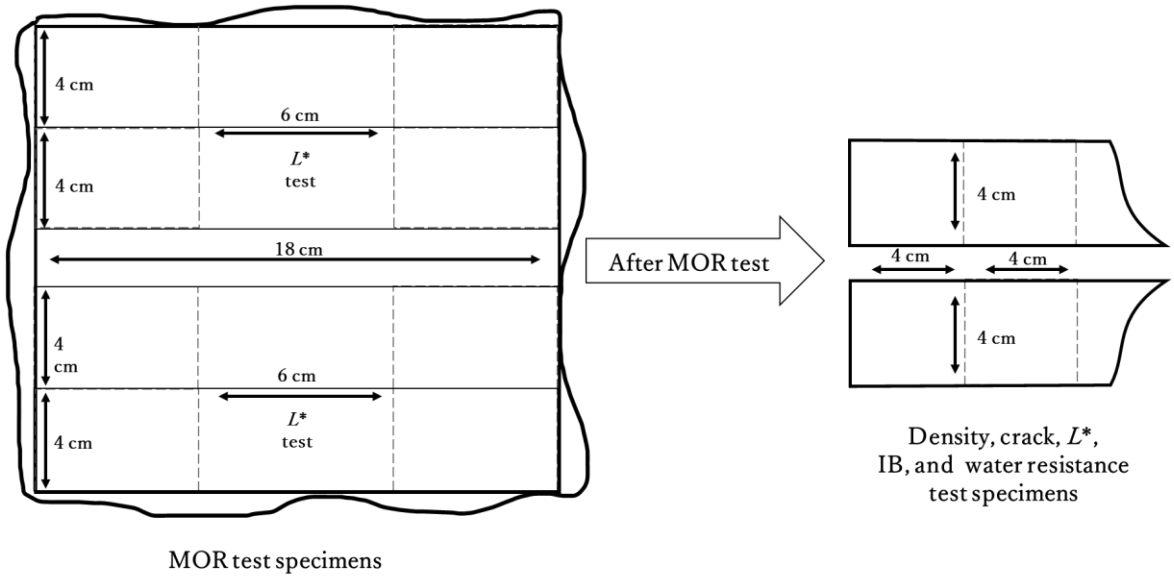

Figure 5-2　　A cutting pattern of the test specimens

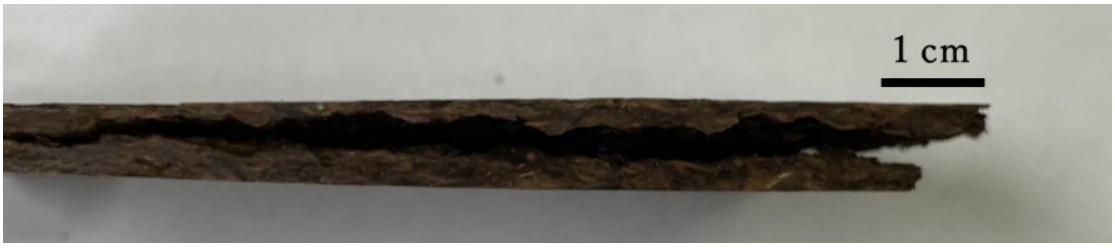

Figure 5-3　　The side-view of the board with an internal crack

2.4 Surface darkening measurement (L^* test)

The brightness L^* in the $L^*a^*b^*$ color system was measured using a Handy Spectrophotometer (NF555, Nippon Denshoku Industries Co.). Five measurements were performed at each of the front and back surfaces within ± 3 mm from the center of the bending test specimens (**Fig. 5-2** left), and at each of the front and back surfaces of the IB and water resistance test specimens (**Fig. 5-2** right). The mean of the ten measurements obtained was used as the L^* for each test specimen.

3. Results and discussion

3.1 Temperature, density, crack, and L^* of the I-Boards

First, we focus on the core temperature (T_C) of the I-Boards. **Figure 5-4** shows an example of the press time (X) – temperature (Y) relationship obtained from a hot-pressing. The temperature of the T_C decreased during the depressurization process after the end of the first compression, but gradually increased after a large amount of water vapor was released during the relaxation period. Therefore, as shown in **Fig. 5-4**, the T_C at the start of the hot-pressing (T_{C1}), the end of the first compression (T_{C2}), max/min temperature of the relaxation period (T_{C3}/ T_{C4}), the end of the relaxation period (T_{C5}), the start/ end of the second compression (T_{C6}/ T_{C7}) were determined, and the speed of change (S) of T_C at each stage was calculated. The calculated results are shown in **Table 5-3**. The higher the residual pressure, the smaller the S of T_C. It can be seen that the S of T_C at each stage of I_S-chip boards (**Table 5-3** left) is slower than that I_L-chip boards (**Table 5-3** right). The reason for this is thought to be that the smaller the voids between the small chips, the more difficult it is water vapor to escape, and the T_C tends to be more stable and has higher self-adhesive ability.

Next, thickness and density of the I-Boards. **Figure 5-5** shows the relationships between the I-Board thickness and density (MC: 3-4%) for each chip size, I_L- and I_S-chip with/without second compression. I-Board thickness was in the range of 5.3–5.9 mm and 4.9–5.4 mm for the I_L- and I_S-chip, respectively. The thickness of the board affected the density, with thinner boards having higher densities, and the thickness and density of the I_S-chip boards were closer to the target thickness of 5 mm and density of 1.0 g/cm^3 than those of the I_L-chip boards. The reason for this is thought to be the slow S of T_C in I_S-chip boards, which allows the raw material to be softened by the action of stable heating and suppresses pressure resistance. In particular, the I-Board with the $I_SR_{10}Y$ condition (thickness: 4.95 mm, density: 0.99 g/cm^3) was closest to the target. The performance of

the second compression brought the density closer to the target level, highlighting the value of this second compression.

Finally, we focus on the internal cracking and L^* (**Table 5-3**). I_S-chip boards tended to have internal cracks, especially when the residual pressure was large, T_C's S_b and S_c were small, such as under the R_{15} and $R_{15}Y$ conditions. It is interpreted that, the smaller the chips, the smaller the gaps between them, which caused the delay in the discharge of water vapor generated during hot-pressing. In addition, I_S-chip boards tended to have smaller L^* than I_L-chip boards, resulting in the elution of self-adhesive components and darkening of the color.

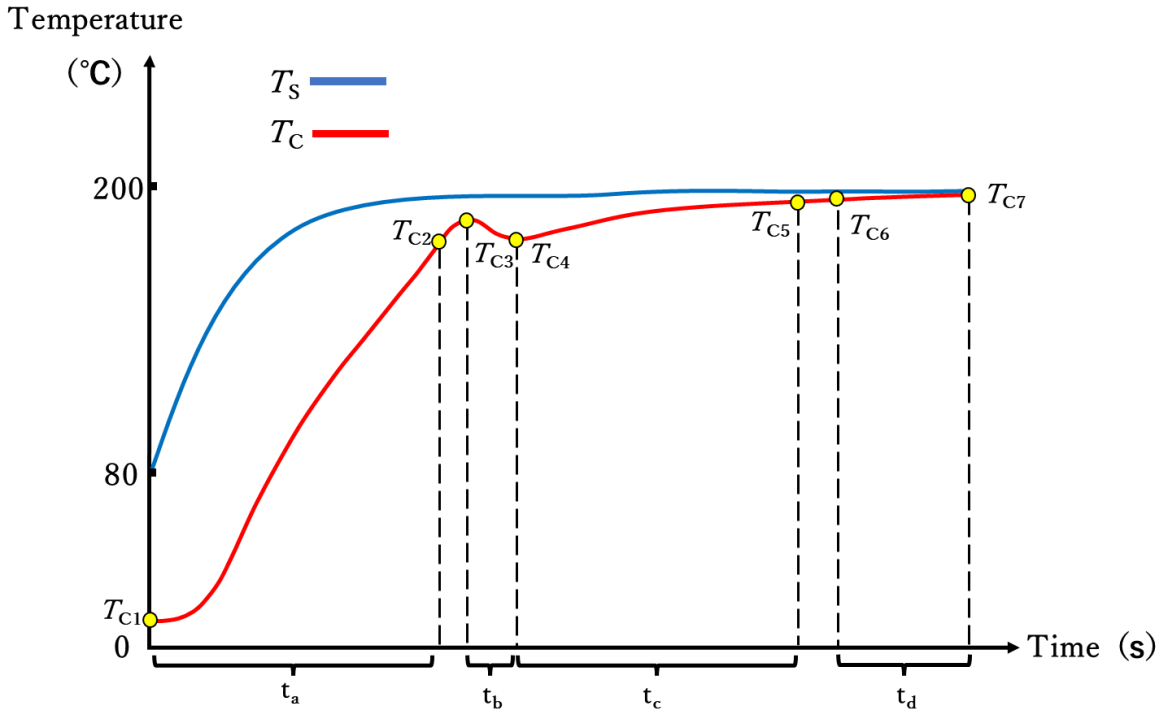

Figure 5-4 Example of the press time (X) – temperature (Y) relationship (I-Board, $I_LR_{10}Y$)

T_{C1}: Core temperature at start of the hot-pressing

T_{C2} / T_{C5} : Core temperature at the end of the first compression/ relaxation period

T_{C3} / T_{C4}: Max/Min core temperature of the relaxation period

T_{C6} / T_{C7}: Core temperature at the start/ end of the second compression

Table 5-3 Temperature, L^* (mean) and the number of cracks of the I-Boards

		I_S						I_L					
		R_5	R_5Y	R_{10}	$R_{10}Y$	R_{15}	$R_{15}Y$	R_5	R_5Y	R_{10}	$R_{10}Y$	R_{15}	$R_{15}Y$
Speed of change of T_C (°C/s)	S_a[1]	0.42	0.41	0.47	0.45	0.42	0.42	0.59	0.59	0.57	0.61	0.59	0.55
	S_b[2]	0.36	0.33	0.17	0.24	0.11	0.04	0.57	0.47	0.16	0.19	0.09	0.11
	S_c[3]	0.07	0.06	0.04	0.04	0.03	0.02	0.10	0.10	0.07	0.05	0.06	0.06
	S_d[4]	–	0.03	–	0.01	–	0.01	–	0.03	–	0.02	–	0.02
L^*[5]		42.8	39.4	40.1	40.0	39.3	38.0	44.7	45.4	53.6	42.9	44.3	42.2
The number of cracks		3	5	4	4	8	13	0	0	0	0	0	0

1) $S_a = (T_{C2} - T_{C1})/t_a$ 2) $S_b = (T_{C3} - T_{C4})/t_b$

3) $S_c = (T_{C5} - T_{C4})/t_c$ 4) $S_d = (T_{C7} - T_{C6})/t_d$

5)The number of specimens is 400 for I_SR_5Y and $I_SR_{15}Y$, 420 for other conditions

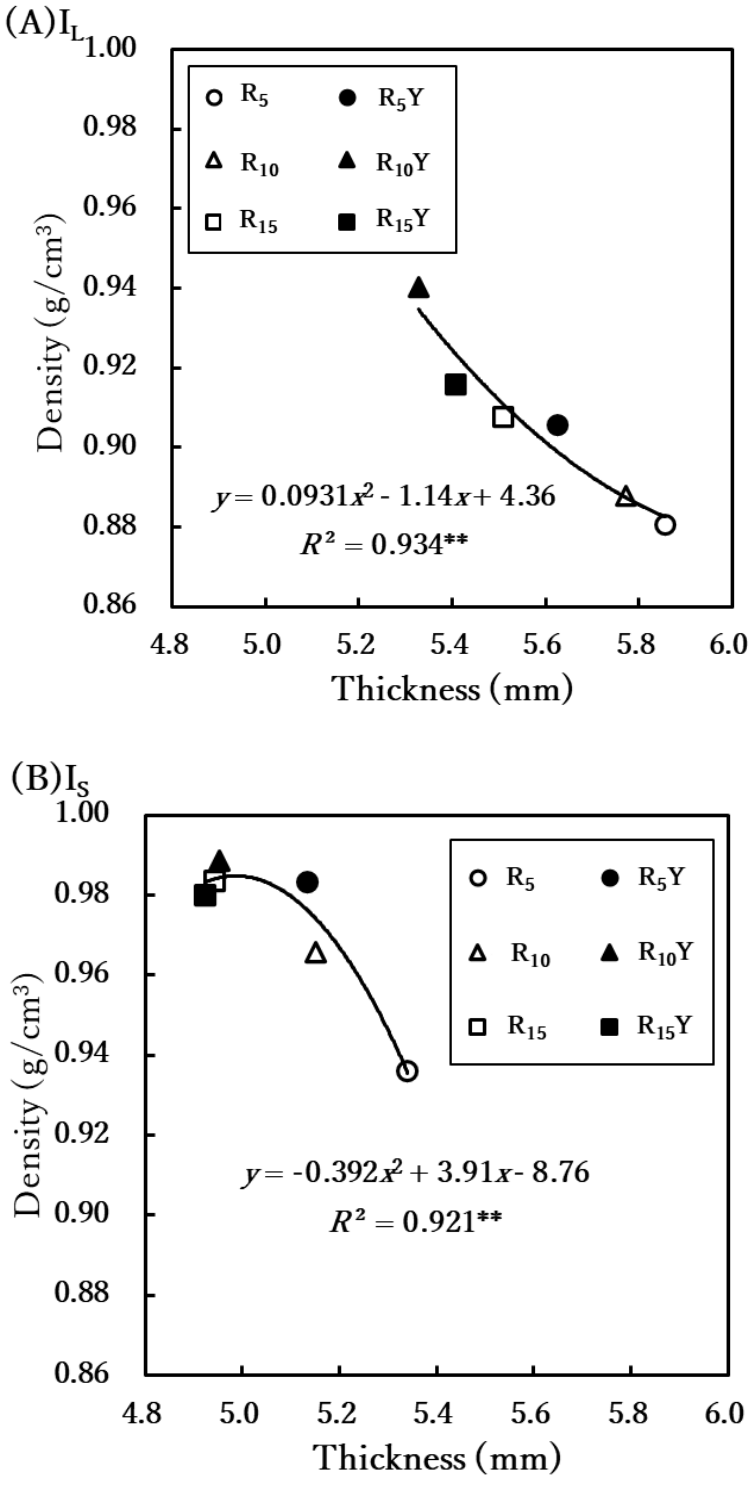

Figure 5-5 Relationships between the thickness and density of the I-Boards

3.2 Internal bond strength (IB) of the I-Boards

The IB of I-Boards shown in **Fig. 5-6** was higher at a residual pressure of 1.0 MPa and 1.5 MPa than at 0.5 MPa, with a maximum IB value of 0.62 MPa in the I_LR_{15} condition, followed by 0.44 MPa in the I_SR_{10} condition. The IB for the 1.0 MPa and 1.5 MPa residual pressure conditions fully met the JIS PB 18 type standard value (0.3 MPa). However, at a residual pressure of 0.5 MPa, the I_SR_5 condition did not meet the standard value (0.15 MPa) of the PB 8 type. A possible reason for this is that excessive water vapor emission may increase the range of T_C change and lead to insufficient self-adhesion capability. Meanwhile, the second compression and the chip size (I_L- and I_S- chips) were not observed to have any effect on IB.

The relationships between L^* and IB are shown in **Fig. 5-7**. Focusing on the plots with IB greater than 0.3 MPa (PB 18 type in JIS), the corresponding range of L^* was 35–50. Many plots in this range were for conditions of residual pressure of 1.0 and 1.5 MPa. This trend can be interpreted as follows: When the residual pressure was large, the excessive discharge of water vapor was suppressed, so the darkening progressed. As a result, the thermoplastic flow in the small chips also progressed, which resulted in increased IB. However, when L^* was less than 35, IB significantly decreased. This could be attributable to the weakening of the substance due to pyrolysis.

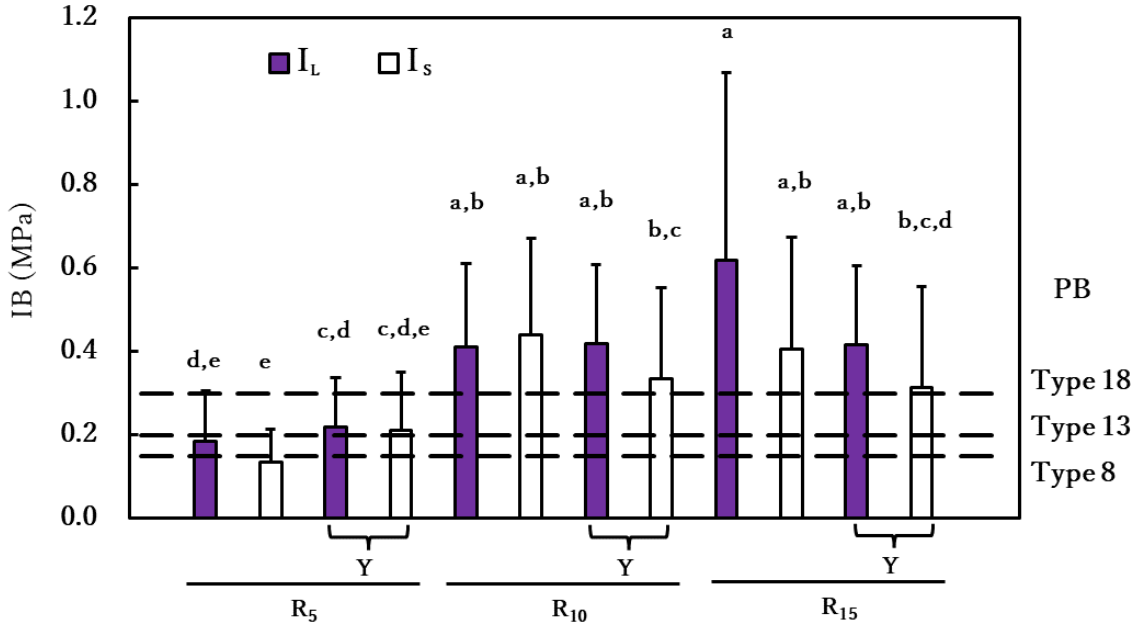

Figure 5-6 IB of the I-Boards and comparison to the JIS standards

Different letters along the bars are significantly different at $P = 0.05$

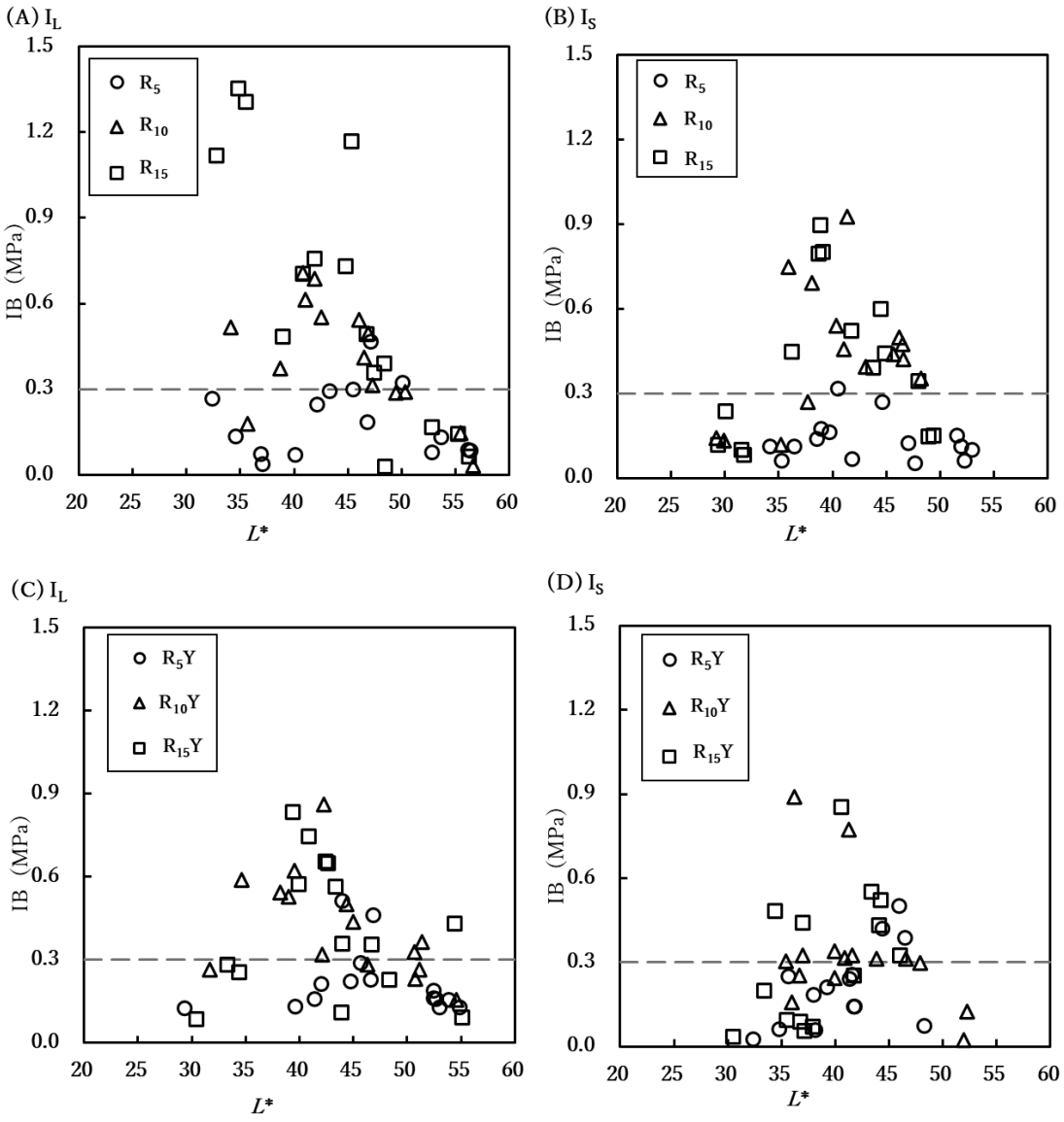

Figure 5-7 Relationships between the IB and L^* of the I-Boards

0.3MPa: standard value required for JIS PB type 18

3.3 Bending strength (MOR) and young's modulus (MOE) of the I-Boards

Figure 5-8 shows the MOR of I-Boards. Under all hot-pressing conditions the standard value (8 MPa) of the JIS PB 8 type was fulfilled. However, at a residual pressure of 0.5 MPa, the MOR was relatively low. As discussed for IB, this factor is thought to be due to excessive water vapor emission, which results in a larger range of T_C change and lack of self-adhesion ability. The second compression and the chip size (I_L- and I_S- chips) had no effects on MOR. **Figure 5-9** shows the relationships between L^* and MOR; plots with MOR greater than 8 MPa (PB 8 type in JIS) were mostly found in the L^* range of less than 45.

Figure 5-10 shows the relationships between MOE and MOR. As with the other wood-based panels, a significant positive correlation was found between them. JIS PB 8 type indicates MOE of 2 GPa or more as a reference value. I-Boards with MORs of more than 8 MPa often had MOEs of more than 2 GPa. Judging from the fact that I_S-chip boards have many plots with higher MOE and MOR than I_L-chip boards, the former tended to have higher bending performance than the latter.

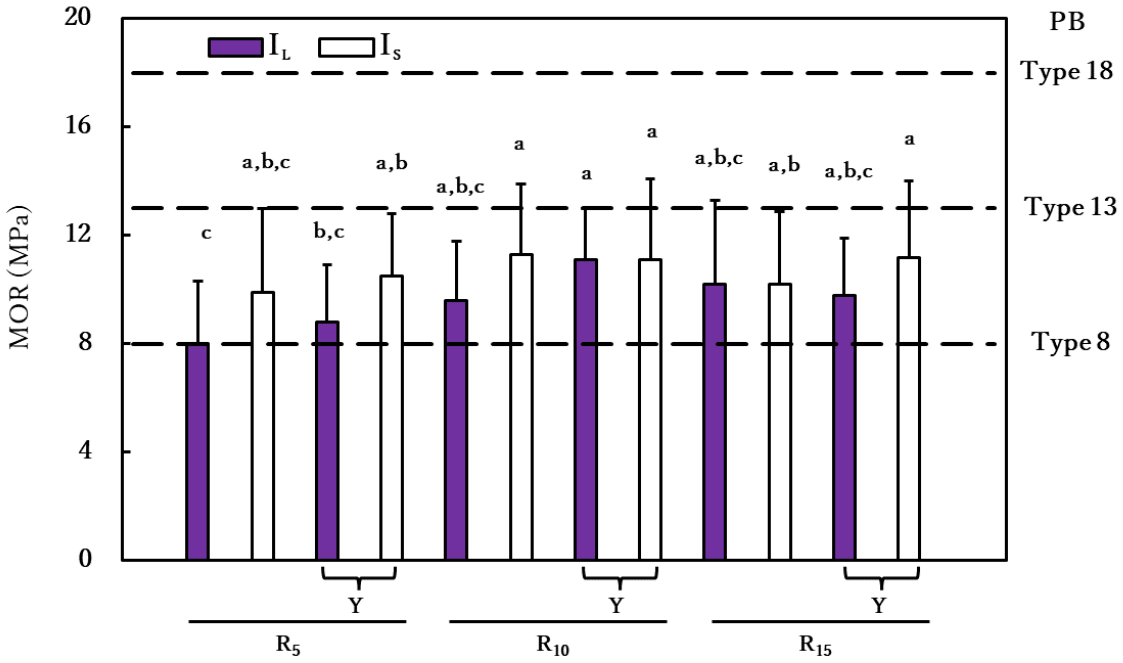

Figure 5-8 MOR of the I-Boards and comparison to the JIS standards

Different letters along the bars are significantly different at $P = 0.05$

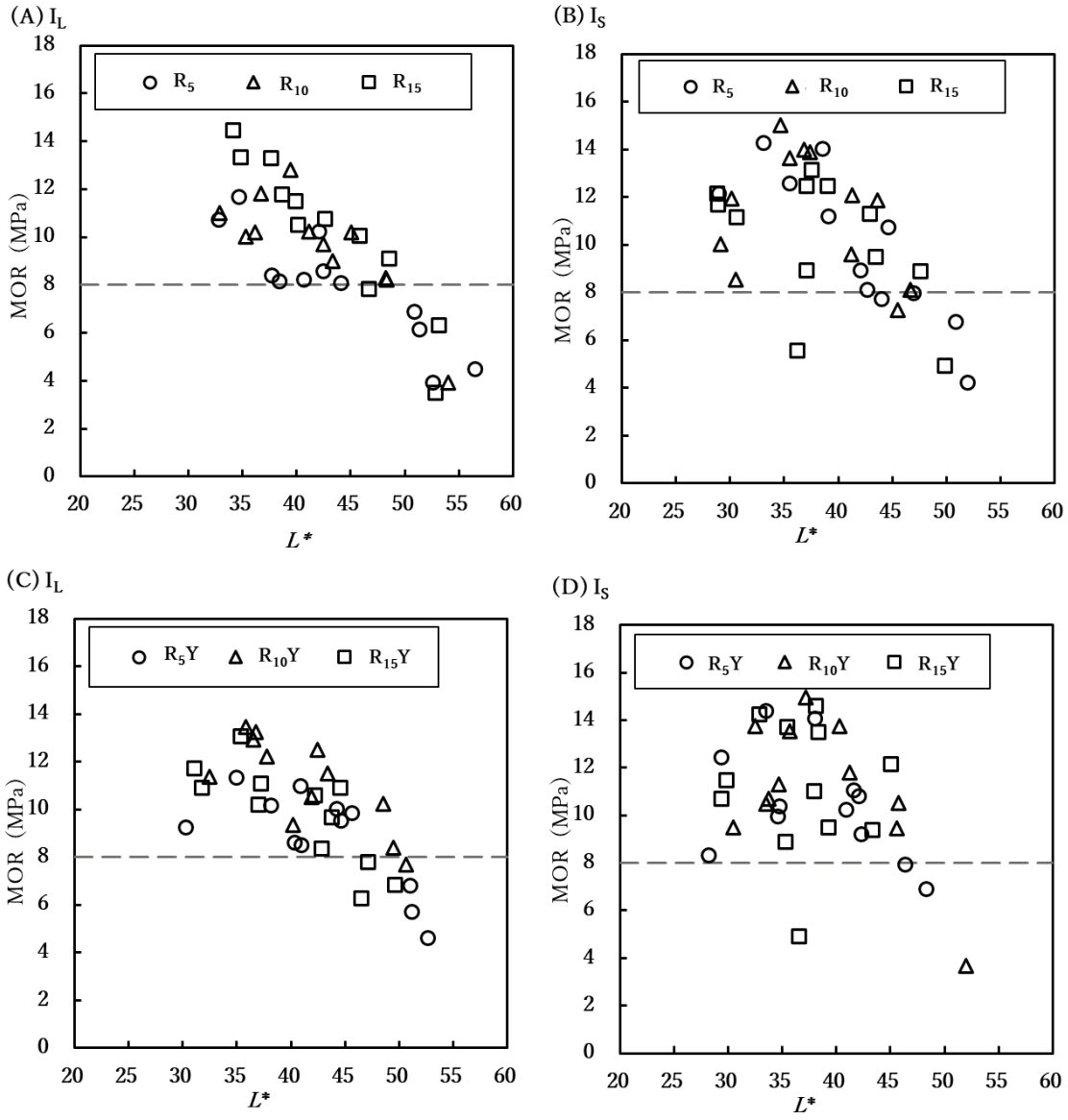

Figure 5-9 Relationships between the MOR and L^* of the I-Boards

8MPa: standard value required for JIS PB type 8

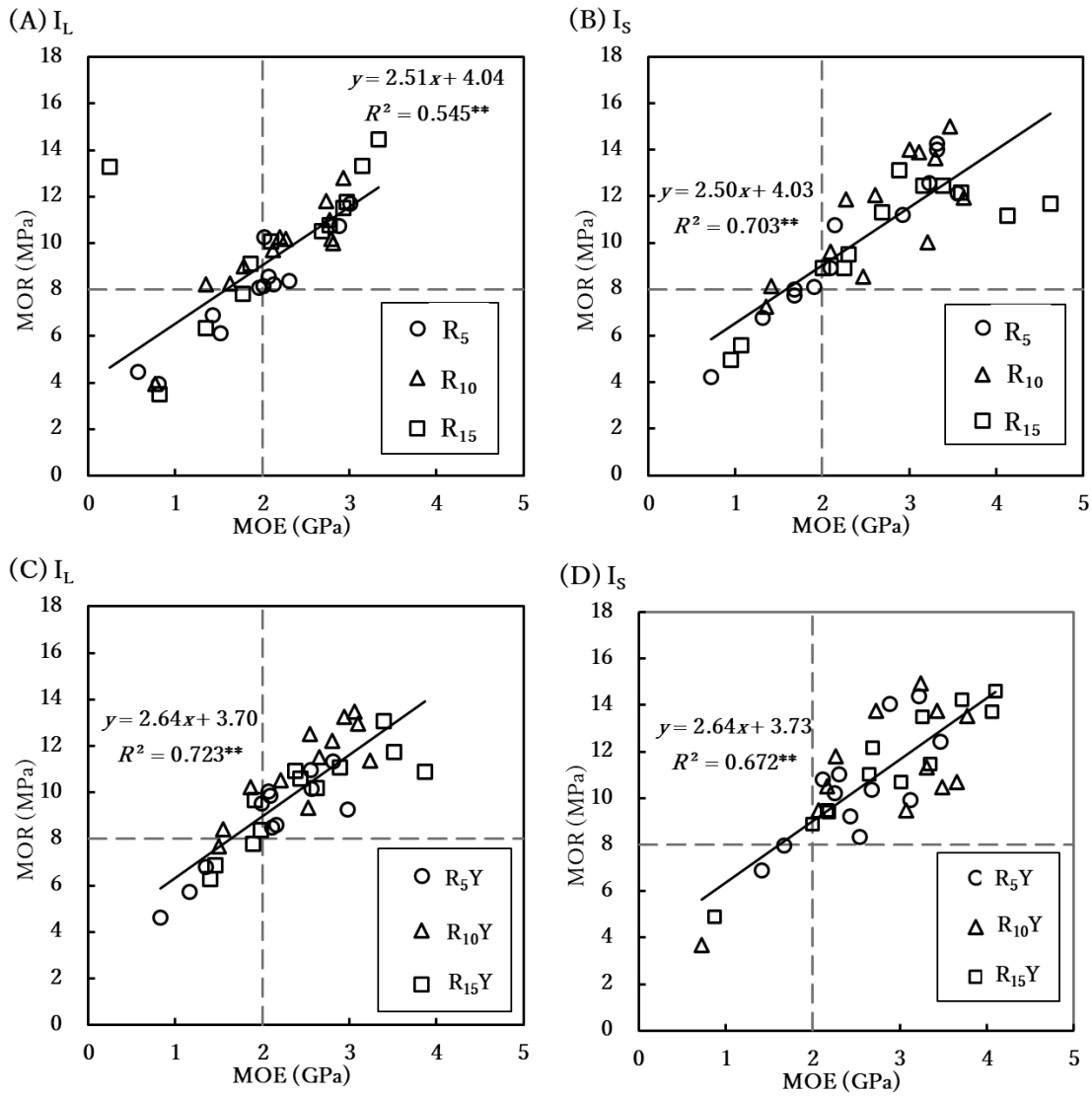

Figure 5-10 Relationships between the MOR and MOE of the I-Boards

2GPa: standard value required for JIS PB

3.4 Water resistance (TS・WA) of the I-Boards

Figure 5-11 shows the water resistance (TS and WA) of the I-Boards. First, we focus on the WA (**Fig.5-11 (A)**), which causes thickness swelling. The WA was about 40–60 %, which was significantly larger than that of commercial hardboard (density: 1.0 g/cm^3, thickness: 5–6 mm, WA: 5–11% [5-8]) with a density similar to that of I-Boards. The WA values of R_5Y, R_{10}, and $R_{15}Y$ conditions were significantly smaller for I_S-chip boards than for I_L-chip boards. No differences in WA were observed with/without the second compression. Next, we focus on TS (**Fig.5-11 (B)**). The differences in TS among the conditions were similar to those in WA. However, the effect of chip size was larger than in WA, with the TS of I_S-chips being about half that of I_L-chips. The reason for this may be that the I_S-chip board density is higher than that of I_L-chip boards (see **Fig. 5-5**). Moreover, there are more adhesion sites between the chips, which may suppress thickness swelling due to water absorption. Meanwhile, as in the case of WA, there were no differences in TS with/without the second compression, and only the $I_SR_{15}Y$ condition met the JIS PB standard value (TS < 12%).

Figure 5-12 shows the relationships between TS and WA. A clear trend of TS tending to increase with increasing WA can be observed for each condition. Focusing on the region below the JIS TS standard of 12%, I_S-chip boards (**Fig. 5-12(B) and (D)**) had more plots that meet this standard than I_L-chip boards (**Fig. 5-12(A) and (C)**). Many of the plots within this range belong to the conditions with residual pressure of 1.5 MPa and 1.0 MPa with the second compression. The WA value on the regression line at the time of 12% of TS was 23.4% for **(A)**, 37.8% for **(B)**, 24.8% for **(C)**, and 39.7% for **(D)**. These results show that I_S-chip boards have higher dimensional stability than I_L-chip boards since the TS does not easily increase even if the water absorption increases.

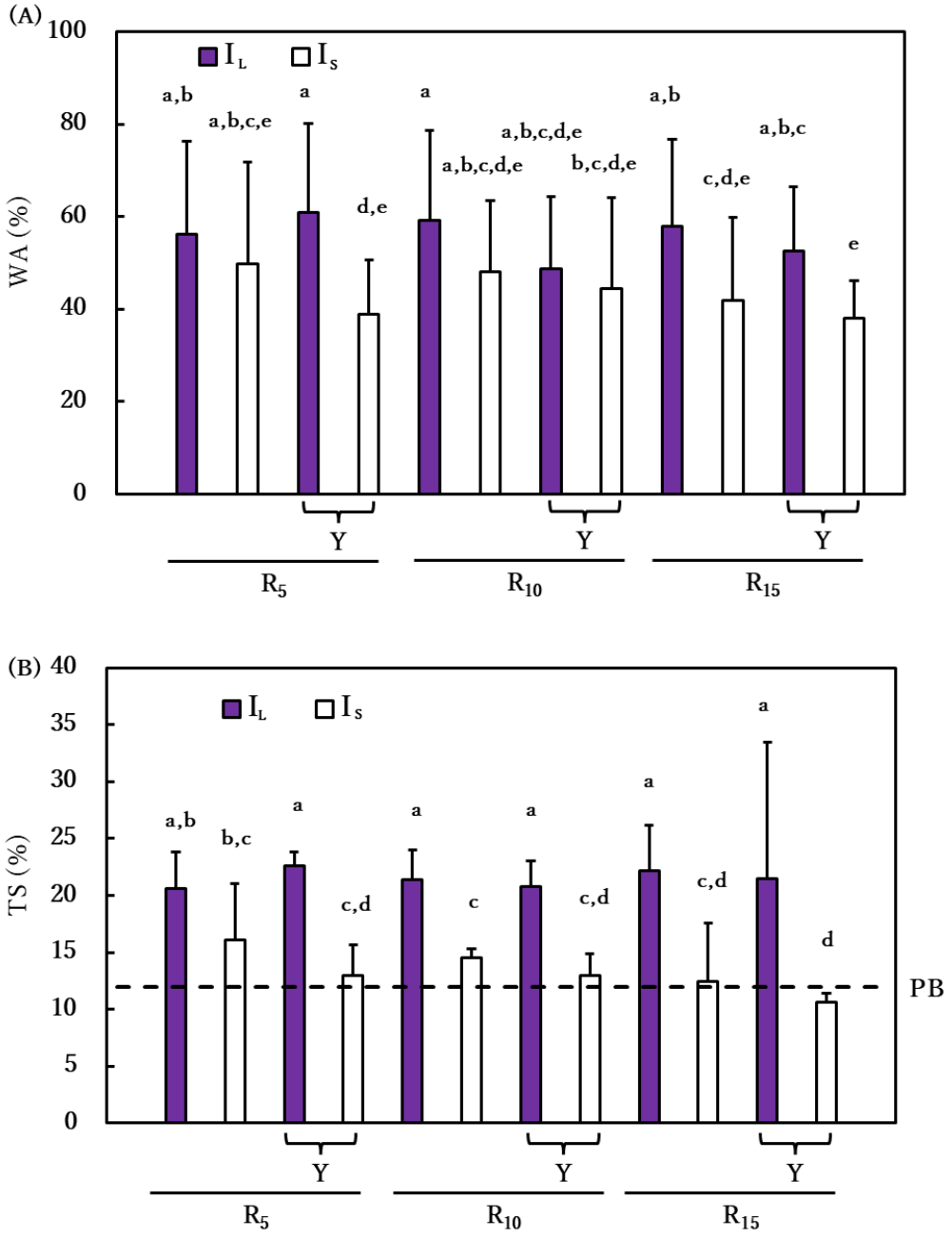

Figure 5-11　Water resistance of the I-Boards and comparison to the JIS standard

(A: WA, B: TS)

Different letters along the bars are significantly different at $P = 0.05$

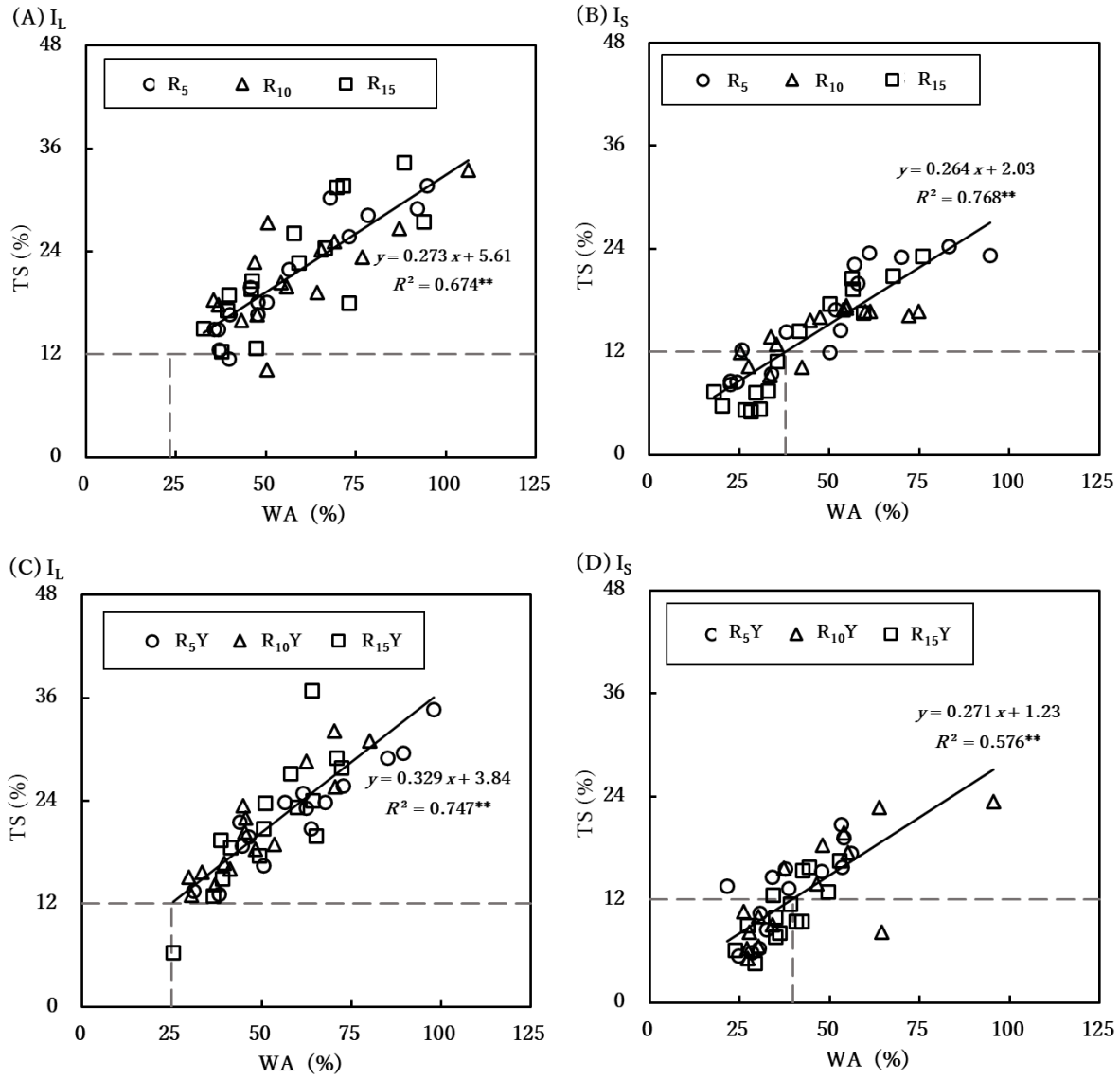

Figure 5-12 Relationships between the TS and WA of the I-Boards

TS 12%: standard value required for JIS PB

3.5 Effect of skin chips on the board properties

Table 5-4 lists the measurement results for the I-, W- and S-Board. First, we focus on the board appearance (thickness, density, internal cracking, and L^*). Boards with S-size chips (**Table 5-4** left) were closer to the target thickness of 5 mm and density of 1.0 g/cm^3 than boards with L-size chips (**Table 5-4** right). In particular, the board using S-size chips of the WMB's skin ($S_SR_{10}Y$) was closest to the target values. This suggests that the skin raw material is more easily compacted by the action of water vapor than the inside raw material. Meanwhile, a significant amount of internal cracking was observed in the W- and S-Boards among the S-size chip series. As discussed previously, the smaller the chips, the smaller the gaps between them, which caused the delay in the discharge of water vapor generated during hot-pressing. Therefore, it is considered that the presence of the WMB's skin strengthened this tendency. The L^* of the S-Board was smaller than those of the I- and the W-Board for both the S- and L-size chip series. This can be attributed to the original darkening of the skin of the WMBs (deposition of melanin pigment) as well as thermoplastic flow.

Next, we focus on the mechanical properties. The IBs met the lowest JIS PB standard (0.15 MPa: PB 8 type) under all manufacturing conditions. In particular, the boards with L-size chips (**Table 5-4** right) and the board with the $I_SR_{10}Y$ condition also met the highest JIS PB standard value (0.3 MPa: PB 18 type). Meanwhile, the MOR and MOE of W- and S-Board were smaller than the lowest JIS PB standard value (MOR: 8 MPa PB 8 type, MOE: 2 GPa). These results indicate that the mechanical properties of the boards deteriorate when the skin of WMBs is mixed.

Finally, we focus on the water resistance. No significant difference in WA was observed among all of the manufacturing conditions. The TS did not meet the JIS PB standard value (<12%) for all of the manufacturing conditions.

Table 5-4　Density, cracks, L^*, mechanical properties, and water resistance values (mean[1)]±std.[2)], n[3)]) of the binder-less boards (MC_d: 3-4%)

		Chip size of S			Chip size of L		
		I-Board ($I_SR_{10}Y$)	W-Board ($W_SR_{10}Y$)	S-Board ($S_SR_{10}Y$)	I-Board ($I_LR_{10}Y$)	W-Board ($W_LR_{10}Y$)	S-Board ($S_LR_{10}Y$)
4×4 cm specimen	Thickness (mm)	4.95^{d} (48)	$5.13^{b,c}$ (30)	$5.00^{c,d}$ (33)	5.33^{a} (48)	$5.31^{a,b}$ (48)	$5.29^{a,b}$ (43)
	Density (g/cm^3)	0.99^{b}	0.97^{b}	1.00^{b}	0.95^{a}	0.93^{a}	0.95^{a}
	The number of cracks	4	18	19	0	0	6
	L^* [4)]	40.0 (420)	41.2 (300)	37.7 (280)	42.9 (420)	40.1 (420)	38.6 (420)
Mechanical properties	IB (MPa)	$0.33^{a,b}$±0.22 (16)	0.23^{b}±0.14 (11)	0.24^{b}±0.11 (10)	0.42^{a}±0.19 (16)	$0.30^{a,b}$±0.12 (15)	$0.33^{a,b}$±0.17 (15)
	MOR (MPa)	11.1^{a}±3.0 (12)	5.5^{b}±1.7 (8)	5.9^{b}±2.1 (9)	11.1^{a}±1.9 (12)	5.8^{b}±1.3 (12)	5.1^{b}±2.0 (12)
	MOE (GPa)	2.8±0.9	1.3±0.7	1.8±0.9	2.5±0.6	1.5±0.6	1.4±0.7
Water resistance (%)	WA	40±20	56±16	50±13	36±16	48±16	50±15
	TS	13^{c}±6 (16)	$19^{a,b}$±4 (11)	$16^{a,b,c}$±3 (9)	21^{a}±6 (16)	$17^{a,b,c}$±6 (15)	$21^{a,b}$±6 (15)

1)　Averages with different letters are significantly different at $P = 0.05$

2) std.: standard deviation

3) Numbers in () indicate the number of test specimens for each test

4) The number of specimens is 300 for $W_SR_{10}Y$, 280 for $S_SR_{10}Y$, and 420 for other conditions

4. Conclusions

The findings obtained from this work are summarized as follows:

(1) The manufacturing conditions involving the use of chips of less than 2 mm and second compression provided the I-Boards with thickness and density closest to the target values. However, at the highest residual pressure of 1.5 MPa, the boards tended to suffer internal cracking.

(2) The manufacturing conditions that provided the boards with the best mechanical properties involved the following combination: chips of less than 2 mm derived from the inside of WMBs, residual pressure of 1.0 or 1.5 MPa at the relaxation period, and a second compression. Under these conditions, darkened test specimens were obtained, with lightness L^* in the range of 35–50, suggesting the ability to perform self-adhesion.

(3) The thickness and density of the W- and S-Boards were similar to those of the I-Boards. However, the mechanical properties of these boards were inferior to those of the I-Boards and they exhibited significant internal cracking when chips of less than 2 mm were used.

CHAPTER SIX

FUTURE PROSPECTS

Aiming for fuel and material utilization of shiitake waste mushroom beds (WMBs), the following three subjects were examined in this study: fuel properties, thermal insulation performance and mechanical properties as an insulation material, manufacturing conditions and properties of binder-less board. Based on the findings obtained from CHAPTER 2 to 5, the three subjects to be further examined are as follows.

1. Wastewater treatment in fuel utilization

A major challenge in using shiitake WMBs as fuel is the decrease in moisture content. If the place and time for air-drying can be secured, natural drying is promising. However, in reality, there are many challenges, such as differences in temperature and humidity depending on the location, time, and season. Therefore, introduction of compression and dewatering machines would make it possible to smoothly reduce moisture content throughout the year. However, the hydrogen ion index of the dewatered wastewater was measured to be pH 3.4. If a large amount of dewatered wastewater is generated, it is necessary to consider methods and facilities for neutralization treatment.

2. Sound absorption properties, moisture and water resistance when used as insulation material

When the shiitake WMBs were compressed and dried, the thermal conductivity was lower than that of wood and similar to that of wood-based panels. As for effects of compression-drying on the mechanical properties, the increase in internal bond strength was small, but the compressive properties were better than that of commercial IFBs. Therefore, it is expected to be used in areas

where compressive performance is required, such as insulation materials installed under the floor. However, the sound absorption properties, moisture resistance and water resistance of the WMBs have not yet been examined and needs to be investigated.

3. Water resistance of WMB binder-less board and utilization of skin material

Using whole WMBs as raw material for binder-less boards caused internal cracking and strength loss of the board due to the hydrophobic skin material. Therefore, it is appropriate to use only the inside of the WMB as raw material. However, it is necessary to find a manufacturing condition of binder-less board that does not cause performance degradation even if the skin of WMBs is mixed with. In addition, the water resistance of binder-less board cannot be said to be high even manufactured with materials from the inside of WMBs. Therefore, it is necessary to add something like a natural adhesive to provide the boards with water resistance.

REFERENCES

Chapter one

1-1. FAOSTAT: http://www.fao.org/faostat/en/#data/QC.

1-2. Non-timber forest products production statistics survey in Japan: http://www.maff.go.jp/j/tokei/kouhyou/tokuyo_rinsan/.

1-3. Sekino N, Jiang Z (2020) Mushroom cultivation in Jilin Province, China and fuel utilization of waste mushroom beds (in Japanese). Wood Industry 75(6):254-257

Chapter two

2-1. The Japan Wood Research Society (2000) Wood science experimental manual, p.92, Buneido Press, Tokyo

2-2. Japanese Industrial Standard M8814 (2000) The method for measuring total calorific value with a bomb calorimeter and the method for calculating gross calorific value, Japanese Standards Association

2-3. Roger M. Rowell (2013) Handbook of Wood Chemistry and Wood Composites 2nd Ed., p.60, CRC Press, New York

2-4. Kufujita H, Ettyu K, Ota M (1999) Characterization of the major components in bark from five Japanese tree species for chemical utilization. Wood Science and Technology 33(3): 223-228

2-5. Sekino N, Kofujita H, Abe K, Higashino T (2011) Charactering calorific value of coniferous bark chips in terms of elemental and chemical composition and its practical range as boiler fuel (in Japanese). Mokuzai Gakkaishi 57(2):101-109

2-6. Jennings D H, Lysek G (1999) Fungal Biology: Understanding the Fungal Lifestyle (2nd Ed.

Japanese translation Ed.), p133, Kyoto University Press, Kyoto

2-7. George Tsoumis (1991) Science and technology of Wood, p.200, Van Nostrand Reinhold, Ney Yor

2-8. The Energy Conservation Center, Japan (Tyuou-Netsukanri Council: 1972) Heat management handbook (in Japanese), p.305, Maruzen, Tokyo

2-9. Standard Tables of Food Composition in Japan: https://www.mext.go.jp/a_menu/syokuhinseibun/1365295.htm

2-10. Itoh S (2016) The recycle utilization of Shiitake (*Lentinula edodes*) cultural waste for sawdust-based cultivation of Shiitake (in Japanese). Kyushu journal of forest research 69:177-179

2-11. Nakaya M, Yoneyama S, Kato Y, Yamamura T (1999) Cultivation of Pleurotus ostreatus and Flammulia velutipes using sawdust of waste Shiitake bed logs (in Japanese). Journal of the Hokkaido Forest Products Research Institute 13 (6):1-6

2-12. Higuchi S, Takahashi M, Yamaji A (2007) Utilization of the functional constituents from wheat (in Japanese). Journal of Saitama Industrial Technology Center Vol.5, Topic No.5 of industry support

2-13. Dinwoodie J M (2000) Timber: Its nature and behaviour (2nd Ed.), p.212, E&FN Spon, London

Chapter three

3-1. Grown Bio: https://www.grown.bio. Accessed 15 Mar 2022.

3-2. Dahmen J (2017) Soft futures: mushrooms and regenerative design. Journal of Architectural Education 71 (1): 57–64

3-3. Jones M, Bhat T, Huynh T, Kandare E, Yuen R, Wang CH, John S (2018) Waste-derived low-

cost mycelium composite construction materials with improved fire safety. Fire and Materials 42: 816–825

3-4. Pelletiera MG, Holta GA, Wanjuraa JD, Bayerb E, McIntyre G (2013) An evaluation study of mycelium based acoustic absorbers grown on agricultural by-product substrates. Industrial Crops and Products 51: 480–485

3-5. Japanese Industrial Standard A 1412-2 (1999) Test method for thermal resistance and related properties of thermal insulations, appendix A: The comparison method with standard plate. Japanese Standards Association Group

3-6. Sekino N, Jiang ZQ (2019) The change in thermal conductivity of wood due to carbonization and the mechanisms behind this (in Japanese). The Wood Carbonization Research Society 16 (1): 13–23

3-7. Japan Society of Thermophysical Properties（2000）Thermophysical properties handbook (in Japanese). Yokendo, Tokyo, p 221

3-8. Saito F, Suzuki T, Nawamaki M（1976）Thermal Conductivity of Particleboards (in Japanese). Mokuzai Gakkaishi 22(5): 297-302

3-9. The Japan Wood Research Society (1985) Wood science experiment book Ⅰ. Physics and Engineering (in Japanese). Chugai Sangyo Chosakai, Tokyo, pp 107-111

3-10. Japan Society of Thermophysical Properties（2000）Thermophysical properties handbook (in Japanese). Yokendo, Tokyo, pp 204-205

3-11. Sekino N, Yamaguchi K (2013) Mechanisms behind better thermal insulation capacity of carbonized binder-less wood shaving insulation panels – Investigation from apparent thermal conductivity of coarse pore – (in Japanese). The Wood Carbonization Research Society 9(2): 68–74

Chapter four

4-1. JIS A 5905 (2014) JIS standard for fiberboard. Japanese Standards Association, Tokyo, p 3, 18 (in Japanese)

4-2. Morisaki, H. (2008) Microbes in Natural Environments – Their Surface Characteristics and Interaction with Interfaces –. Japan Oil Chemists' Society. 8:2

Chapter five

5-1. Umemura, K. (2015) Wood adhesion technology without using fossil resources. Journal of The Adhesion Society of Japan. 51: 491-495 (in Japanese)

5-2. Okuda, N., Sato, M. (2004) Manufacture and mechanical properties of binderless boards from kenaf core. The Japan Wood Research Society. 50: 53–61

5-3. Widyorini, R., Xu, JY., Umemura K., Kawai, S. (2005) Manufacture and properties of binderless particleboard from bagasse I: effects of raw material type, storage methods, and manufacturing process. Journal of Wood Science. 51: 648–654

5-4. Sekino, N., Sasaki, T., Taniuchi, H. (2005) Manufacturing and performance of high density sugi bark boards without synthetic resins (Part 1) Effects of mat moisture content and hot-pressing schedule on basic properties of the boards. Bulletin of The Iwate University Forests. 36: 21–37 (in Japanese)

5-5. S. Chow. (1975) Bark boards without synthetic resins. Forest Products Journal. 25 (11), 32-37

5-6. Lui, FHY., Kurokochi, Y., Narita, H., Saito, Y., Sato, M. (2018) The effects of chemical components and particle size on the mechanical properties of binderless boards made from oak (*Quercus* spp.) logs degraded by shiitake fungi (*Lentinula edodes*). Journal of Wood Science. 64: 246–255

5-7. JIS A 5905 (2022) JIS standard for particleboard. Japanese Standards Association, Tokyo (in Japanese)

5-8. Sekino, N., Suzuki, S. (2003) Durability of wood-based panels subjected to ten-year outdoor exposure in Japan. Bulletin of The Iwate University Forests. No. 34: 23–36

ACKNOWLEDGMENTS

This thesis marks the end of a long and memorable journey that I could not have completed without the dedicated support of my supervisors. I am extremely grateful to my dedicated supervisors, and it is with sincere appreciation that I acknowledge Prof. Noboru SEKINO for his consistent and invaluable support throughout my PhD studies. I owe a great debt to him for his patience, guidance, and academic expertise. Prof. SEKINO provided me with excellent opportunities and advice in writing research papers, and his thorough reviews and constructive feedback have significantly improved my work. I consider myself fortunate to have benefitted from Prof. SEKINO's vast knowledge and admirable character. I would also like to express my gratitude to my associate advisors, Prof. Atsushi MARUI, Hisayoshi KOFUJITA, Motohei KANAYAMA, Tatsuya ASHITANI, as well as the members of my dissertation committee. Their valuable feedback, advice, and critical insights have played an instrumental role in shaping the direction of my research. I would like to extend my thanks to Koshido Mushroom Co., Ltd. for providing the waste mushroom bed samples, and Daiken Corp. for providing the Insulation fiberboard samples. Their generosity has contributed to the success of my research.

I would also like to express my heartfelt appreciation to my family. I rarely say thank you to you because I think it’s too official, but now I want to sincerely thank you for your constant encouragement and unwavering support.

Last but not least, I wish to thank my partner for his unwavering support, he never stopped encouraging me and stood by me through all of the hardships I had endured. His support allowed me to concentrate on my studies and complete my thesis.

LIST OF ABBREVIATIONS

1. WMB: Waste mushroom bed
2. MC: Moisture content
3. MC_d: Moisture content on a dry basis
4. MC_w: Moisture content on a wet basis
5. *n*: The number of sample/ test specimen
6. mean: Mean value
7. std.: Standard deviation
8. PB: Particleboard
9. IFB: Insulation fiberboard
10. IB: Internal bond strength

Chapter two

1. R: Radial direction
2. T: Tangential direction
3. L: longitudinal direction
4. C: Carbon
5. H: Hydrogen
6. N: Nitrogen
7. *COV*: Coefficient of variation
8. H_h: Calorific value
9. H_{ho}: Calorific values on a dry basis

10. H_{ho}': Correction value

11. H_n: Net calorific value

12. h: weight ratio

Chapter three

1. H_{120}: Uncompacted WMB (120 mm high)

2. H_{60}: The WMB compacted to 60 mm high

3. H_{50}: The WMB compacted to 50 mm high

4. H_{30}: The WMB compacted to 30 mm high

5. H_{25}: The WMB compacted to 25 mm high

6. MDF: Medium-density fiberboard

7. OSB: Oriented strand board

8. λ: Thermal conductivity of the test specimen

9. λ_0: Thermal conductivity of the standard plate

10. $\triangle \theta$: Temperature difference between upper and lower surfaces of the test specimen

11. $\triangle \theta_0$: Temperature difference between upper and lower surfaces of the standard plate

12. d: The height of the test specimen

13. d_0: The height of the standard plate

14. V: Void's ratio

15. λ_s: Thermal conductivity of the substance

16. λ_a: Thermal conductivity of the air

17. ρ_o: Oven-dry density

18. ρ_h: Substance density

19. λ_m: Thermal conductivity of the mat

Chapter four

1. P_{max}: Maximum load
2. A: load surface
3. ε_y: yield strain
4. σ_y: yield stress
5. E: Elastic modulus
6. E_s: Elastic modulus of the substance

Chapter five

1. t : Sample thickness of consolidation test
2. I_L: Inside of the WMB chip, size is 4–2 mm
3. I_S: Inside of the WMB chip, size is less than 2 mm
4. S_L: Skin of the WMB chip, size is 4–2 mm
5. S_S: Skin of the WMB chip, size is less than 2 mm
6. W_L: Whole WMB chip, size is 4–2 mm
7. W_S: Whole WMB chip, size is less than 2 mm
8. T_S: Surface temperature of the caul-plate
9. T_C: Core temperature of the Binder-less board
10. T_{C1}: Core temperature at start of the hot-pressing
11. T_{C2}: Core temperature at the end of the first compression
12. $T_{C3:}$ Max core temperature of the relaxation period

13. $T_{C4:}$ Min core temperature of the relaxation period
14. T_{C5}: Core temperature at the end of the relaxation period
15. T_{C6}: Core temperature at the start of the second compression
16. T_{C7}: Core temperature at the end of the second compression
17. I-Board: Binder-less board made from the inside of the WMB
18. S-Board: Binder-less board made from the skin of the WMB
19. W-Board: Binder-less board made from the whole of the WMB
20. MOR: Bending strength
21. MOE: Young's modulus in bending
22. TS: Thickness swelling rate
23. WA: Water absorption rate
24. L^*: Surface darkening of the test specimen

LIST OF TABLES

Chapter two

Table 2-1. Details of the cultivation bed……15

Table 2-2. Weight and moisture content of WMB……20

Table 2-3. Results of the elemental analysis……25

Table 2-4. Weight composition of the cultivation bed……33

Table 2-5. Elemental weight composition of an oven-dry cultivation bed……35

Table 2-6. Comparison of the elemental weight composition between the cultivation bed and WMB in an oven-dry base……36

Chapter three

Table 3-1. Wood and wood-based panels for thermal conductivity measurement……47

Table 3-2. Air-dry densities of the WMB for thermal conductivity measurement……49

Table 3-3. Values used in model calculations and the optimal substance thermal conductivity λ_s……56

Table 3-4. Comparison of the thermal conductivity of WMB with the same density band……59

Chapter four

Table 4-1. Internal bond strength test specimens and their densities……72

Table 4-2. Compressive test specimens and their densities……74

Table 4-3. IB values at different air-dry density bands of WMB……81

Table 4-4. Elastic modulus of substance E_s (powder samples) ……85

Chapter five

Table 5-1. Symbols of the raw material chips……95

Table 5-2. Hot-pressing conditions of the binder-less boards……98

Table 5-3. Temperature, L^* (mean) and the number of cracks of the I-Boards……105

Table 5-4. Density, cracks, L^*, mechanical properties, and water resistance values of the binder-less boards…… 118

LIST OF FIGURES

Chapter one

Figure 1-1. Pellet fuel production process from WMBs (wood ear) ……9

Figure 1-2. Production process of Shiitake mushroom using hardwood chip cultivation bed……11,13,44

Figure 1-3. Three types of voids inside the dried WMB……11,41

Chapter two

Figure 2-1. Weight histogram of WMB……20

Figure 2-2. Changes in the structure of a mushroom bed……21

Figure 2-3. Results of the ash content tests……23

Figure 2-4. Gross calorific values on a dry basis (H_{ho})……27

Figure 2-5. Relationships between moisture content on a wet basis (MC_w) and the net calorific value for both the WMB (whole) and the raw wood chips……31

Chapter three

Figure 3-1. Air-dry density distribution of the WMB……45

Figure 3-2. Compaction equipment for the WMB (a: front view, b: side view, c: top view, d: cross section of compression formwork) …46

Figure 3-3. Cut surface of the WMB for chip inclination angle measurement……46

Figure 3-4. A heat-flow model applied to the WMB……52

Figure 3-5. Relationship between the density and thermal conductivity for the powder mat ……55

Figure 3-6. Relationship between the density and thermal conductivity of the WMB ……58

Figure 3-7. Relationship between the density and thermal conductivity for the WMB and comparison materials……61

Figure 3-8. Relationship between the height of the WMB after compaction and inclination angle of the decayed chip ……63

Figure 3-9. Thermal conductivity of the coarse void varying with a WMB density……63

Figure 3-10. WMB's estimated substance thermal conductivity along the heat-flow direction……65

Chapter four

Figure 4-1. Elimination of internal voids by compression drying (four levels of the heigh)
a: 120 mm high (before compression, uncompressed WMBs),
b: 60 mm high, c: 50 mm high, d: 30 mm high, e: 25 mm high……68

Figure 4-2. Air-dry density of the WMBs ……71

Figure 4-3. Schematic draw of the stress – strain curve of the compressive test……75

Figure 4-4. Schematic draw of the stress – thickness curve of the powder consolidation test……77

Figure 4-5. Relationships between the air-dry density and the internal bond strength of the WMB and IFB……80

Figure 4-6. Example of the powder sample thickness – stress relationship (WMB, F7) ……83

Figure 4-7. Schematic draw of the compaction behavior for the WMB (density 300 kg/m^3 or more)……88

Figure 4-8. Compression behavior of the WMB and IFB
(A: relationships between the density and the *E*, B: yield point) ……89

Figure 4-9. The yield point of the WMB and IFB……91

Chapter five

Figure 5-1. Hot-pressing schedules of the binder-less boards……97

Figure 5-2. A cutting pattern of the test specimens...……100

Figure 5-3. The side-view of the board with an internal crack……100

Figure 5-4. Example of the press time (X) – temperature (Y) relationship (I-Board, $I_LR_{10}Y$) ……104

Figure 5-5. Relationships between the thickness and density of the I-Boards……106

Figure 5-6. IB of the I-Boards and comparison to the JIS standards……108

Figure 5-7. Relationships between the IB and L^* of the I-Boards……109

Figure 5-8. MOR of the I-Boards and comparison to the JIS standards……111

Figure 5-9. Relationships between the MOR and L^* of the I-Boards……112

Figure 5-10. Relationships between the MOR and MOE of the I-Boards……113

Figure 5-11. Water resistance of the I-Boards and comparison to the JIS standard

(A: WA, B: TS) ……115

Figure 5-12. Relationships between the TS and WA of the I-Boards……116